Effect of Climate Change on Flooding in King County Rivers: Using New Regional Climate Model Simulations to Quantify Changes in Flood Risk

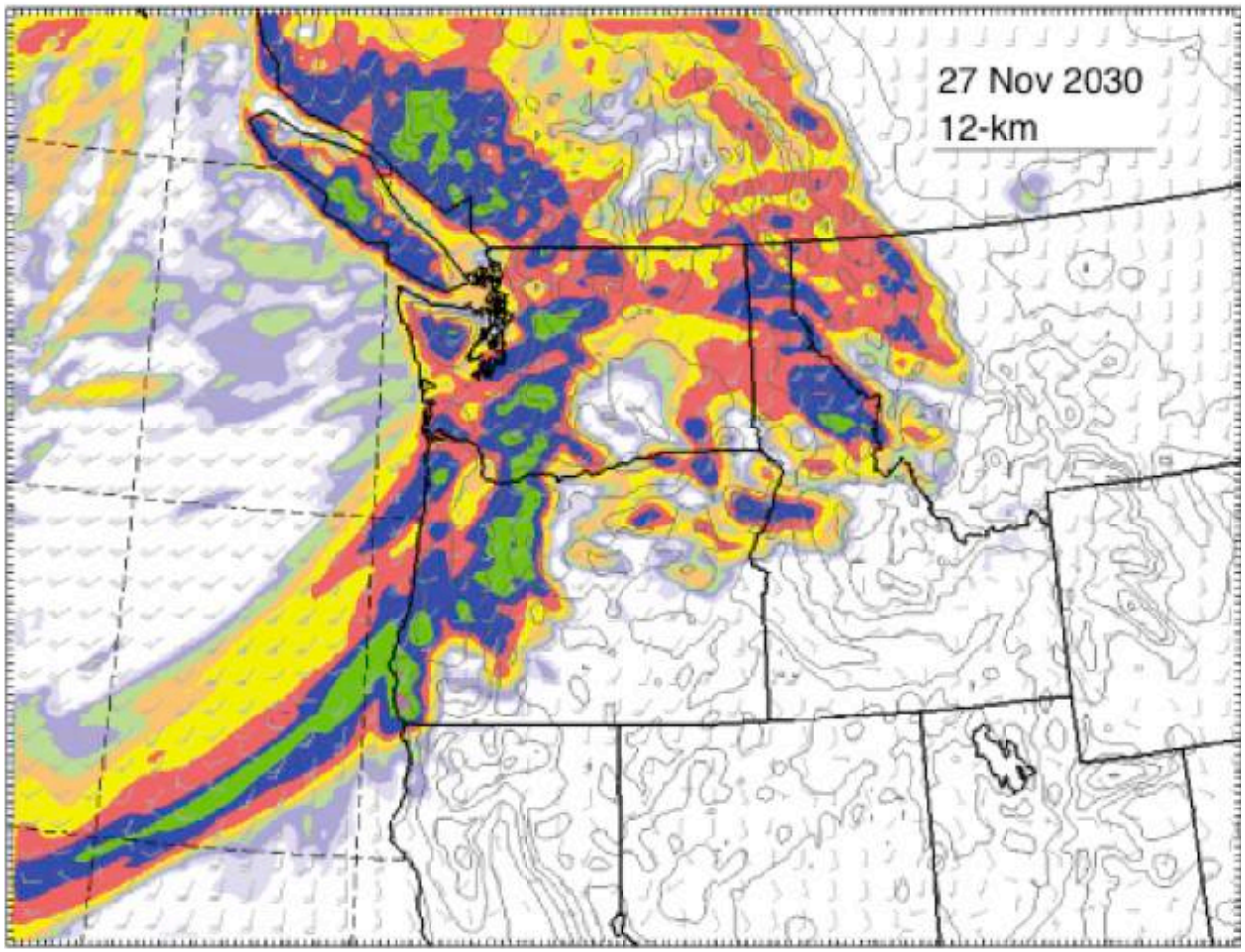

Prepared by the

Climate Impacts Group | University of Washington

May 2018

Se-Yeun Lee
Guillaume Mauger
Jason Won

Contributors

A total of 8 staff members at King County participated in regular project meetings, providing invaluable feedback and suggestions over the course of the project.

Department of Natural Resources and Parks Director's Office

Lara Whitely Binder

Water and Land Resources Division River and Floodplain Management Section

Kyle Comanor
Fred Lott
Brian Murray
Lorin Reinelt
Jeanne Stypula

Water and Land Resources Division Science and Technical Support Section

Curtis DeGasperi (Project Manager)
Jim Simmonds

Acknowledgements

The authors would like to acknowledge Eric Salathé for his help in a number of closely related and leveraged efforts aimed at better characterizing changes in extreme precipitation. David Rupp provided the RegCPDN data and advice on the analysis. Additional help came from Mike Warner, who made the initial foray into the RegCDPN statistics. Ken Brettman and Logan Osgood-Zimmerman at the U.S. Army Corps of Engineers (USACE) provided invaluable help on both the reservoir modeling and the key flow metrics of interest to reservoir operators. The WRF simulations were produced by Rick Steed and Raquel Lorente, in part thanks to computing resources provided by Cliff Mass. Robert Norheim produced the interactive online visualizations using Tableau as well as all of the maps in the report. This project was funded by the King County Flood Control District, with additional support from the Critical Infrastructure Resilience Institute (CIRI), a U.S. Department of Homeland Security S&T Center of Excellence (award number 2015-ST-061-CIRC01).

Cover image: Future storm projected by the regional climate model used in this study (Source: Eric Salathé, University of Washington)

Citation: Lee, S.-Y., G.S. Mauger, and J.S. Won. 2018. *Effect of Climate Change on Flooding in King County Rivers: Using New Regional Climate Model Simulations to Quantify Changes in Flood Risk.* Report prepared for King County. Climate Impacts Group, University of Washington.

Errata

The following errors have been identified and corrected since the initial publication of this report:

October 19th, 2018	Correction to Table 6.3. In the previous version, the projections listed in the RCP 8.5 column for bcMACA were incorrect. These were replaced with the correct values.

Table of Contents

1 Executive Summary

Climate projections indicate an increase in flooding in many Pacific Northwest watersheds over the course of the 21st century, in response to an increasing proportion of mountain precipitation falling as rain instead of snow. Global climate models also project an increase in the intensity in the type of heavy rain events that cause most river-scale flood events. A parallel study, funded by the King County Department of Natural Resources and Parks (DNRP) and the Washington State Department of Ecology,[1] has produced a new set of projections of 21st century climate, developed using a regional climate model. A key feature of these projections is that they provide hourly estimates of future weather conditions (temperature, precipitation, humidity, wind, etc.) and account for changes in both the form of precipitation (i.e., rain vs snow) and storm event intensity. Results from that study are described in a separate report (Mauger et al. 2018). In this study, we used the new projections to model changes in future streamflow and evaluate potential changes in peak flows on the Snoqualmie, South Fork (SF) Skykomish, and Green rivers. For the Green River, we also accounted for the effect of reservoir operations by the U.S. Army Corps of Engineers (USACE) at Howard Hanson Dam. Funding for this study was provided by the King County Flood Control District, with additional support from the Critical Infrastructure Resilience Institute.

We modeled future streamflow using the Distributed Hydrology Soil Vegetation Model (DHSVM, Wigmosta et al. 2002) to estimate changes in future streamflow. The model was calibrated to match observations on each river, and the calibrated model showed good performance for both monthly and extreme flow statistics. Changes in streamflow were estimated by using the new regional climate model projections, developed under the parallel King County study, as input to the DHSVM model simulation. The new regional model projections were selected to bracket the range from the low- to the high-end of precipitation changes among global models. For comparison, we also simulated future streamflow using an existing set of climate projections. Although developed using a simpler approach (“statistical downscaling”), these provide a larger set of estimates of future climate, which can be helpful for evaluating the range among projections. For the Green River, we then performed an additional set of simulations to evaluate the effect of reservoir management on peak flows downstream of Howard Hanson Dam.

As temperatures warm, winter precipitation will increasingly fall as rain, reducing the amount of snow that accumulates at high elevations. The smaller amount of snow that does accumulate then melts more quickly, both because there is less snow to melt and because temperatures are warmer. All of our simulations show this behavior, and the resulting increase in winter streamflow and corresponding decrease in summer. For

[1] Specifically, the parallel study was funded by King County’s Stormwater Services Group (within DNRP’s Water and Land Resources Division), the Wastewater Treatment Division (also within DNRP), and a grant from the Washington State Department of Ecology.

example, by the 2080s, average streamflow for Oct-Mar is projected to increase by 15-25% for the Snoqualmie near Snoqualmie (USGS ID: 12144500), by 17-33% for the SF Skykomish near Index (USGS ID: 12133000), and by 10-22% for the Green near Auburn (USGS ID: 12113000), relative to the 1970-1999 average. The changes are more pronounced for the Snoqualmie and SF Skykomish rivers than for the Green, possibly due to the larger amount of historical winter snowpack in that basin.

Changes in peak flows are influenced by both the declines in snowpack and by higher intensity heavy rain events. Although both act to increase the risk of flooding, we find that the decrease in snowpack, and resulting increase in flow during rain events, has the greatest impact on peak flows in the first half of the 21st century. Later in the century, the increase in rain intensity is the more important driver of changing peak flows in the Green and Snohomish. As a result, our projections reflect the changes in precipitation intensity projected by the two regional climate model simulations. The high-end simulation, which projects a large increase in precipitation intensity, shows a correspondingly large increase in peak flows. For example, by the 2080s (relative to 1970-1999), the amount of flow associated with a 10-year peak flow is projected to increase by +72% for the Snoqualmie near Snoqualmie (USGS ID: 12144500), by +72% for the SF Skykomish near Index (USGS ID: 12133000), and by +58% for the Green near Auburn (USGS ID: 12113000). This increase is larger than the increase projected by the median (in some cases even the maximum) of the projections in the statistically-downscaled comparison dataset. It is not clear whether the differences between the statistically-downscaled projections and the new regional climate model results are due to differences among global climate models or the method used to “downscale” the global projections to local scale changes in climate. This could be tested by creating a paired set of downscaled projections stemming from the same global model projection.

In contrast with the high-end projection, the low-end simulation shows high variability in precipitation and no clear trend over time. Specifically, the model projects a decrease of -35% in the 10-year peak flow for the Snoqualmie near Snoqualmie), -32% for the SF Skykomish near Index (USGS ID: 12133000), and -33% for the Green near Auburn, for the 2080s relative to 1970-1999. However, our analysis indicates that the changes projected in this low-end simulation are really a consequence of a few apparently random spikes in rainfall in the early 1980s and in the middle of the 21st century. Apart from these spikes, the time series shows no appreciable trend in rainfall extremes. Random variability is present in all climate projections – including both the ACCESS and GFDL simulations. However, its influence is greater in the ACCESS simulation because of the small number of particularly large events in the record. For the GFDL simulation, in contrast, peak flows remain relatively consistent throughout the record, showing a gradual increase over time. Two interpretations are possible: (1) that these events reflect random variability which could occur at any time in the record, or (2) that these spikes accurately represent a decrease in peak flows over the course of the 21st century. In either case, a small number of anomalously large storm events are insufficient to obtain a robust estimate of the long-term trend. Additional model simulations would be needed to determine which interpretation is correct.

We present a separate analysis, showing that uncertainty in the estimates of extreme event statistics can be important. This is primarily a consequence of sample size, and is a challenge for both the observations and the model results. For example, our results suggest that for 60 years of observations (about the length of the Sea-Tac record), the uncertainty in the 100-year precipitation extreme is about ±10%. This means that changes in the 100-year storm that are smaller than 10% could potentially be masked by the noise in the observations. For the 30-year time periods used to evaluate projected changes, the uncertainties are greater. We present one approach, using a moving window, to begin account for this issue.

The Howard Hanson Dam on the Green river has significant capacity for retaining higher peak flows in its reservoir. We simulated reservoir operations at HHD using the model developed by USACE. Most projections suggest that the largest floods in the future are still within the dam's capacity to manage flows downstream. However, a few of the statistically downscaled climate projections indicate the potential for large floods that exceed the capacity of the reservoir to mitigate peak flows downstream. As above, it is not clear if these represent an accurate projection of future peak flows or if they are a result of random variability. Furthermore, the method used to produce these older projections (statistical downscaling) may not accurately represent changes in heavy rain events. The best way to test these results would be to develop additional regional climate model simulations, allowing for a better characterization of the mean and range among projections.

There are two priorities for future work: (1) Expand the number of regional climate model projections used to evaluate future peak flows. As noted above, it is not clear how to interpret some of the results of the current study. Additional regional climate model simulations would help with this interpretation by clarifying which trends are consistent among multiple models. (2) Expand the streamflow modeling to include other King County rivers (e.g., Cedar, White). The Cedar River watershed is warmer than either the Snoqualmie or Green watersheds, while the White River watershed is colder. As a result, changes in peak flows for these basins will likely be different than those estimated for the Green and Snohomish rivers; these differences have important implications for flood risk management. In addition, reservoir operations on the South Fork Tolt River (a tributary to the Snoqualmie) can only be simulated in tandem with reservoir operations on the Cedar River, since the two reservoirs are managed in coordination with one another.

Beyond these two near-term efforts, there are many possibilities for using the existing results to further quantify impacts. One possibility would be to develop future flood maps by modeling changes in the extent and depth of flooding. A current pilot in Snohomish County serves as a proof-of principle for developing future flood maps that cover an entire county. The approach could be translated to King County and applied using the new streamflow projections described in this report.

2 Background & Motivation

Climate projections indicate an increase in flooding in many Pacific Northwest watersheds over the course of the 21st century, a result of both decreasing snowpack and more intense heavy rain events (e.g., Salathé et al. 2014). Flooding poses significant threats to public health and safety, transportation corridors and economic activities throughout King County. Flooding affects residents throughout King County; the County has experienced 12 federally declared flood disasters since 1990, and tens of thousands of county residents commute through, live, and work in floodplains. Assessments of projected changes in magnitude and timing of river flows have been conducted at multiple scales, ranging from the entire Pacific Northwest, the Puget Sound basin, and specific watersheds. Historical trends (e.g., Mass et al. 2011) and climate projections (e.g., Salathé et al. 2014) suggest that climate change will lead to more intense heavy precipitation and consequently larger flood events in western Washington, especially in fall and early winter.

This document summarizes the methods and results of a study aimed at developing new estimates of the impacts of climate change on flooding in the Snohomish and Green rivers (Figure 2.1). The specific objective of this work was to develop new projections of flooding for King County. To aid in interpretation, we also performed a separate analysis to quantify the uncertainty in estimates of extreme precipitation.

Past work has emphasized the need for dynamically-based – as opposed to statistically-based – methods for "downscaling" coarse-scale global model projections to scales that can capture the interactions of weather systems with the complex terrain of the Pacific Northwest (e.g., Salathé et al. 2014). Our study used new dynamically-downscaled projections developed under a parallel effort that was also funded by King County. For comparison, we also included results from a statistically downscaled set of climate projections.

Recent advances in computing power have also made it more feasible to implement fine-scale hydrologic models. In this study we employed a fine-scale hydrologic model to develop a more detailed characterization of the hydrology in each watershed. On the Green River, we used a reservoir model to characterize the impact of climate change on regulated flows. Finally, we evaluated changes in peak flows in terms of changes in both the magnitude and frequency of peak flow events.

3 Data

Observed Streamflow

Observed flows were used for calibration and validation of the hydrologic model, as well as to bias-correct the model streamflow estimates. Since the hydrologic model used in this study does not include reservoir management, an adjusted set of “naturalized” flows was obtained for the Green River.

We obtained daily mean streamflow observations from USGS sites where effects of reservoir management on streamflow are minimal or non-existent (Table 3.1 and Figure 3.1). The U.S Army Corps of Engineers (USACE) provided historical naturalized (unregulated) streamflow estimates for sites downstream of Howard Hanson Dam (i.e. the Green River at Howard Hanson Dam and the Green River near Auburn). The sites with more than 30 years of overlap between observed and simulated flows were used for the final streamflow bias-correction.

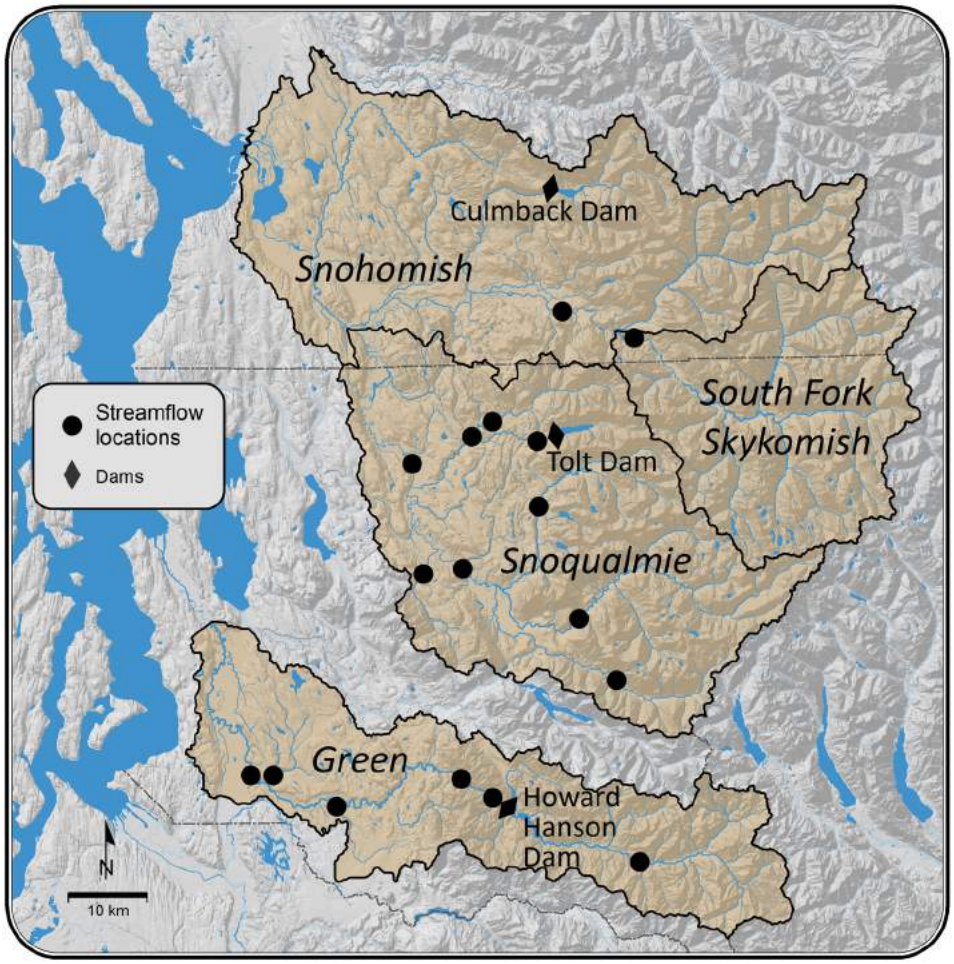

Figure 3.1. Streamflow locations for the Green, Snoqualmie, and SF Skykomish basins. Only sites with at least 30 years of observations are included in the map.

Site Name	USGS ID	Water Years	Nat. Flows
Snohomish River basin			
SF Snoqualmie R. AB Alice Creek near Garcia	12143400	1961-1989, 1991-2015	USGS
MF Snoqualmie near Tanner	12141300	1962-1991, 1993-2015	USGS
NF Snoqualmie near Snoqualmie Falls	12142000	1962-1989, 1991-2015	USGS
Snoqualmie near Snoqualmie	12144500	1959-2015	USGS
Raging R. near Fall City	12145500	1975-2015	USGS
NF Tolt R. near Carnation	12147500	1953-1963, 1969-2015	USGS
SF Tolt R. near Carnation	12148000	1970-2015	n/a
Tolt R. near Carnation	12148500	1939-2015	n/a
Mainstem Snoqualmie near Carnation	12149000	1929-2015	n/a
SF Skykomish R. near Index	12133000	1902-1982	USGS
Skykomish River near Gold Bar	12134500	1928-2015	USGS
Green River basin			
Green River near Lester	12104500	1945-1990, 1993	USGS
Green River at Howard A. Hanson Dam (HHD)	--------	1963-2002	USACE
Green R. at Purification Plant near Palmer	12106700	1963-2015	USGS
Newaukum Creek near Black Diamond	12108500	1944-2015	USGS
Big Soos Creek above Hatchery near Auburn	12112600	1960-2018	USGS
Green R. near Auburn	12113000	1963-2001	USACE

Table 3.1. Streamflow sites used in this study. The table lists the water years (Oct-Sep) of quality-controlled observations, along with the source of naturalized flow data. Naturalized flows were not obtained for the three sites listed as “n/a”: flows at these sites are affected by the SF Tolt Reservoir.

Observed and Simulated Climate

This section describes the “downscaled” climate projections used in the current study. Downscaling refers to the approaches used to relate large-scale changes in climate, obtained from coarse-scale global climate model (GCM) simulations, to the local-scale changes that are relevant to planning and needed to drive hydrologic model simulations. Global climate models are typically much too coarse to be used directly to assess climate change impacts, with scales ranging from 50 to 200 km between grid cells. GCM projections are typically downscaled one of two ways: “statistically”, via empirical relationships with surface weather observations; or “dynamically”, via a regional climate model. As noted previously, recent research has emphasized the need to use regional

climate model projections (or "dynamical downscaling") in order to better quantify changes in extreme precipitation (e.g., Salathé et al. 2014).

GCM projections were obtained from the Climate Model Inter-comparison Project, phase 5 (CMIP5; Taylor et al., 2012). As part of the CMIP5 project, international modeling groups coordinate to create a set of consistent future simulations, driven by predetermined greenhouse gas scenarios ("Representative Concentration Pathways", or RCPs, van Vuuren et al. 2011; a more detailed discussion of greenhouse gas scenarios is included in Mauger et al. 2018). In this study we use RCPs 4.5 and 8.5, representing a low- and high-end greenhouse gas scenario, respectively. The RCP 2.6 scenario (lower than RCP 4.5) is not used because recent research suggests it is not achievable (e.g., Davis and Socolow 2014). Current research does not suggest that either the RCP 4.5 or RCP 8.5 scenario is more likely than the other.

The primary objective of this study was to estimate changes in peak flows using two new dynamically downscaled projections. Although it would be preferable to evaluate more than two projections, dynamical downscaling remains expensive to implement and only two simulations could be completed with the time and resources available. Mauger et al. (2018) provide a detailed description of the methods and results of the new projections;

Downscaling Method	***Dataset***	***Global Model***	***Resolution***	***Historical***	***Low Emissions (RCP 4.5)***	***High Emissions (RCP 8.5)***
Dynamical	WRF	GFDL	12 km	1970-2005	--	2006-2099
	WRF	ACCESS		1970-2005	2006-2099	--
	RegCPDN	HadAM3	25 km	1986-2015	--	2031-2060
Historical	bcLivneh	n/a *(obs.-based)*	1/16° (~5×7 km)	1950-2013	--	--
Statistical	bcMACA	bcc-csm1-1-m		1950-2005	2006-2099	2006-2099
	bcMACA	CanESM2		1950-2005	2006-2099	2006-2099
	bcMACA	CCSM4		1950-2005	2006-2099	2006-2099
	bcMACA	CNRM-CM5		1950-2005	2006-2099	2006-2099
	bcMACA	CSIRO-Mk3-6-0		1950-2005	2006-2099	2006-2099
	bcMACA	HadGEM2-CC		1950-2005	2006-2099	2006-2099
	bcMACA	HadGEM2-ES		1950-2005	2006-2099	2006-2099
	bcMACA	IPSL-CM5A-MR		1950-2005	2006-2099	2006-2099
	bcMACA	MIROC5		1950-2005	2006-2099	2006-2099
	bcMACA	NorESM1-M		1950-2005	2006-2099	2006-2099

Table 3.2. Gridded climate datasets used in this study.

here we provide a brief summary. Global climate models were evaluated for their ability to accurately represent the historical climate and storm characteristics in the Pacific Northwest. The best models were then ranked, and two GCM-scenario pairs were chosen to bracket the range from low- to high-end future changes in precipitation extremes. The ACCESS 1.0 model, forced by the RCP 4.5 greenhouse gas scenario, was chosen to represent the low end. For the high-end projection, we used the GFDL CM3, model, forced by the RCP 8.5 greenhouse gas scenario. We refer to these as the "Low-Low" and "High-High" scenarios, respectively. As with the model selection, the choice of greenhouse gas scenario is discussed in more depth in Mauger et al. (2018). Regional climate model simulations were performed using the Weather Research and Forecasting model (WRF, Skamarock et al. 2005), which has been optimized to accurately represent the climate of the Pacific Northwest. The WRF model is run at a resolution of 12 km.

As a complement to the dynamically downscaled projections, and because a much larger number of projections were available, we also used an adjusted version of the statistically downscaled Multivariate Adaptive Constructed Analogs (MACA, Abatzoglou and Brown et al. 2012) dataset, including the observationally-based Livneh dataset (Livneh et al. 2013) that is the basis of the downscaling. MACA is a statistical downscaling approach that works by identifying analogs in the observed record and using these to downscale from the large-scale GCM fields to the local variations that are present in the observations (in this case, the Livneh dataset). Recent work has shown that the Livneh et al. dataset has significant biases resulting from an erroneous assumption of a constant temperature lapse rate (the rate of temperature change with elevation). Although this approximation affects the results in a number of ways, the primary issue of concern was the resulting cold bias at high elevations, which affects the model estimates of snow accumulation and melt. Both the Livneh and MACA data were therefore adjusted via comparison with the 1950-2011 climatology from the Parameter Regression on Independent Slopes Model (PRISM; Daly et al. 2004, 2008). The corrected datasets are referred to as "bcMACA" and "bcLivneh," respectively (Mauger et al. 2016).

Finally, we used an additional set of dynamically downscaled projections to evaluate the uncertainty in extreme precipitation estimates. These stem from the Regional Climate Prediction (dot) Net (CPDN) experiment, termed "RegCPDN" in this analysis, and are described in depth in the following section.

The datasets used in this study are listed in Table 3.2. Figure 3.2 compares the grid spacing for each set of regional climate model simulations, as well as for the hydrologic model used in this study.

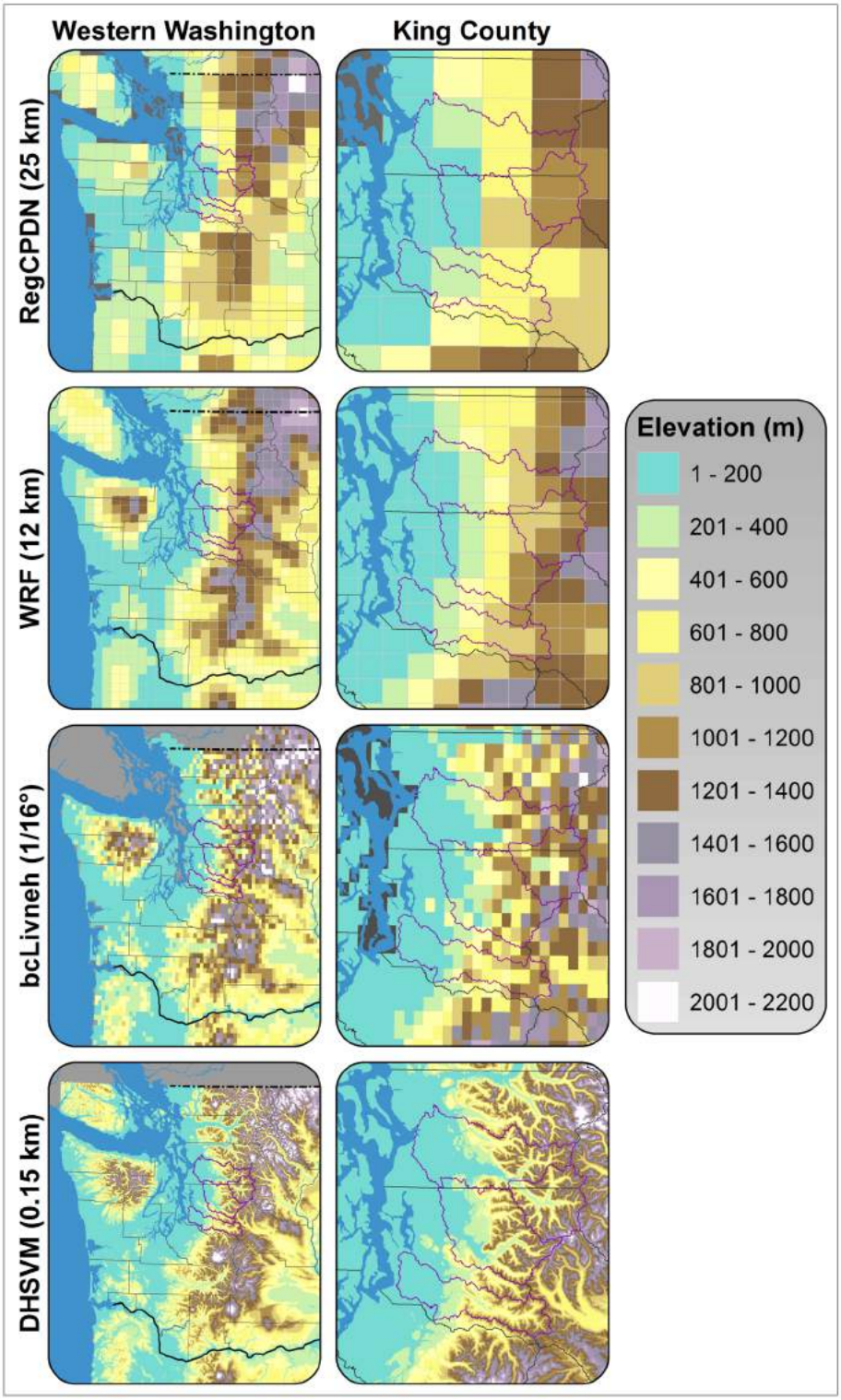

Figure 3.2 Resolution of the RegCPDN (25 km), WRF (12 km), and bcMACA/bcLivneh (1/16°, ~5×7 km) climate datasets (top, 2nd, and 3rd rows, respectively), compared to the hydrologic model topography (0.15 km, bottom panel). Results are shown for both western Washington (left) and King County (right). The Green, Snoqualmie, and SF Skykomish river basins are outlined in each map, and the shading denotes elevation.

Quantifying the Uncertainty in Extreme Precipitation Statistics

Description of the RegCPDN dataset

We used the RegCPDN set of dynamically downscaled projections to evaluate the uncertainty in extreme precipitation estimates. These were not used as input to the hydrologic modeling. Instead, this work was intended to complement the remainder of the study by quantifying the uncertainty in extreme statistics (e.g., 100-year event) given that extreme statistics are often estimated from a limited sample size.

Termed Climate Prediction (dot) Net (CPDN), this dataset stems from simulations produced with volunteered computer time. The result is a “superensemble”, in which numerous independent simulations are produced for each year, all with slightly perturbed initial conditions (Mote et al. 2016). We refer to this dataset as “RegCPDN”, since it stems from the regional climate model simulations being produced by the CPDN project.

At the global scale, the RegCPDN simulations are driven by the atmospheric portion of the global Hadley Centre Coupled Model, version 3 (HadAM3), implemented at a horizontal resolution of 1.25° latitude by 1.875° longitude. This global model information is then regionally downscaled by the Hadley Centre Regional Climate Model, version 3P (HadRM3P), which is run at a horizontal resolution of 25 km. For RegCPDN, the model is run in an atmosphere-only mode (HadAM3), which means that it takes boundary conditions (e.g., sea surface temperature) from a previous simulation of the coupled HadCM3 GCM that simulates the interactions between the atmosphere, land, and ocean.

Each simulation year is completed by a volunteer by downloading and running a year-long simulation on their personal computer. The results are then uploaded to a master database for use in climate studies such as this one. This process allows for the resources necessary for creating a large ensemble of high resolution climate simulations. More details on the RegCPDN model and approach can be found in Mote et al. (2016).

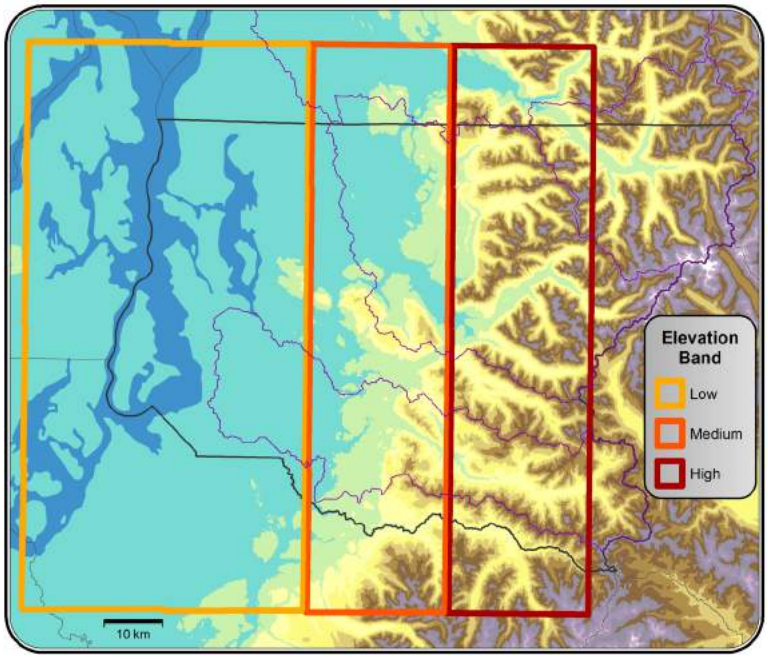

Figure 3.3. Elevation bands used for averaging the RegCPDN results. Calculations were applied separately for each elevation band.

The RegCPDN experiment that we are using includes two 29 water year simulations:

one for 1986-2015 (historical) and another for 2031-2060 (future). Each water year is simulated separately, with one month of spin-up prior to the start of the water year (since these are atmosphere-only simulations, one month is sufficient for spin-up). The future simulation is driven by the RCP 8.5 scenario. Although changes might be more pronounced later in the 21st century, the model was only run for one 30-year period in the future. The implications of this choice are discussed in the following section.

The effects of climate change, including the simulated changes in extreme precipitation, are likely to be more pronounced at the end of the 21st century, rather than for 2031-2060. However, no such simulations are available for RegCPDN. The time period was chosen to be representative of projected changes for the 2040s, for application to a wide range of near-term climate adaptation planning purposes. In addition, a primary reason to look at more distant projections is to maximize the "signal" of changing precipitation extremes, relative to the "noise" of natural variability. With RegCPDN, this is less important: the large sample size allows us to average out natural variability thus making it easier to isolate and detect the effects of climate change.

For both the historical and future simulations, each year is simulated 100 times with slightly modified initial conditions. The result is a dataset that includes 2900 years each for the historical and future time periods. Given the large sample size, we use these to quantify the uncertainty in precipitation extremes statistics.

Quantifying the Uncertainty in Extremes

In this analysis we focus on the RegCPDN results over King County (see RegCPDN grid in Figure 3.2). Since precipitation changes significantly with elevation, results were averaged over three north-south bands that roughly correspond to elevation, based on the 25 km RegCPDN grid (Figure 3.3). We analyzed precipitation extremes separately for each elevation band.

Extreme statistics were calculated for the 2-, 10-, 25-, 100-, and 500-year return frequencies in daily precipitation (corresponding to the (50%, 10%, 4%, 1%, and 0.2% annual chance of exceedance). We took the typical block maximum approach, in our case taking the maximum daily precipitation for each water year (Oct-Sep) in the simulations. As with flood statistics (discussed below), we used the Generalized Extreme Value (GEV) distribution with L-moments to estimate the extreme statistics, following the same methodology described in Salathé et al. (2014) and Tohver et al. (2014).

We used a Monte Carlo approach to estimate the probability distribution of each statistic. Specifically, we resampled from the 2900 simulations in each time period, with replacement, to create 10,000 estimates of each statistic. A critical sampling detail is that each year in the simulations (e.g., 1993, 2047) is given the same pattern of sea surface temperatures. In order to control for the effect of sea surface temperatures we needed to sample uniformly from all years in each time period. Our sampling procedure was as follows:

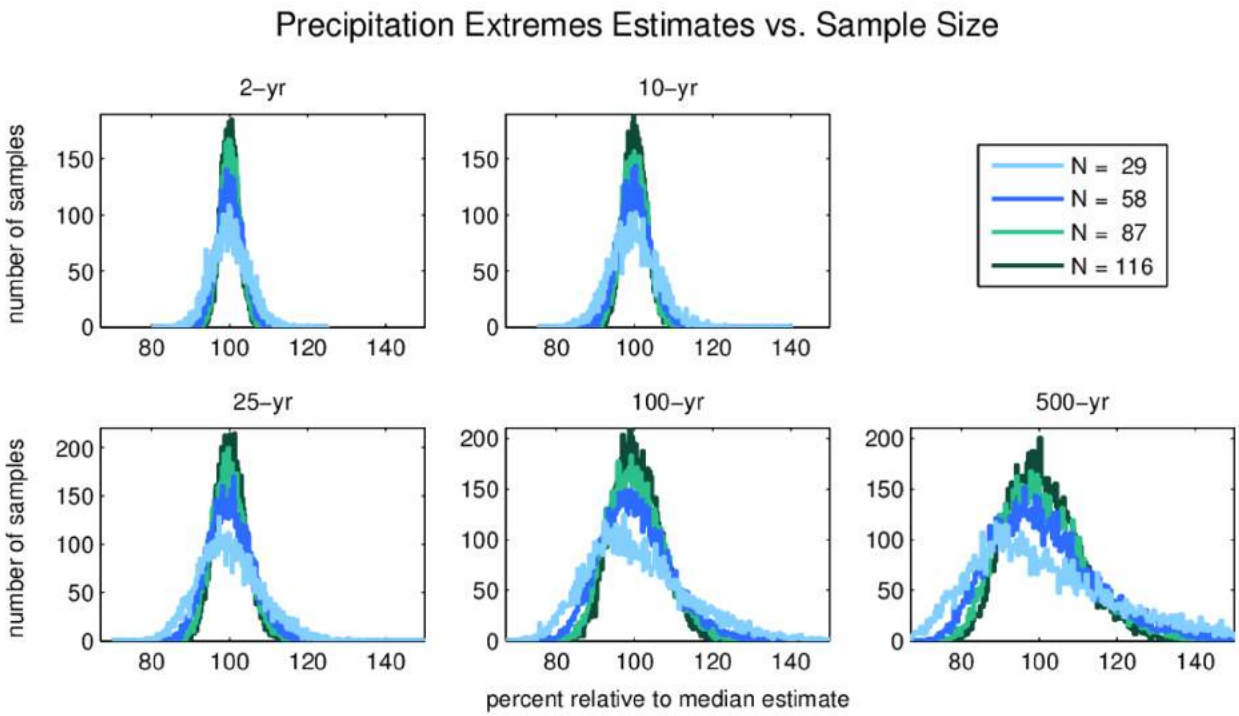

Figure 3.4. Probability distributions of daily precipitation extremes for the historical (1986-2015) average over the low elevation areas in King County (Figure 4.2). Results are shown for five return intervals: the 2-, 10-, 25-, 100-, and 500-year extremes. In each plot, four distributions are shown: one each for the Monte Carlo results corresponding to sample sizes of 29, 58, 87, and 116 years. In order to allow side-by-side comparisons, results are expressed relative to the median estimate for the 116-year samples, and the x-axis limits are the same across all five plots.

- For each year, randomly select N years from its 100-member ensemble,
- Repeat for all 29 years,
- Combine all of the selections (sample size = 29 × N) and compute extreme statistics.

This process was then repeated 10,000 times to obtain a probability distribution for each extreme statistic. We repeated the process for four separate sample sizes of: 29, 58, 87, and 116 years (corresponding to N=1, 2, 3, and 4). These were selected to roughly span the range of observed precipitation and streamflow records, so that our results might provide insight on the likely uncertainties in extremes estimates obtained from observations.

Results from the historical simulation, for the high elevation band (Figure 3.3), are shown in Figure 3.4 and summarized in Table 3.3. Precipitation statistics are expressed as a percent of the median estimate obtained from the largest sample size used (N=116 years). Although the precipitation totals were different for each elevation band, the percent ranges were nearly identical when evaluated relative to the median estimate for

each return interval. This means that the results presented here apply to precipitation at all elevations in King County.

Return Period	Sample Size	Percent Relative to Median		
		Std-Dev	66% Range	95% Range
2-yr	N=29	5%	96-105%	91-110%
2-yr	N=58	3%	97-103%	93-107%
2-yr	N=87	3%	97-103%	95-105%
2-yr	N=116	2%	98-102%	96-105%
10-yr	N=29	6%	95-106%	89-112%
10-yr	N=58	4%	96-104%	92-108%
10-yr	N=87	3%	97-103%	94-107%
10-yr	N=116	3%	97-103%	95-106%
25-yr	N=29	8%	93-107%	86-116%
25-yr	N=58	5%	95-105%	90-111%
25-yr	N=87	4%	96-104%	92-109%
25-yr	N=116	4%	96-104%	93-107%
100-yr	N=29	12%	90-112%	81-127%
100-yr	N=58	8%	93-108%	86-118%
100-yr	N=87	7%	94-107%	88-114%
100-yr	N=116	6%	95-106%	90-112%
500-yr	N=29	18%	86-119%	75-145%
500-yr	N=58	12%	90-112%	81-128%
500-yr	N=87	10%	92-110%	84-122%
500-yr	N=116	8%	93-108%	86-118%

Table 3.3. Summary of the distributions shown in Figure 3.4. Range among daily precipitation extremes for the historical (1986-2015) average over the low elevation areas in King County. Results are expressed as a percent of the median estimate, based on the N=116 sample size, for each return interval. The 66% range gives the difference between the 17th and 83rd percentiles, while the 95% range gives the difference between the 2.5th and 97.5th percentile in each distribution. Results are nearly identical for other elevation bands.

A number of observations that can be made from these results. First, it is important to note that the uncertainties quantified here stem primarily from natural variability. Since we are estimating the magnitudes of rare events, random fluctuations in weather and climate patterns can result in short term periods that differ substantially in the magnitude of large events. Second, there are appreciable uncertainties for all return intervals and all sample sizes. Not surprisingly, the uncertainty decreases with increasing sample size. However, even with a sample size of 116 years, the 95% confidence limits can deviate from the median estimate by up to 5% for the 2-year event and over 20% for the 500-year event. Finally, the median estimates are remarkably constant regardless of sample size. This confirms that a GEV fit with L-moments provides an unbiased estimate of the extreme statistics. For all but the 29-year sample size, the distributions are nearly symmetric, indicating that the sampling is sufficient to produce an unbiased GEV fit. For the 29-year sample size, however, the effect of sampling is apparent in the skewness of the distribution, particularly for the larger events. This is simply a reflection of the fact that not every 29-year sample will include a 100-year or 500-year event (or, more specifically, an event large enough to sufficiently

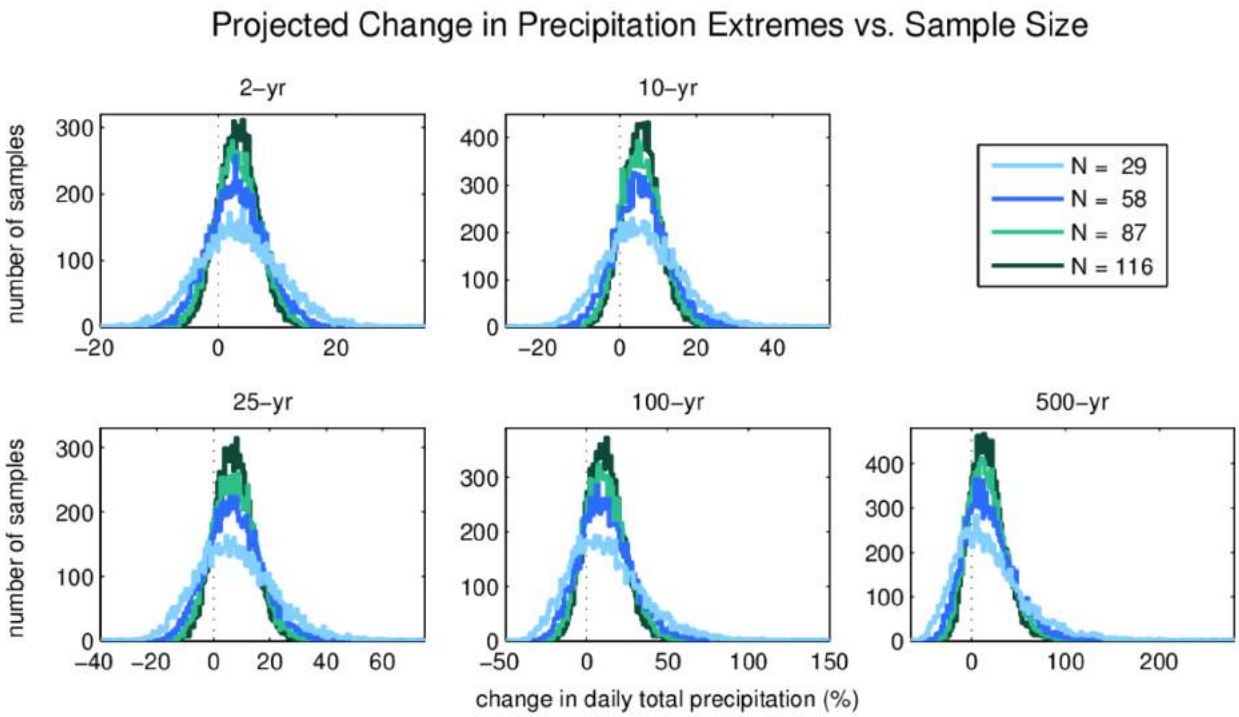

Figure 3.5. Probability distributions of daily precipitation extremes for the historical (1986-2015) average over the low elevation areas in King County (Figure 4.2). Results are shown for five return intervals: the 2-, 10-, 25-, 100-, and 500-year extremes. In each plot, four distributions are shown: one each for the Monte Carlo results corresponding to sample sizes of 29, 58, 87, and 116 years. In order to allow side-by-side comparisons, results are expressed relative to the median estimate for the 116-year samples, and the x-axis limits are the same across all five plots.

constrain the fit for extremes of these magnitudes). The results for the 29-year samples are particularly relevant to the current analysis, since the historical and future flood frequency statistics presented later in this report were calculated from a 30-yr record.

The particularly large uncertainties for the 500-year event suggests that these estimates should be treated with caution. For example, although the median estimates are not shown here, the median estimate for the 500-year event is only about 12% higher than the median estimate for the 100-year event. This means that the 100-year event is well within the uncertainty range of the 500-year estimate, suggesting a very large difference in impacts between the low and high end of the 500-year uncertainty range.

Of course, another reason for caution is that the statistics of extreme precipitation will not remain stationary. The RegCPDN simulations are particularly well suited to this question, allowing us to quantify the uncertainty in the projected changes for each return interval (Figure 3.5 and Table 3.4). The projections are roughly consistent with those reported in the companion report by Mauger et al. (2018). As noted above, by considering the average or median values among a large sample, the influence of natural variability can be minimized. The near-perfect correspondence of the median change estimates for all

Return Period	Sample Size	Median	Std-Dev	66% Range	95% Range
2-yr	**N=29**	**+5%**	**+7%**	**-1 to +12%**	**-8 to +21%**
2-yr	N=58	+5%	+5%	+0 to +10%	-4 to +16%
2-yr	N=87	+5%	+4%	+1 to +9%	-2 to +14%
2-yr	N=116	+5%	+4%	+2 to +9%	-2 to +12%
10-yr	**N=29**	**+6%**	**+9%**	**-2 to +14%**	**-10 to +24%**
10-yr	N=58	+6%	+6%	+0 to +12%	-5 to +18%
10-yr	N=87	+6%	+5%	+1 to +11%	-3 to +16%
10-yr	N=116	+6%	+4%	+2 to +10%	-2 to +14%
25-yr	**N=29**	**+6%**	**+11%**	**-4 to +17%**	**-13 to +31%**
25-yr	N=58	+6%	+8%	-1 to +14%	-8 to +23%
25-yr	N=87	+6%	+6%	+0 to +13%	-6 to +20%
25-yr	N=116	+6%	+6%	+1 to +11%	-4 to +18%
100-yr	**N=29**	**+6%**	**+18%**	**-9 to +24%**	**-22 to +47%**
100-yr	N=58	+6%	+12%	-4 to +19%	-15 to +33%
100-yr	N=87	+7%	+10%	-3 to +16%	-11 to +28%
100-yr	N=116	+6%	+8%	-1 to +15%	-9 to +25%
500-yr	**N=29**	**+6%**	**+27%**	**-15 to +34%**	**-33 to +72%**
500-yr	N=58	+7%	+18%	-9 to +26%	-23 to +48%
500-yr	N=87	+7%	+15%	-6 to +22%	-18 to +39%
500-yr	N=116	+7%	+12%	-4 to +19%	-14 to +34%

Table 3.4. Summary of the distributions shown in Figure 3.5. Projected change in daily precipitation extremes for 2031-2060 relative to 1986-2015 for a high (RCP 8.5) greenhouse gas scenario. Results are nearly identical for other elevation bands.

but the 500-year event confirm this: if natural variability were affecting the median estimates, then these would be less uniform. This means that the RegCPDN results can be used to consider changes in precipitation extremes in spite of the fact that changes by 2031-2060 will be small compared to the changes projected for the end of the century.

The uncertainties in Figure 3.5 and Table 3.4 provide information on the detectability of these changes in the absence of a superensemble, where the smaller sample size does mean that natural variability can limit the accuracy of change estimates. In practice, changes are rarely assessed using sample sizes larger than 30 years, so for convenience these rows are highlighted in Table 3.4. The results show that, regardless of return interval or sample size, the 95% confidence bounds include both negative and positive projections. It is possible that greater confidence could be gained by considering changes later in the century. However, in general these results suggest that changes estimated by comparing extremes estimates from two 30-year samples may not be sufficient to isolate the projected change from the confounding influence of natural variability.

Overall, these results show that there are appreciable uncertainties in the estimates of extremes events from limited samples, but that these uncertainties are relatively small for all but the 100- and 500-year events. More importantly, we find significant uncertainty in the projected change when comparing historical and future extremes estimates. Since this is a consequence of natural variability, it implies that the issue could be addressed with improved sampling. Although there is some improvement in the range with sample size, this may not be sufficient to constrain projections. Instead, a more fruitful approach may be to apply the same Monte Carlo sampling used in the current analysis to a smaller number of years available in each projection. For example, extremes could be estimated by resampling 20-year records from a 30-year time period and re-computing the extreme statistics for each random subsample. As in the current analysis, this could provide a more robust median estimate of extremes than could be obtained from a single estimate based on the entire 30-year record.

Developing Meteorological Forcings for the Hydrologic Model

Six variables in 3-hour time steps are required to run the hydrologic model used in this study: temperature (°C), relative humidity (%), precipitation (m), wind speed (m/s), incoming shortwave radiation (W/m^2), and incoming longwave radiation (W/m^2). In the past, the most common approach to developing meteorological forcings was to develop statistically downscaled projections of daily temperature and precipitation, simply interpolate winds from coarse-scale GCM simulations, temporally disaggregate from daily to a 3-hour time step, and apply the MtClim (Thornton and Running 1999, Bohn et al. 2013) empirical formulations to estimate humidity and radiation.

Previous studies have established that dynamically downscaled projections provide an improved representation of precipitation extremes, a key driver of flood events. Based on these findings, we use dynamically downscaled projections ("**MtClim-WRF**" in Figure 3.6) and compare those with statistically downscaled projections ("**bcMACA**" in Figure 3.6). Although recent work has emphasized the need to use dynamical downscaling in order to accurately characterize changes in precipitation extremes, we include the statistically-downscaled projections both to provide context for the new WRF projections, and because the bcMACA projections include a much larger ensemble of models and scenarios.

We also explore ways of improving simulations by replacing interpolated GCM winds with those simulated by WRF, and evaluating the benefits of using WRF-simulated estimates of humidity and radiation ("**Direct-WRF**" in Figure 3.6). WRF-simulated estimates of humidity and radiation are tested by including them alongside results that are based on the empirical MtClim estimates. Although the effect on hydrology is likely small, WRF-simulated winds are undoubtedly better than those interpolated from GCMs; we do not perform any additional tests to confirm this.

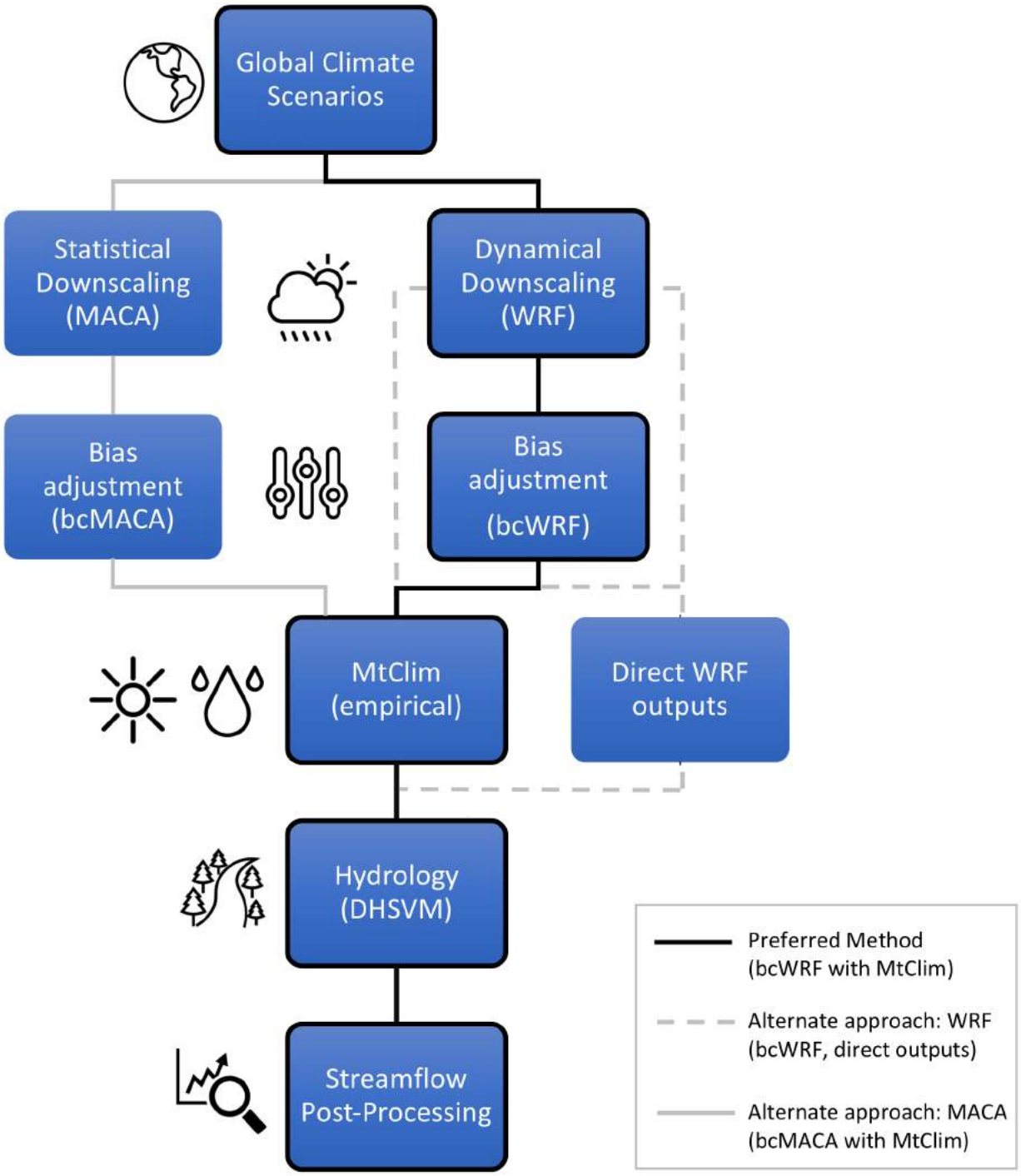

Figure 3.6. Diagram illustrating the process used to develop future streamflow simulations. As described in the text, we tested several approaches to developing meteorological forcings for the hydrologic model, and selected a preferred approach based on the results. The preferred approach is highlighted with the thick black lines, and is described in the text.

Figure 3.6 illustrates the three different ways that the forcings were produced:

1. Using all six variables directly from the WRF outputs ("**Direct-WRF**"),
2. Using direct WRF estimates of daily temperature, precipitation, and winds but using the MtClim empirical formulations to estimate humidity and radiation ("**MtClim-WRF**"), and
3. Using the statistically-downscaled bcMACA projections for temperature, precipitation, and winds, but using the MtClim empirical formulations to estimate humidity and radiation ("**bcMACA**"). These runs are included for comparison with the newer dynamically-downscaled projections.

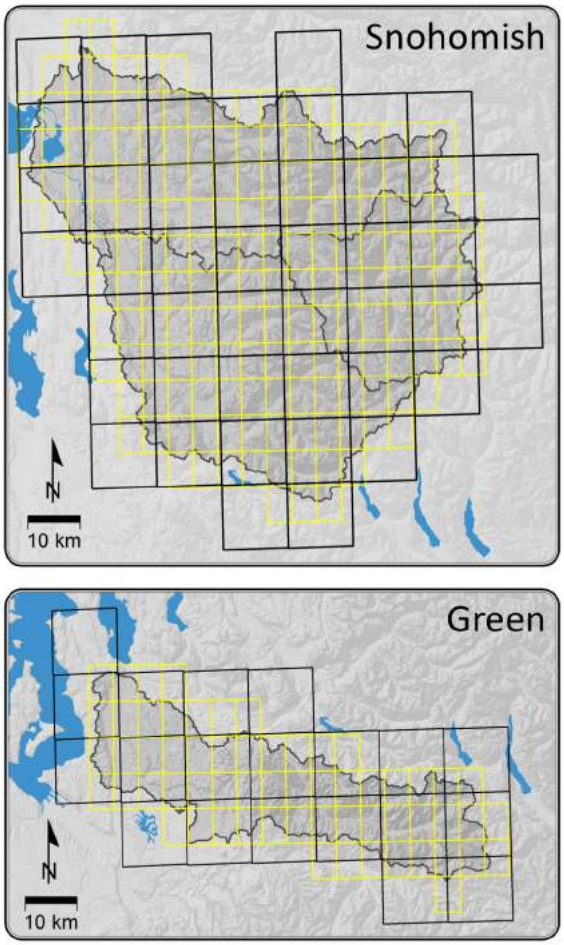

Figure 3.7. Grid cell boundaries for the two meteorological input grids: 1/16-degree (about 5 × 7 km) in yellow, and 12 km in black. The DHSVM input locations are at the center of each grid cell.

The Variable Infiltration Capacity (VIC) hydrologic model (Liang et al. 1994), which includes MtClim, was used as a pre-processing step to temporally disaggregate the daily bcMACA data to a three-hourly time step and develop the empirical estimates of humidity and radiation. For MtClim-WRF, VIC was also used to develop empirical estimates of humidity and radiation after bi-linearly interpolating to the VIC resolution (in both cases, the VIC pre-processor was implemented at a resolution of 1/16-degree). For Direct-WRF, humidity and radiation were extracted directly from the raw WRF outputs and the native resolution of 12 km was maintained. Figure 3.7 shows the resolution of the 12 km and 1/16-degree grids over the Green, Snoqualmie, and SF Skykomish rivers.

4 Models

This study used a fine-scale hydrologic model, the Distributed Hydrologic Soil Vegetation Model (DHSVM), to produce historical and future streamflows at sites in the Snohomish and Green Rivers (Table 3.1, Figure 3.1). The reservoir model for the Green River was obtained from the U.S. Army Corps of Engineers (USACE), and used to simulate the impacts of climate change on regulated flows. This section briefly describes the configuration and inputs for the hydrologic model and the reservoir model for the Green River.

Hydrologic Model

The DHSVM model **(**Wigmosta et al. 1994) is a physically-based, spatially-distributed hydrological model that explicitly solves the water and energy balance at each grid cell. The model requires spatially distributed land surface characteristics such as surface topography, vegetation cover, soil type and depth, stream network and digital elevation data. The model forcings are time-series of meteorological variables such as precipitation, temperature, wind speed, relative humidity and incoming shortwave and longwave radiation at a sub-daily time step (typically 1 to 3 hours). The model contains two unsaturated soil layers and a saturated bottom layer (see Figure 4.1). Subsurface flow in the saturated zone is based on a quasi-equilibrium approach described by Wigmosta and Lettenmaier (1999) and also includes an energy balance snow accumulation and ablation algorithm (Andreadis et al. 2009), which represents the interaction of snow with forest canopies. Stream channel routing is performed using a storage accounting scheme,

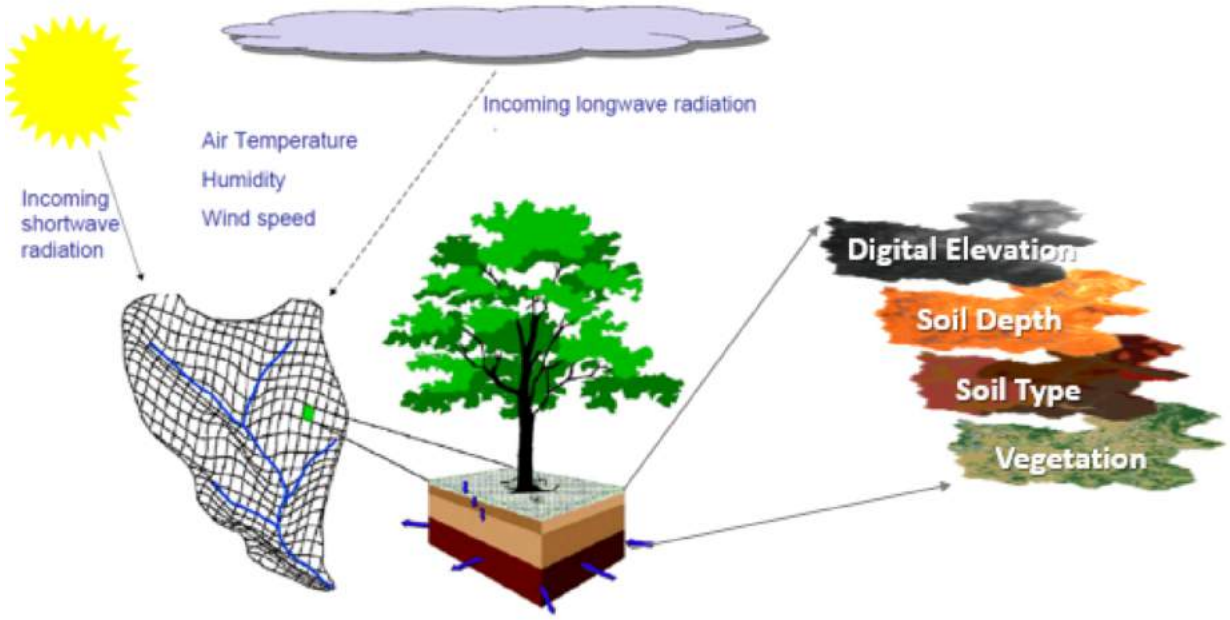

Figure 4.1 Diagram of DHSVM model and its inputs.

which is capable of producing hydrographs at any location along the channel network represented by the digital topography. Typical spatial resolution of DHSVM implementations ranges from about 10 m to 200 m. DHSVM has been widely applied in the mountainous western United States (e.g., Storck et al., 1998, Bowling and Lettenmaier, 2001; Whitaker et al., 2003) and for assessing the impacts of climate change (e.g., Elsner et al. 2010, Vano et al. 2010, Cuo et al. 2011, Cristea et al. 2014, Naz et al. 2014) and land use (e.g., Sun et al. 2013, Cuo et al. 2009, 2011) on streamflow.

For this study we implemented DHSVM for the Green and Snohomish basins (including the Snoqualmie and SF Skykomish basins) at 150 m spatial resolution with a 3-hour time step. With its finer spatial resolution of 150 m, the model can capture some of the local scale differences in topography, soils, and vegetation that make up the many tributaries of interest in the Green and Snoqualmie/Snohomish rivers.

Geospatial Inputs

The DHSVM requires spatial inputs that are managed in ArcGIS, primarily as raster files. The spatial inputs such as elevation, watershed, land cover, soil type, soil depth, and stream network are described in this section.

Digital Elevation Model (DEM)

The digital elevation models were downloaded from the National Elevation Dataset at http://viewer.nationalmap.gov/basic/ (Elevation products, 3DEP). The DEM provides the base layer of spatial information and is used to generate soil depth, stream network and watershed boundaries using ArcGIS tools such as ArcGIS hydrology modeling tools and

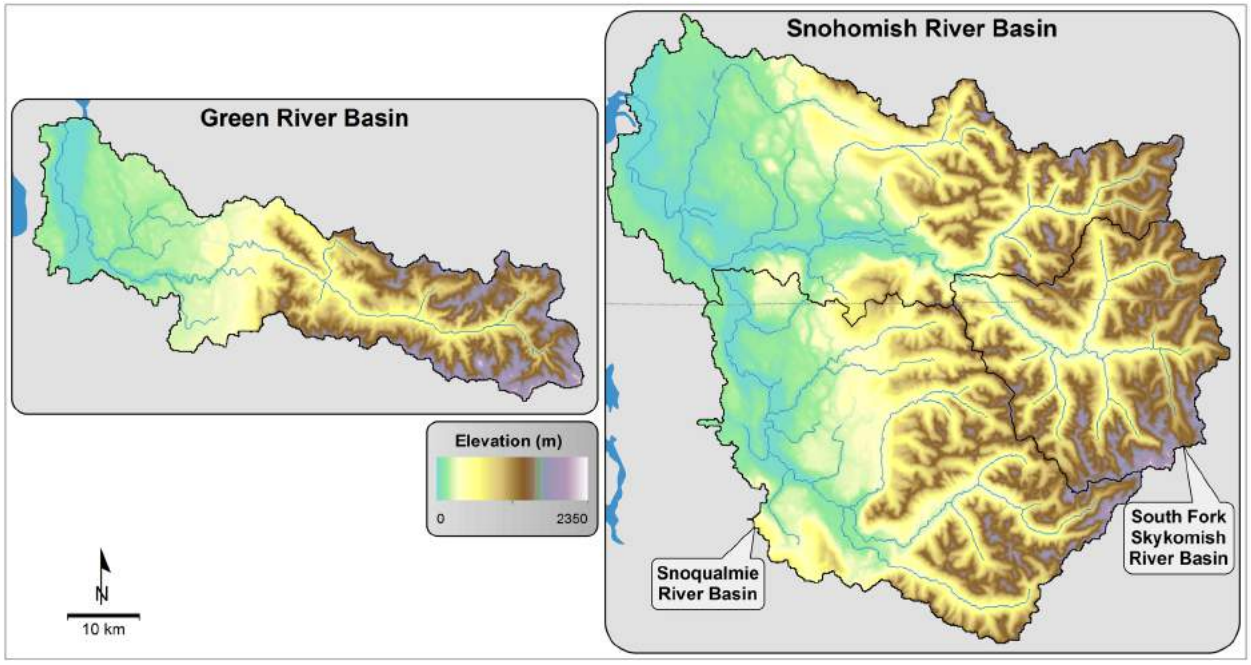

Figure 4.2. Digital Elevation Maps (DEMs) for the Green and Snoqualmie/Skykomish/Snohomish Basins.

Arc Macro Language scripts (Wigmosta et al. 2002). The stream network is used to route streamflow using flow direction relationships between upstream (higher elevation) and downstream (lower elevation) grid cells. Figure 4.2 shows DEM for the Green and Snoqualmie/Snohomish basins.

Land Cover

The land cover information was developed using the National Land Cover Database 2011 (NLCD 2011; Figure 4.3). This is the most recent national land cover product, with a 16-class land cover classification scheme applied at a spatial resolution of 30 meters based on circa 2011 Landsat satellite data and created by the Multi-Resolution Land Characteristics Consortium (Homer et al, 2015). For both basins, the upper basins are mainly covered by evergreen forest and the lower basins are highly developed (Figure 4.3).

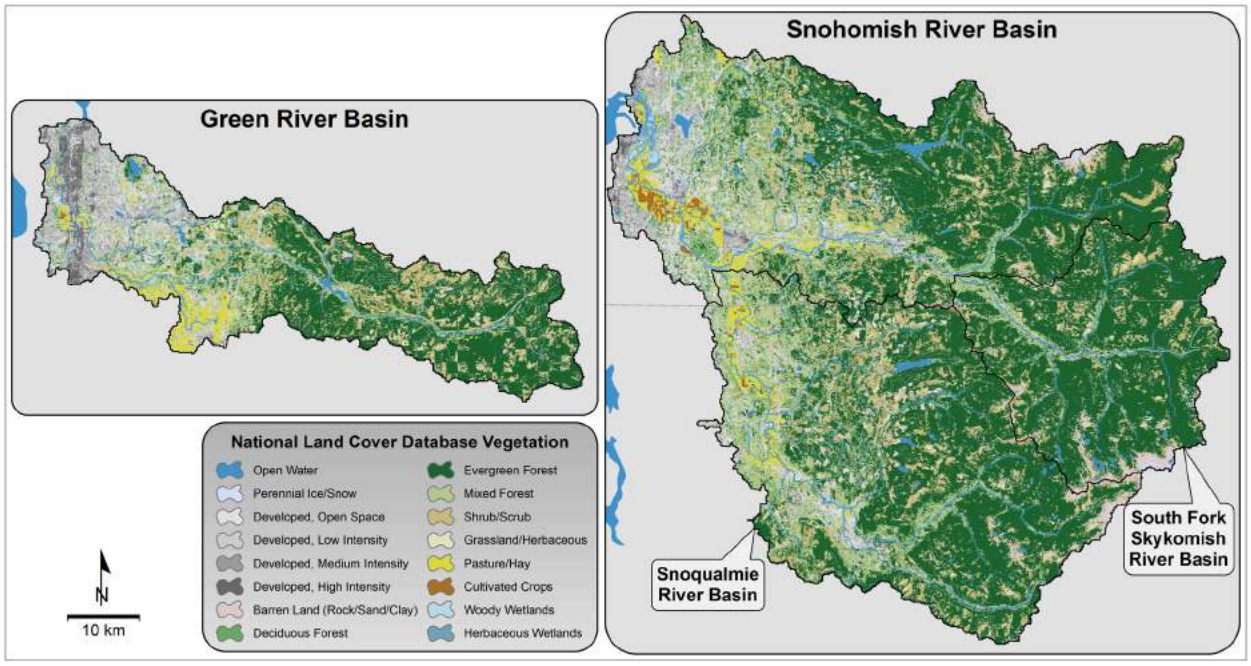

Figure 4.3. Land Cover classification (NLCD 2011) for the Green and Snoqualmie/Skykomish/Snohomish Basins.

Soils

The Digital General Soil Map of the United States, or STATSGO dataset (http://www.soilinfo.psu.edu/index.cgi?soil_data&statsgo) was developed for regional and national studies designed for broad planning and management uses requiring estimates of soil characteristics. The soil units are distributed as spatial and tabular datasets. The geospatial data maps soil units on a 1-kilometer resolution grid for the conterminous United States by weighting average soil values computed by aggregating soil layers. The STATSGO database resolves 16 different soil map units from which DHS-

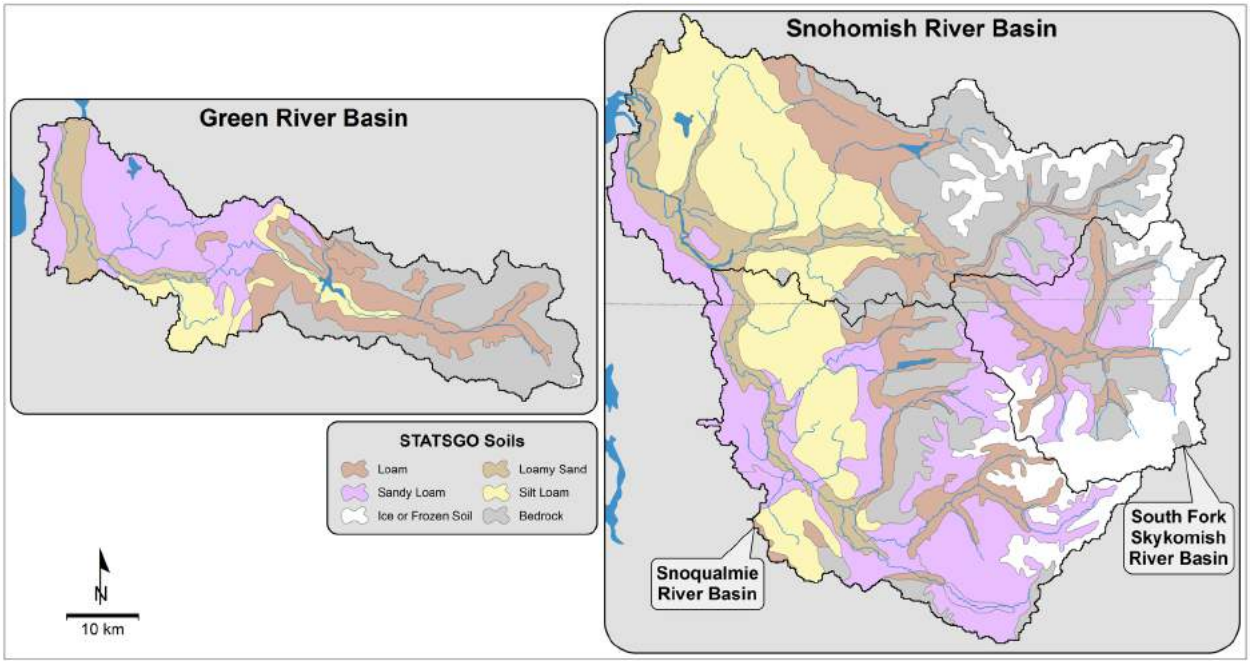

Figure 4.4. STATSGO soil types for the Green and Snoqualmie/Skykomish/Snohomish Basins.

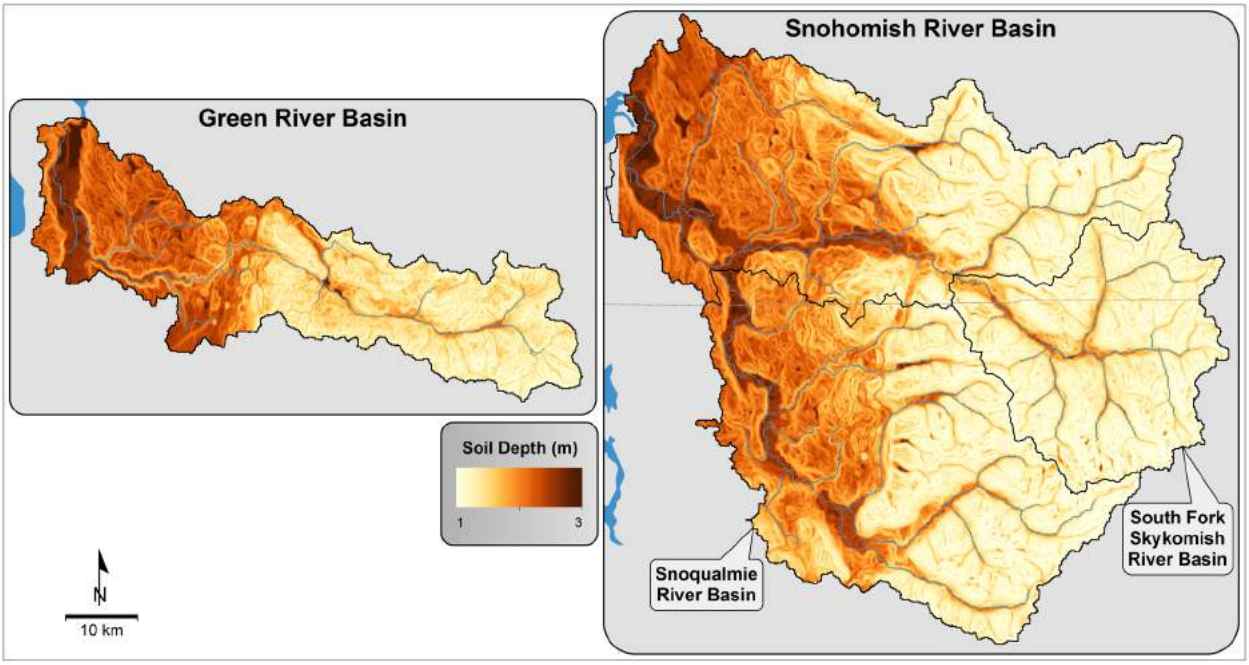

Figure 4.5. Soil Depth for the Green and Snoqualmie/Skykomish/Snohomish Basins.

VM soil parameters can be derived. Sandy loam is one of major soil types in both basins (Figure 4.4).

Soil Depth

Soil depths across the Green and Snoqualmie/Snohomish basins were empirically estimated from topography, based on elevation, local slope and contributing area. This algorithm gives thin soils on steep slopes and ridge tops and thick soils on gentle slopes and in depressions, within a defined range of 1.0 – 3.0 m (Figures 4.5).

Reservoir Model

The Howard Hanson Dam RiverWare model is currently used by the U.S. Army Corps of Engineers, Seattle District to simulate regulation at the dam (USACE 2014). We applied the same model to simulate the effects of climate change on regulated flows for the Green River. Although the dam operations are complex and the management is constrained by multiple objectives, the primary objective during flood events is to keep instantaneous peak flows at Auburn below 12,000 cfs.

The RiverWare model has two inputs: Inflow to Howard Hanson Dam and local flow between the dam and Auburn (Figure 4.6). Hanson Dam and the control point at Auburn were selected as the upstream and downstream boundaries of the model. Upstream of Palmer, Washington, the model simulates the City of Tacoma diversion for municipal and industrial (M&I) water supply. Daily streamflows for the two input points were developed for historical and future time period to assess the changes in peak flows due to climate

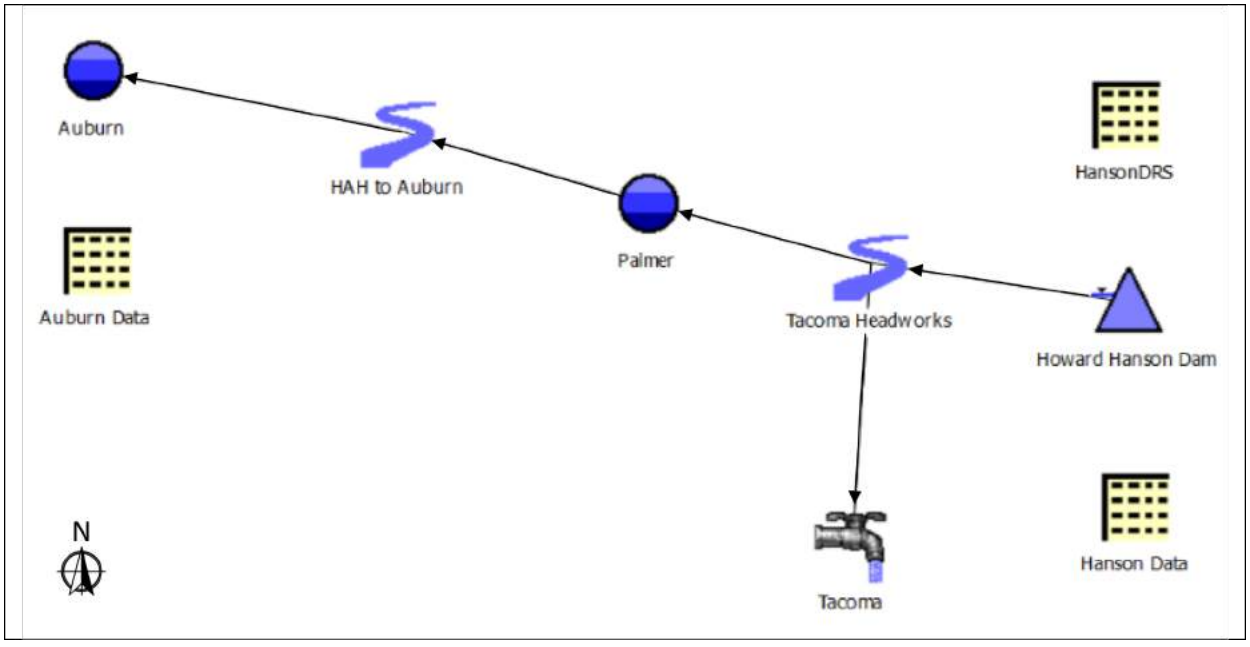

Figure 4.6. Schematic of RiverWare Model used to simulate Howard Hanson Dam reservoir regulations.

change. See USACE (2014) for further details on the model, including dam operation rules and model assumptions.

Streamflow Post-Processing

Time periods

Monthly averages and extreme statistics were calculated for three 30-year time periods: 1970-1999 (“1980s”), 2040-2069 (“2050s”), and 2070-2099 (“2080s”). Although longer time periods might be desired to estimate extreme statistics, 30 years was deemed an appropriate compromise between longer and shorter periods. Since our purpose is to quantify trends in climate and hydrology, using a time frame that is too long would risk underrepresenting changes – by averaging times with less change with others when the changes are more important – while making the estimate less applicable to a specific time horizon for decision-making. Shorter time periods, of course, can limit the reliability of extreme statistics. As noted in Section 3 Data, a bootstrap approach may be the best approach to limiting such uncertainties.

Extreme Statistics

Our comparison of 15-min and 3-hour flows from the observations suggests that DHSVM’s 3-hour time step is sufficient to capture changes in instantaneous peak flows (Figure 4.7). As a result, we used 3-hour streamflow estimates from DHSVM as a proxy for changes in instantaneous peak flows on the Snoqualmie and Green Rivers. An additional analysis was performed on 3-day average flows since these can affect reservoir operations at Howard Hanson dam (personal communication with Ken Brettman at USACE).

To estimate flood magnitude, the maximum in 3-hour, daily, or 3-day flows (depending on the metric) were extracted for each water year (October to September) at each site. These were ranked for each 30-year period and fitted to the generalized extreme value (GEV) distribution with L-moments (Wang 1997, Hosking and Wallis 1993, Hosking 1990), following the methodology described in Salathé et al. (2014) and Tohver et al. (2014). We

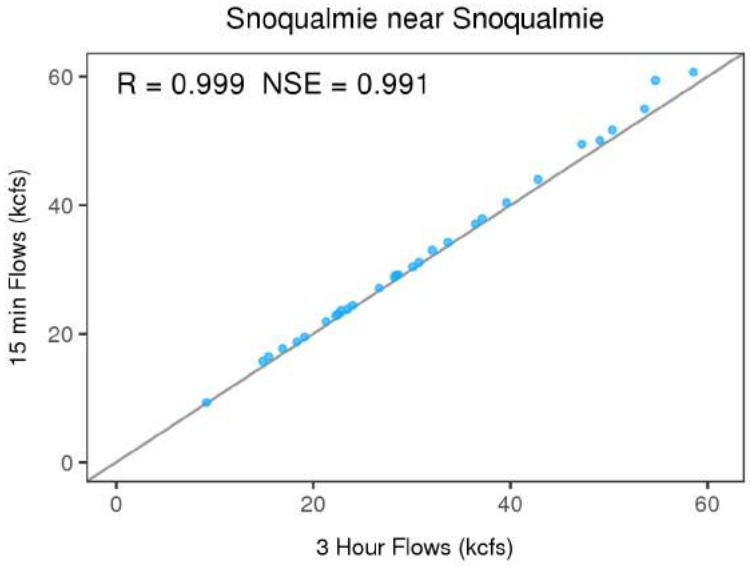

Figure 4.7. Relationship between 15 minute flows and 3 hour flows for the Snoqualmie River near Snoqualmie gauge.

chose the generalized extreme value (GEV) distribution based on findings that indicate it is superior to other distributions, such as Log-Pearson type 3 (LP3; Rahman et al., 1999, 2015; Vogel et al., 1993, Nick et al., 2011).

Flood flows were computed for return intervals of 2, 10, 50, and 100 years. In addition, we evaluated changes in the frequency of a number of key thresholds that are relevant to current management. Specifically, for the Snoqualmie River we evaluated changes in the 20- and 50-year events since these bracket the estimated magnitude of the 2009 floods. For the Green River we evaluated changes in frequency for a range of metrics related to reservoir management. Table 4.1 lists all of the return frequency metrics that we considered.

Site	Naturalized	Regulated	3-hour	3-day	Water Year	Monthly	Threshold	Notes
Snoq. nr. Snoq.	✓		✓		✓		20-yr	Low end for 2009 flood
Snoq. nr. Snoq.	✓		✓		✓		50-yr	High end for 2009 flood
Green nr Auburn	✓		✓		✓		10 kcfs	“trigger threshold”
Green nr Auburn	✓			✓	✓		25 & 28 kcfs	100- and 200-yr events
Green nr Auburn	✓			✓		✓	15 kcfs	
Inflows blw HHD	✓		✓		✓		8 kcfs	100-yr event, 3-hour
Inflows blw HHD	✓			✓	✓		5 kcfs	100-yr event, 3-day
Green nr Auburn		✓		✓		✓	12 kcfs	From ~2- to ~150-yr
Green nr Auburn		✓		✓	✓		10 & 12 kcfs	

Table 4.1. List of alternative metrics, emphasizing the change in the return frequency as opposed to magnitude of flooding. The thresholds for the Snoqualmie are based on the high and low estimates from the King County (2016) assessment of the 2009 flood in that basin. The thresholds for the Green follow the recommendations of Ken Brettman at USACE. “Inflows blw HHD” refers to the contributions from creeks and tributaries that enter the Green between Howard Hanson Dam and the USGS gauge near Auburn. “Trigger threshold” refers to the threshold for flood control operations at HHD.

5 Methods

Calibration of the DHSVM Model

DHSVM is calibrated using a multi-objective complex evolution global optimization method (MOCOM-UA) which was developed by the Land Surface Hydrology group at the University of Washington, following the approach of Yapo et al. (1998). The objective of the model calibration was to maximize the Nash-Sutcliffe Efficiency (NSE) between observed and simulated monthly mean streamflow and log transformed streamflow. During calibration, sensitive parameters such as precipitation lapse rate (m/m), temperature lapse rate (°C/m), lateral saturated conductivity (m/s) for sandy loam (one of

Parameters	Description	Range	Reference	Snohomish River	Green River
Precipitation Lapse Rate (m/m)	Rate of change of precipitation with altitude	0.00010 – 0.00080	Chris Frans 2015, Dickerson 2010, Cuo et al. 2009	0.000328	0.000103
Temperature Lapse Rate (^{o}C/m)	Rate of change of temperature with altitude	-0.0090 – -0.0025	Chris Frans 2015, Dickerson 2010, Minder et al. 2010	-0.008721	-0.006097
Lateral Saturated Conductivity for sandy loam (m/s)	Used in calculation of lateral flow movement	0.0000117 – 0.001	Meyer et al. 1997, Cuo et al. 2011, Dickerson 2010	0.000561	0.001376
Exponential Decrease for sandy loam	Exponent describing the decrease of Lateral Saturated Conductivity with soil depth	0.03 – 5.0	Ziegler, 2000, Cuo et al. 2009, Cuo et al. 2011	2.929152	0.531405
Precipitation Multiplier	Used to adjust precipitation by a factor proportional to the discharge of the basin	0.0 – 0.00020	Wigmosta et al. 1994, Storck et al. 1998, Palmer and Hahn 2002, Whitaker et al. 2003	0.000015	0.000035
Snow Roughness Length (m)	A measure of aerodynamic drag, which affects heat and moisture fluxes	0.0005 – 0.0100	Frans 2015, Andreadis et al 2009, Franz et al. 2008	0.0010	0.0026

Table 5.1. Calibrated parameters of the DHSVM for the Green, Snoqualmie, and SF Skykomish basins.

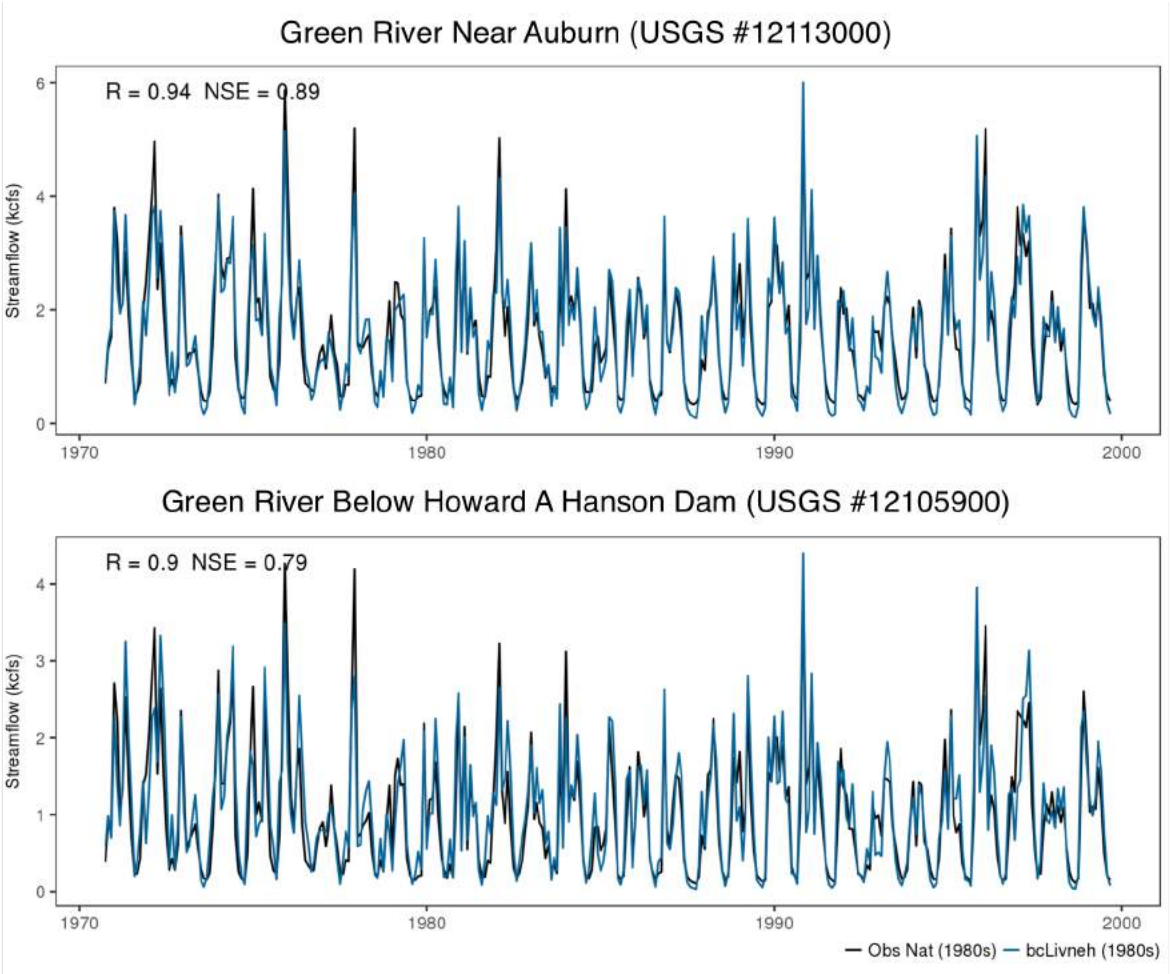

Figure 5.1 Comparing the monthly time series in observed streamflow (black) with simulated flows based on bcLivneh (blue) for the Green River near Auburn (top) and the Green River below Howard A. Hanson Dam (bottom).

major soil types in the basins), exponential decrease for sandy loam, precipitation multiplier, and snow roughness length (m) were adjusted to fit the simulated streamflow to the observed naturalized streamflow. To provide ranges for realistic calibration parameters, we conducted initial trial and error parameter sensitivity analyses using parameter values in the published literature shown in Table 5.1. Our calibrated parameter values for the Snohomish and Green basins were within the ranges in the published literature. As illustrated in Figures 5.1-5.4, these result in good agreement with observed flows.

Although the emphasis of this study is on peak flows, we performed our calibration using a continuous time series of monthly mean flows, based on the reasoning that doing so includes multiple different hydrologic processes that are important for accurately characterizing peak flows. An alternative approach, commonly used in flood studies, is to calibrate the model to a series of observed flood events. We chose not to take this approach because of a concern that the parameter estimates may not be sufficiently

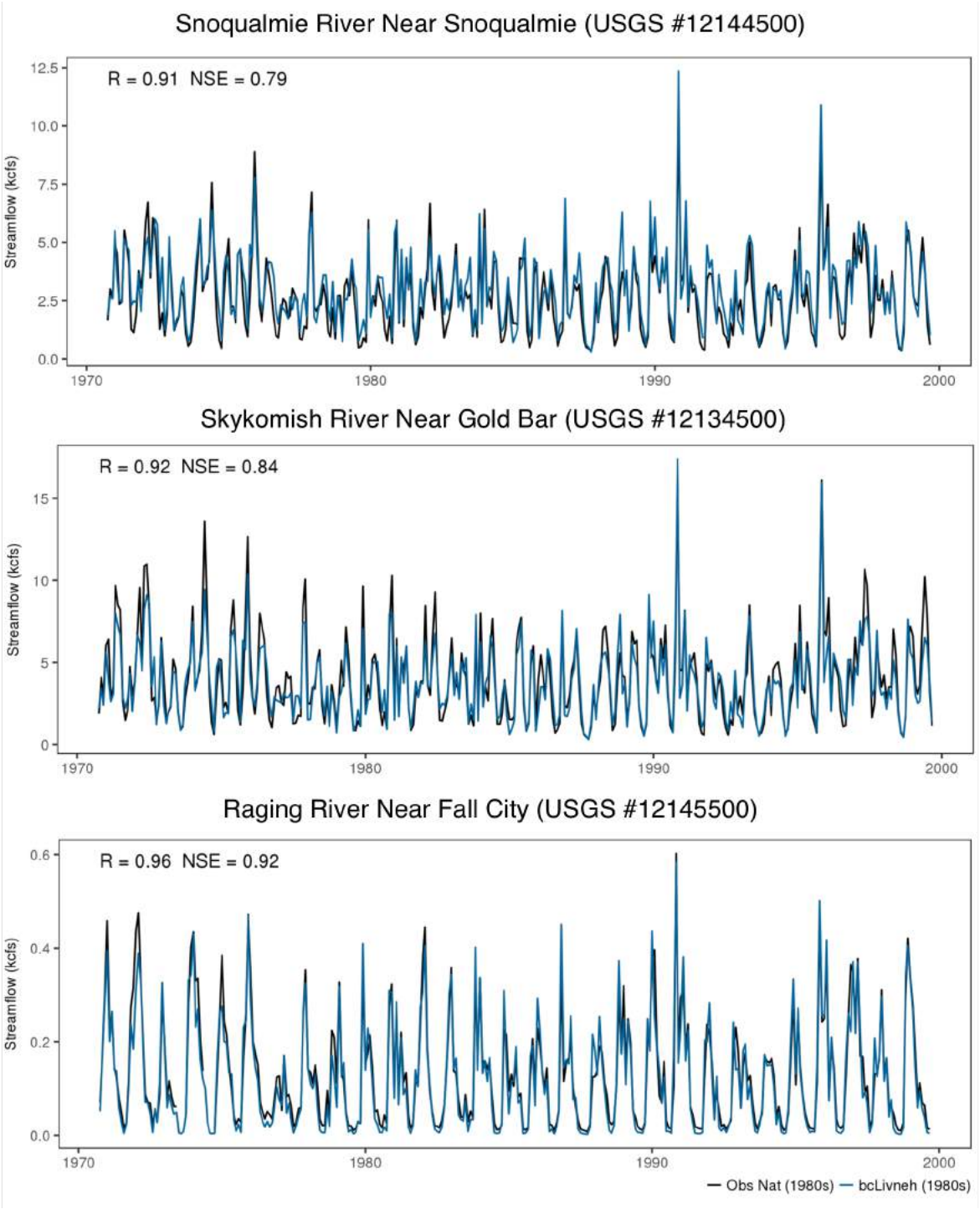

Figure 5.2 As in Figure 5.1 but showing results for the Snoqualmie River near Snoqualmie (top), the Skykomish R. near Gold Bar (middle), and the Raging River near Fall City (bottom).

constrained. We have found that climate change simulations are particularly sensitive to choices of model parameters, particularly for hydrologic models which tend to be over-parameterized. By considering a wide range of flow conditions, the calibration is more constrained by the observations and therefore more likely to center on a set of parameter estimates that more closely resembles the actual soil and vegetation characteristics of each basin.

Comparisons between observed and simulated monthly flows are shown in Figures 5.1 and 5.2. For monthly flow, the correlation (R) and Nash-Sutcliffe Efficiency (NSE) were 0.94 and 0.89 for the Green River near Auburn, and 0.91 and 0.79 for the Snoqualmie River near Snoqualmie, respectively, for water years 1971-1999 (Figures 5.1 and 5.2).

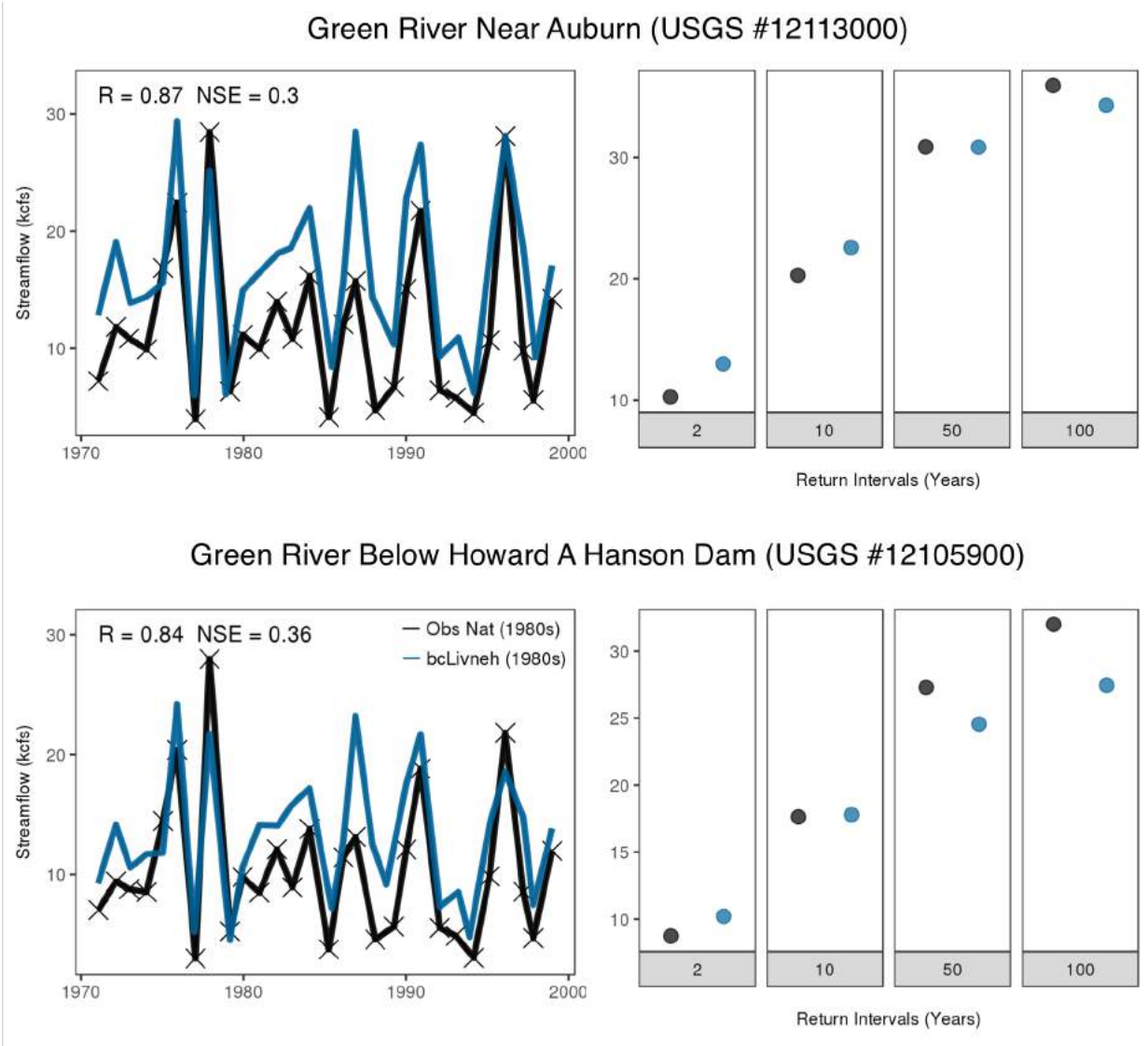

Figure 5.3 Comparing the time series for the water year maximum in daily mean flows (left) and flood statistics for the 2-, 10-, 50- and 100-year events (right) for the observations (black) and simulated flows based on bcLivneh (blue). Results are shown for the Green River near Auburn (top) and the Green River below Howard A. Hanson Dam (bottom).

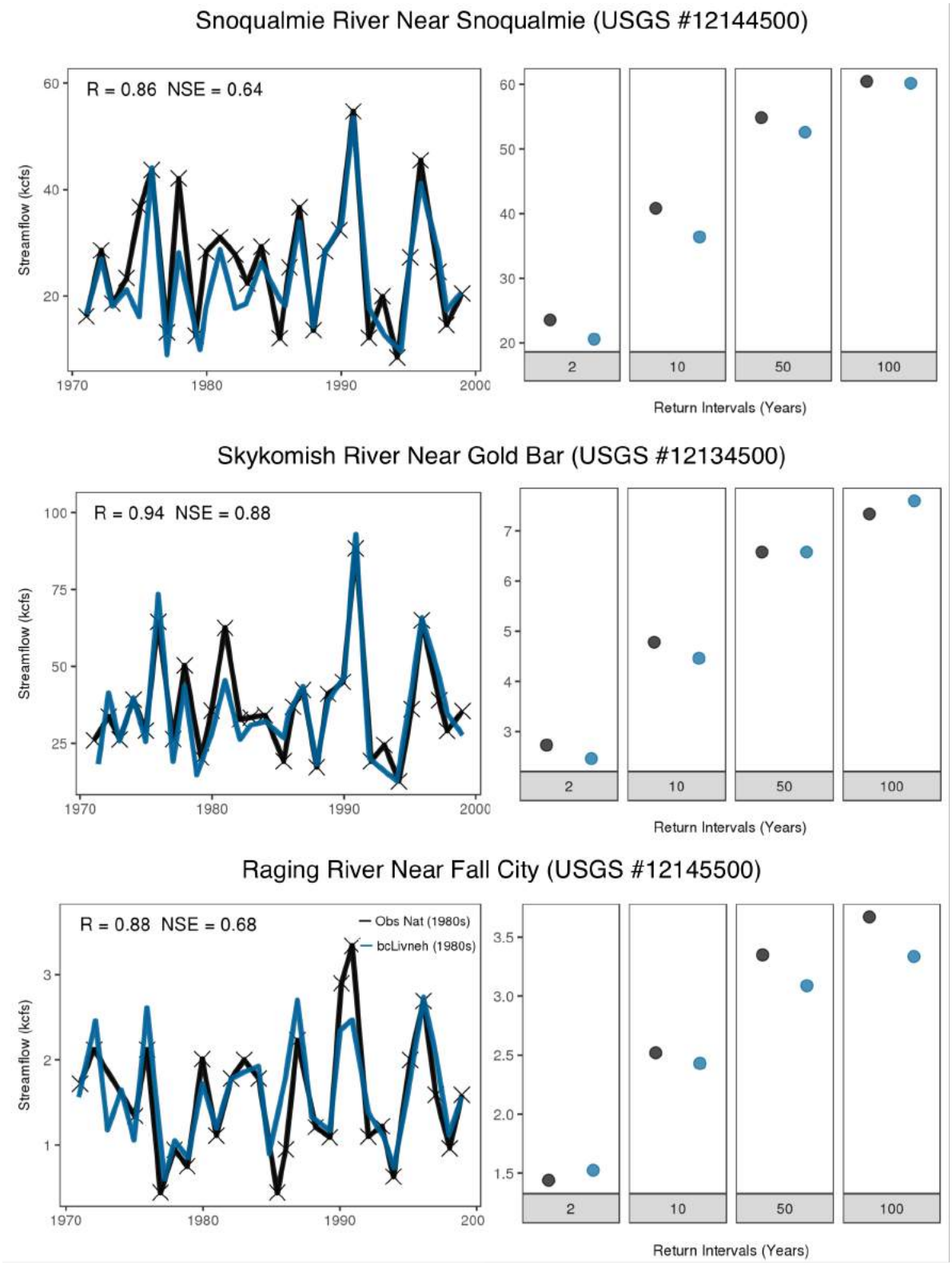

Figure 5.4 As in Figure 5.3 but showing results for the Snoqualmie River near Snoqualmie (top row), the Skykomish R. near Gold Bar (middle), and the Raging River near Fall City (bottom).

Other sites that were not used to calibrate DHSVM are also included in the two figures. These also showed good agreement between the simulation and observations (R >= 0.80 and NSE >= 0.52).

Since the focus of the current study is on flooding we also evaluated the agreement between observed and simulated peak flows (Figures 5.3 and 5.4). We used the annual maximum in daily mean flows (as opposed to 3-hour) for this comparison since sub-daily naturalized flows were not available for some sites. This is a much more stringent test on model performance, especially given that the calibration was optimized for year-round model performance as opposed to just flood events. Although the agreement (R >= 0.84 and NSE >= 0.3) is not quite as good as for monthly flows, the model clearly captures the sequence of variability. The extreme statistics also compare well (right-hand panels in Figures 5.3 and 5.4), especially for high frequency flood statistics (i.e. 2- and 10-year flood stats). As demonstrated in the previous section, flood statistics computed from a single 30-year record can be heavily influenced by natural variability. This may explain the better agreement for the 2- and 10-year events.

Bias-correcting the dynamically downscaled meteorology

Although WRF projections represent a substantial improvement over previous downscaled precipitation estimates, the simulations do contain biases. Accurate hydrologic modeling is contingent on meteorological inputs that reflect the observed temperatures and precipitation totals. As shown in Figure 5.5, the raw WRF simulations tend to be too warm and generally too dry relative to the bcLivneh historical dataset. As a result, we bias-corrected the raw WRF data to match the statistics of the bcLivneh dataset.

Recent work has shown that bias correction can introduce artifacts in the case of climate change, especially when considering changes in extremes (Mauger et al. 2016). Specifically, Mauger et al. (2016) found large changes in the flood projections when comparing hydrologic model results for raw and bias-corrected meteorology. The differences were an unintended side effect of the bias correction, resulting in erroneous estimates of future changes.

This section briefly summarizes an updated bias correction approach that we developed as part of a companion project, also supported by King County, to develop new WRF projections for use in stormwater planning. This new approach is intended to serve as a compromise between improved accuracy in the historical simulations while preserving the projected changes from the raw WRF data. Additional detail can be found in Mauger et al. (2018).

Approach

The bcLivneh data were first aggregated to the 12 km resolution WRF output grid. We then applied the new bias correction approach, called the “Percentile-Delta” method. In

this approach, the historical and future WRF data are adjusted by correcting mean biases in temperature and precipitation in each quantile range (i.e. 0-1, 1-2, … 99-100). For precipitation, all model values below 0.001 inch (0.025 mm) were set to zero. This is a common approach since models simulate a continuous distribution of precipitation yet measurements cannot resolve quantities less than about 0.01 inch (0.25 mm). Next, adjustments were computed in each percentile range as the difference (temperature) or ratio (precipitation) of the average from the historical WRF data (1970-2005) to that from the full historical record from bcLivneh (1950-2013). The result is a different set of "deltas" for each percentile. A separate set of percentiles was calculated for the future WRF simulation (2006-2099). The differences and ratios were then applied to all values in each

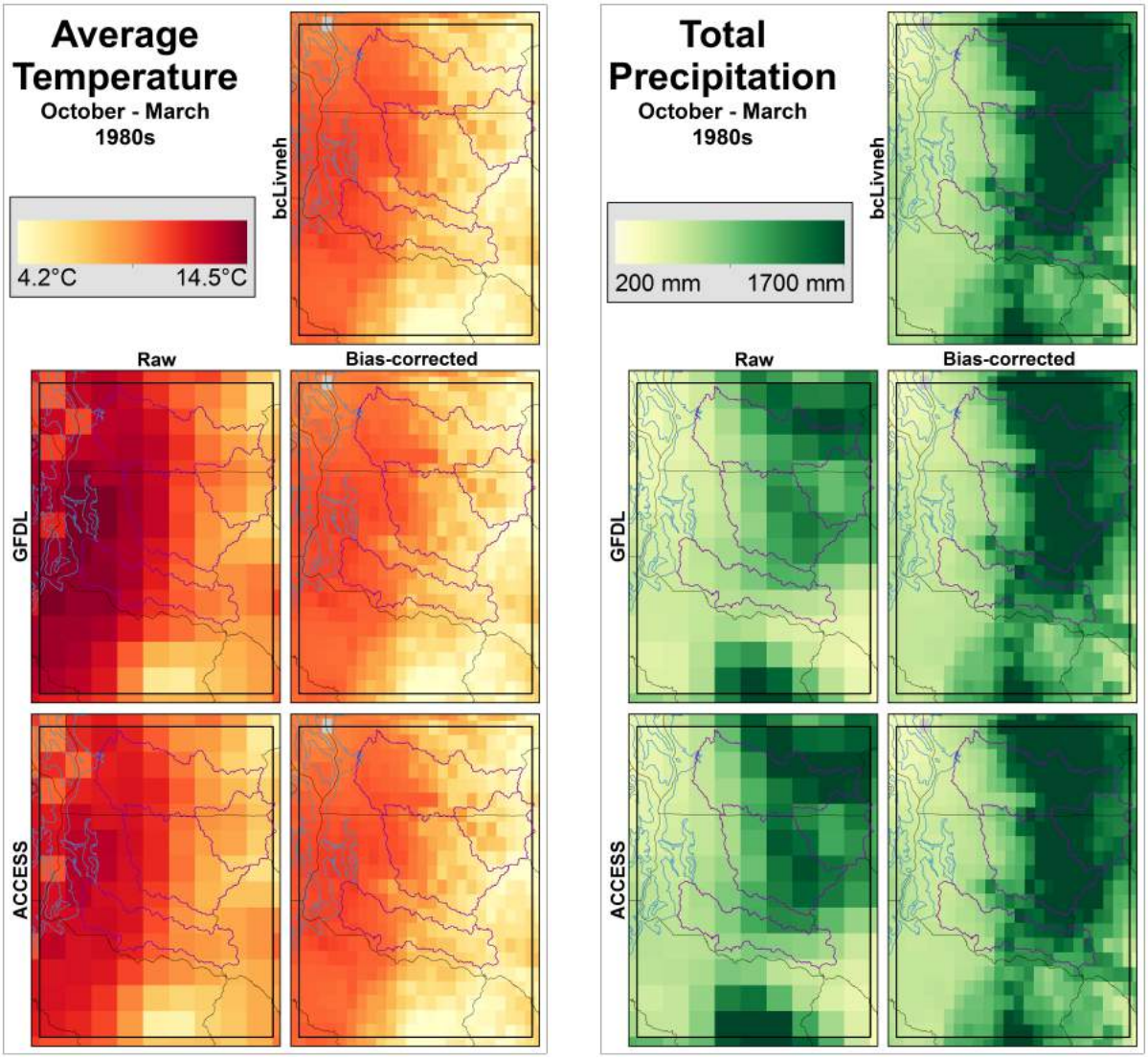

Figure 5.5. Comparing gridded observations (bcLivneh) with raw and bias-corrected WRF simulated weather conditions for the historical GFDL and ACCESS simulations. All maps are based on the 1970-1999 average ("1980s"), showing the average temperature (°C, left) and total precipitation (mm, right) for the cool season (Oct-Mar). Both WRF model simulations tend to be warm and a bit dry; there is a particularly strong warm bias in the GFDL simulation.

percentile of the historical and future WRF data, respectively. Note that since the percentiles are calculated separately, the adjustment applied to a specific value (e.g., 30 mm in daily precipitation) may be different for the historical and future simulations. This is equivalent to assuming that the mechanisms governing precipitation are a function of the quantile in daily precipitation as opposed to the total amount. Recent research supports this assumption (e.g., Warner et al. 2015), indicating that changes in storm thermodynamics (water vapor concentration) and not dynamics (e.g., strength or direction of winds) is the primary driver of increases in precipitation intensity. Finally, the hourly data within each day were simply scaled to match the change applied to the daily average (temperature) or total (precipitation). The bias correction was applied separately for each grid cell.

The Percentile-Delta method was chosen over other methods after extensive testing and evaluation of alternative approaches, applied to both daily and hourly precipitation. Temperature was not found to be as sensitive to the specific approach. Projected changes in return intervals of hourly precipitation were best preserved when performing the Percentile-Delta method versus other methods. For all approaches, including the Percentile-Delta method, Mauger et al. (2018) found that the both the degree of historical agreement with observations and the consistency with raw model projections differed greatly for each location.

Sensitivity Tests

As noted in Figure 3.6, we considered multiple alternative approaches to developing meteorological forcings for the hydrologic simulations. Specifically regarding the WRF simulations, we identified two primary methodological choices that could be made: (1) bias-correcting the meteorology ("bc") vs. using the raw model values ("raw"), and (2) using the MtClim empirical formulations to estimate radiation and humidity ("MtClim") or extracting those values directly from WRF ("Direct", Table 5.2). In order to determine which to use, we ran four separate historical simulations – one for each combination – and evaluated model performance for each set of forcings. There was one additional difference, which is that the Direct-WRF simulations were performed at the native WRF resolution of 12 km, whereas the MtClim-WRF simulations were performed at the typical VIC resolution of 1/16-degree. Separate tests confirmed that this does not influence the results.

Experiment	*Raw*	*Bias-Corrected*	*VIC Preprocessor*	*Direct WRF inputs*
raw MtClim-WRF	✓		✓	
bc MtClim-WRF		✓	✓	
raw Direct-WRF	✓			✓
bc Direct-WRF		✓		✓

Table 5.2. Model experiments used to select among approaches to generating climate forcings. In this case "Raw" and "Bias-corrected" refer to corrections applied to the meteorological data, not the modeled streamflow.

Figure 5.6 compares the monthly mean si-

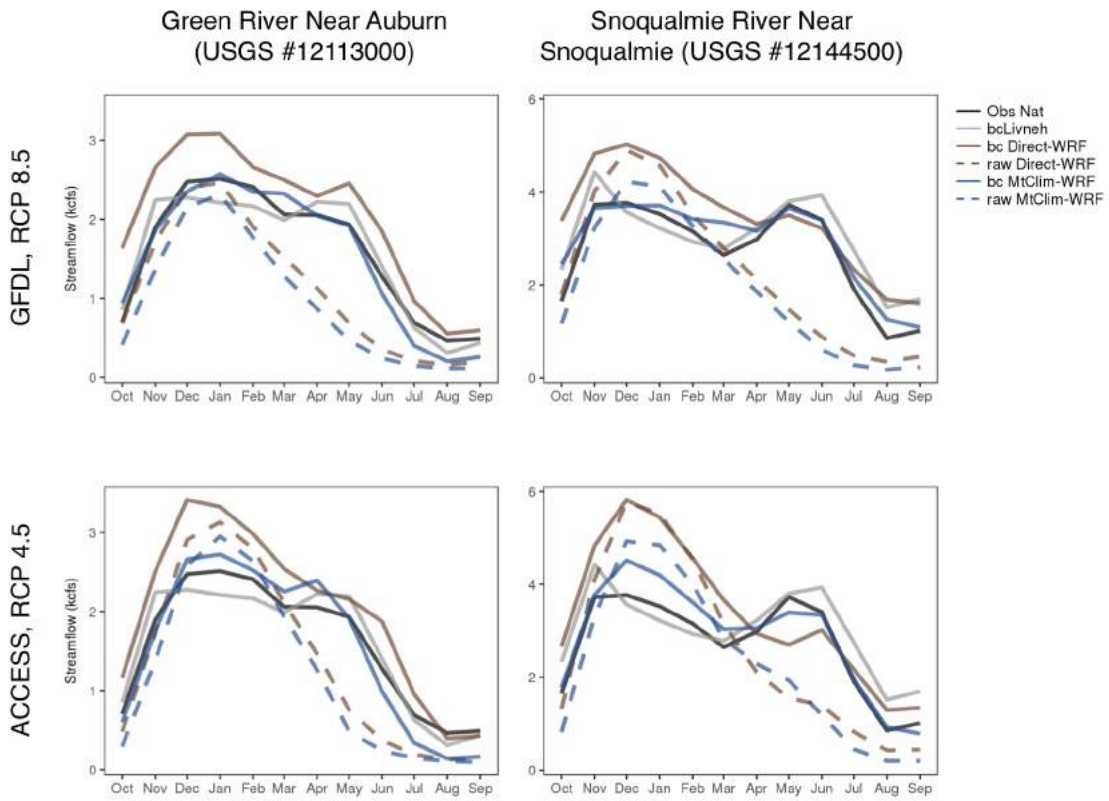

Figure 5.6. Comparing monthly average streamflow both before (dotted lines) and after bias-correcting the meteorological forcings (solid lines), and using the MtClim preprocessor (blue) vs. direct WRF outputs (brown) for GDFL-RCP8.5 (top) and ACCESS-RCP 4.5 (bottom) for the Green River near Auburn (naturalized flows, left) and Snoqualmie River near Snoqualmie (right). Observed flows are shown in black, and the bcLivneh simulation is shown in grey.

-mulated and observed flows for the Green and Snoqualmie Rivers. Warmer and drier conditions in the raw WRF simulations (dashed lines) result in a single streamflow peak in winter due to low snow accumulation, and lowered annual flow volumes compared to the observations (black line). When bias-corrected forcings were used (solid blue and brown lines), both MtClim-WRF and Direct-WRF showed dual winter and spring streamflow peaks, as in the observations, and increased annual flow volume, again aligning more closely with observations. The MtClim-WRF simulation more closely matches the observed annual streamflow volume than Direct-WRF, especially for GFDL.

Bias-correcting the meteorological forcings also resulted in improved estimates of the flood statistics, especially for the ACCESS model (Figure 5.7). Although there were some variations depending on the site, GCM, and return interval, generally the bias-corrected MtClim-WRF forcings performed best at reproducing the observed flood statistics. This is especially true for the GFDL simulations. Based on these results we chose to use the MtClim-WRF with bias-corrected meteorological forcings for the remainder of the current study.

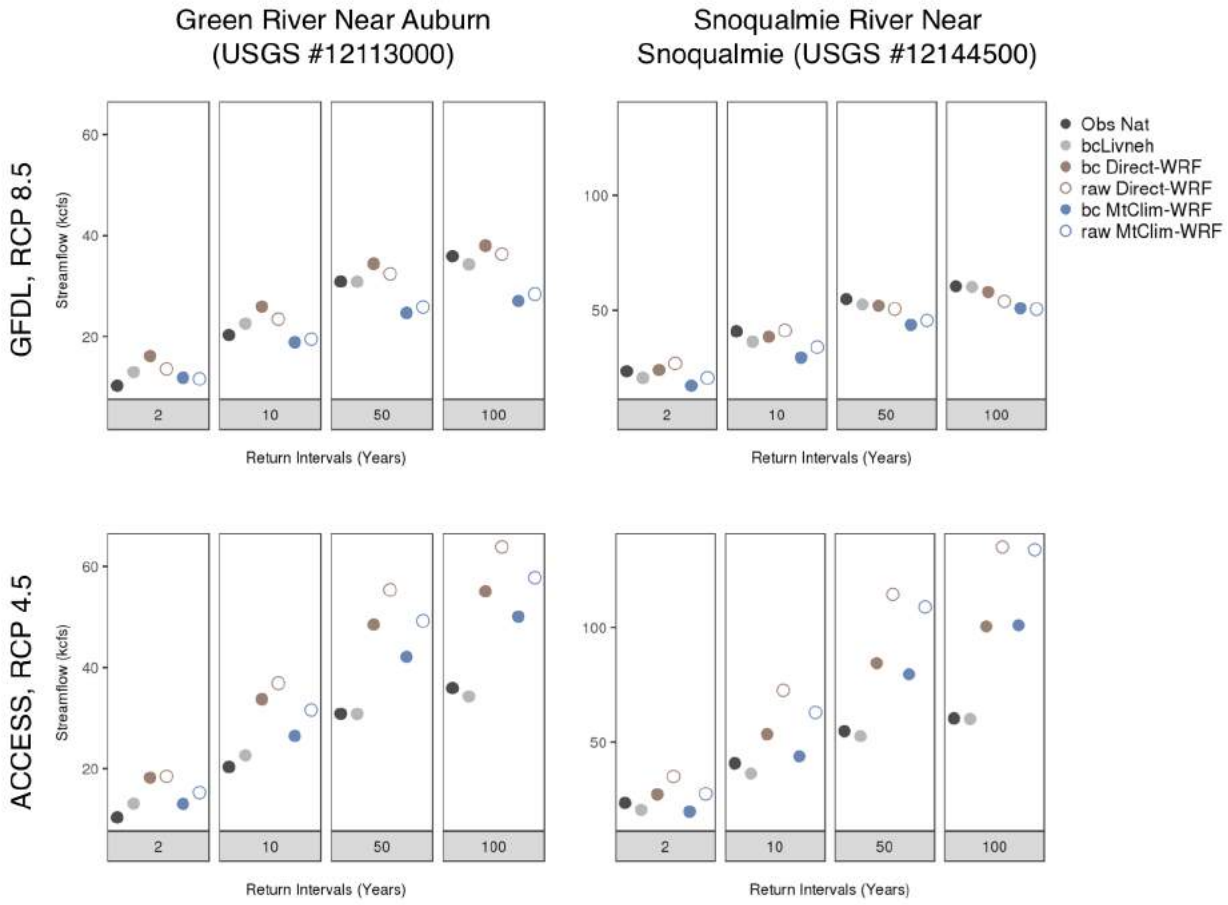

Figure 5.7. As in Figure 5.6 except comparing the historical extreme statistics for each sensitivity test. Observed and bcLivneh flows are shown in black and gray, respectively.

Streamflow Bias-Correction

Our intent in this work was to minimize the need for streamflow bias correction by (a) optimizing DHSVM through calibration and (b) improving the quality of the meteorological forcings. As is evident from Figures 5.1 through 5.4, this goal was largely achieved. Nonetheless, differences between modeled and observed flows remain.

As noted previously, bias correction can often lead to artifacts in the projected changes. One alternative to bias correction is to simply use the relative (e.g., percent) change in the raw DHSVM flows to evaluate impacts. We recommend taking this approach whenever possible.

However, many applications require estimates of absolute flows, especially those that involve continuous simulation. As a result, we have applied a bias correction to bring the DHSVM streamflow estimates into closer alignment with the observations.

Approach

In previous approaches (Hamlet et al. 2013, USACE 2014), bias correction was applied at monthly time scales – adjusting naturalized streamflow using a quantile mapping approach outlined by Snover et al. (2003). A primary concern in monthly bias correction is that biases in the sub-monthly distribution of streamflow – daily flows, in particular – will not be removed in the process.

Given the emphasis on daily extremes in this study, a daily bias-correction approach was developed. This method closely follows the approach outlined in the previous section, in which each percentile (i.e. 0-1, 1-2, … 99-100) in streamflow is scaled based on the average ratio between modeled and observed flows for that percentile range.

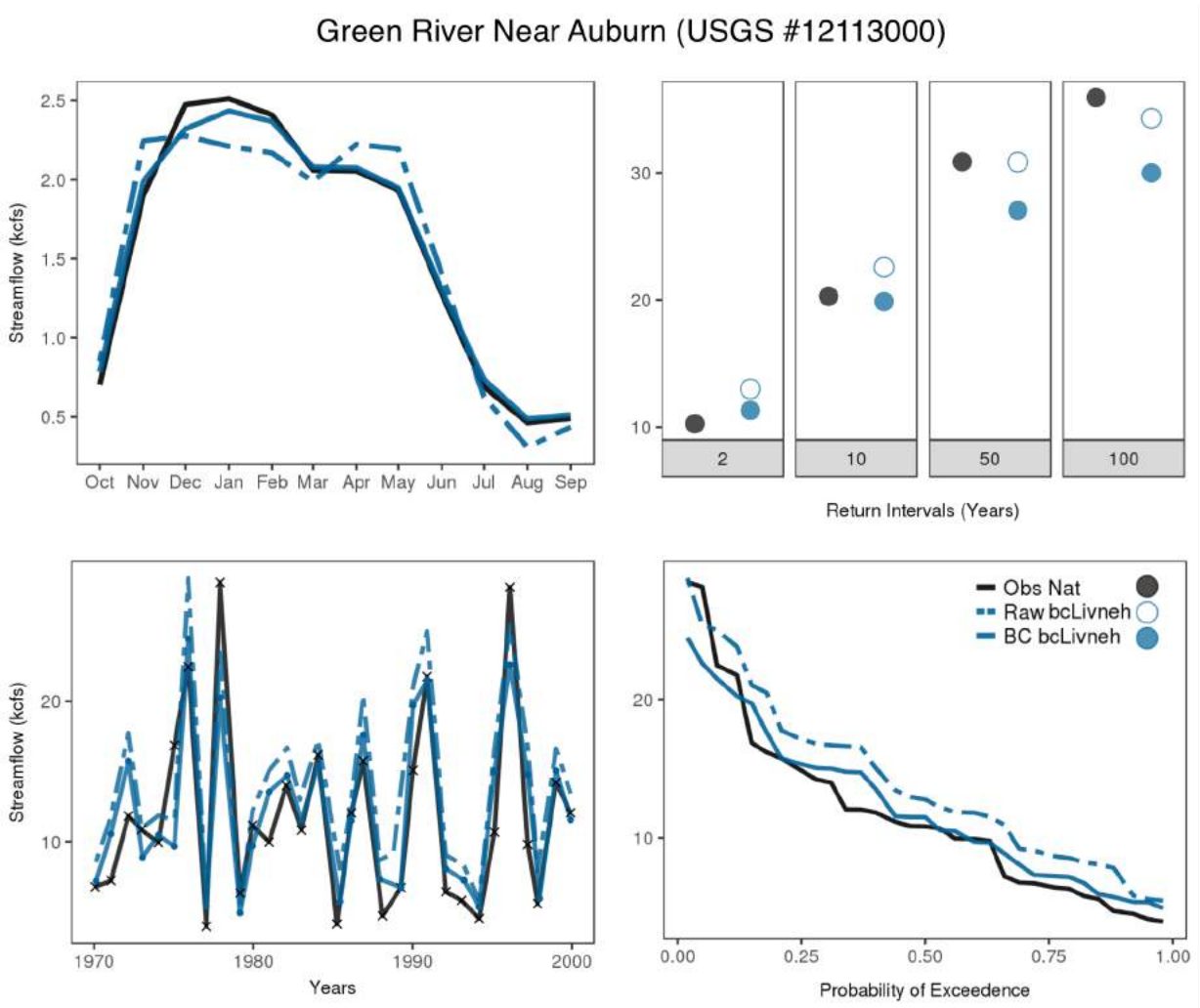

Figure 5.8 Comparing monthly average streamflows (top left), and three plots showing the statistics of the water year maximum in daily mean flows: the time series (bottom left), extreme statistics for the 2-, 10-, 50- and 100-year events (top right), and the cumulative distribution function (bottom right) for naturalized flows on the Green River near Auburn (USGS #12113000). Each plot compares results for the observations (black) with simulated flows based on bcLivneh (blue). Dotted lines and open circles show the raw simulation results, and solid lines and closed circles show bias-corrected streamflows.

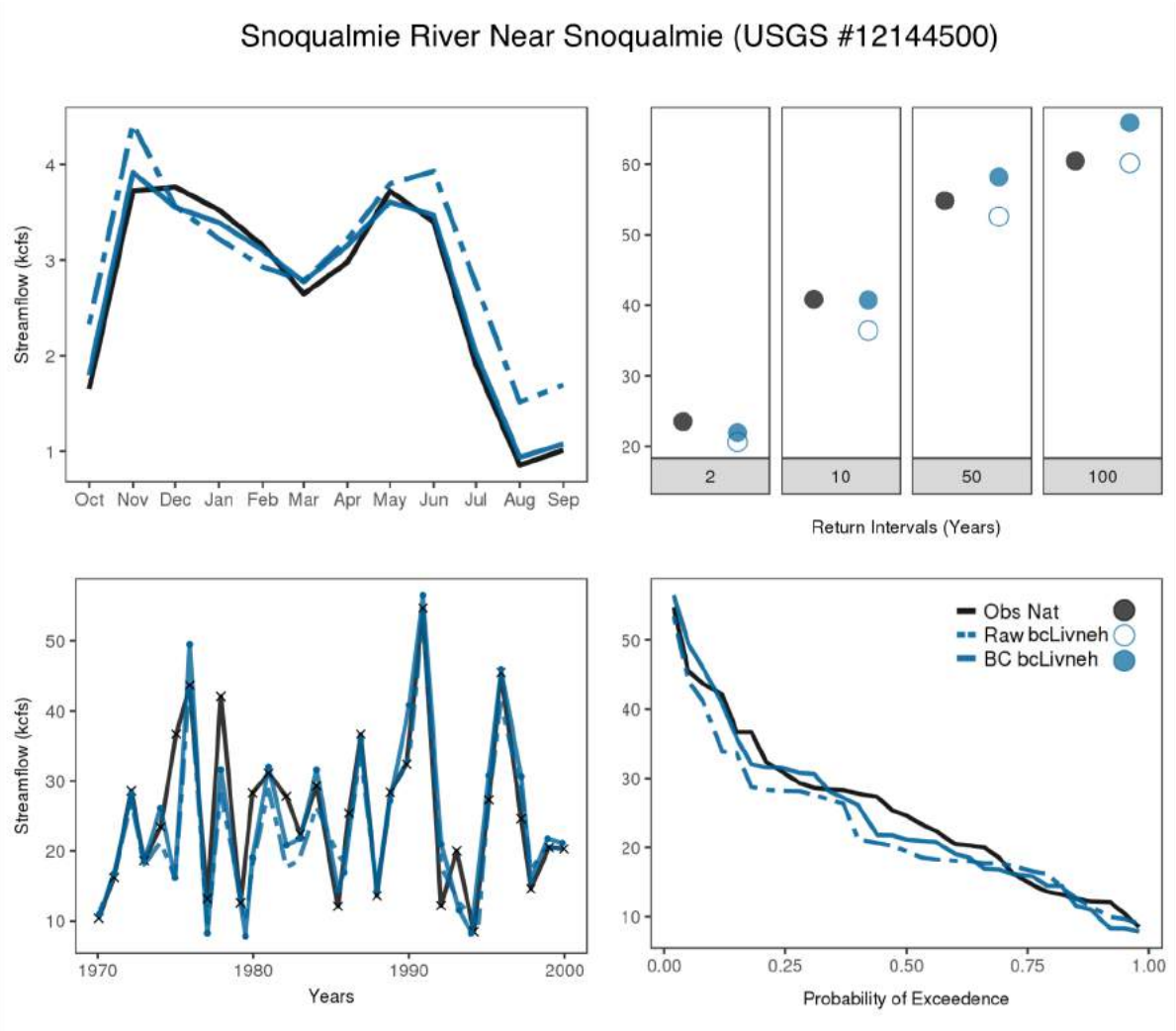

Figure 5.9 As in Figure 5.8 except that results are shown for the Snoqualmie River near Snoqualmie.

While the mechanisms governing temperature and precipitation variations are largely the same throughout the year, the same cannot be said for streamflow. As a result, we modified the bias correction to be applied to a moving window, centered on each day's streamflow. Specifically, we used an 81-day window, calculating the ratio for each percentile for all observed and modeled data that fell within the window for any years that were included in the analysis. This ratio was then applied the quantile for the one day at the center of the window. Moving to the next day, a new window is defined, along with a new set of ratios, and the process is repeated. The 81-day window was selected based on sensitivity tests comparing a year-round bias correction (i.e. no moving window) to 41-, 81-, 121-day moving windows. Tests indicate that the results are improved by using a moving window but are not very sensitive to the exact window width. As above, this approach assumes that bias correction should be applied as a function of quantile as opposed to absolute flows. Future work should explore the trade-offs associated with removing the long-term trend in streamflow before applying the bias correction – such tests were not feasible within the scope of the current project.

Observed monthly average naturalized streamflow at the Green River near Auburn shows the dual streamflow peaks in January and April, a classic pattern observed in snow-influenced watersheds. The same can be seen at the Snoqualmie River near Snoqualmie, though the peaks occur in November and June. Conditions in the Green River basin are likely warmer than the Snoqualmie, given the higher winter peak relative to the spring peak in streamflow. Raw simulations using bcLivneh reproduced the timing of the dual peaks in both rivers, although the simulated flows were slightly higher or lower than the observations for some months (dotted lines in top left panels in Figures 5.8 and 5.9). When we applied daily streamflow bias-correction, these systematic biases were removed (solid lines in top left panels in Figures 5.8 and 5.9).

Similar improvements were seen for the estimates of the water year maximum daily streamflow and the associated flood statistics for the Green and Snoqualmie Rivers, although bias-corrected flows underestimated the two highest peaks for the Green River

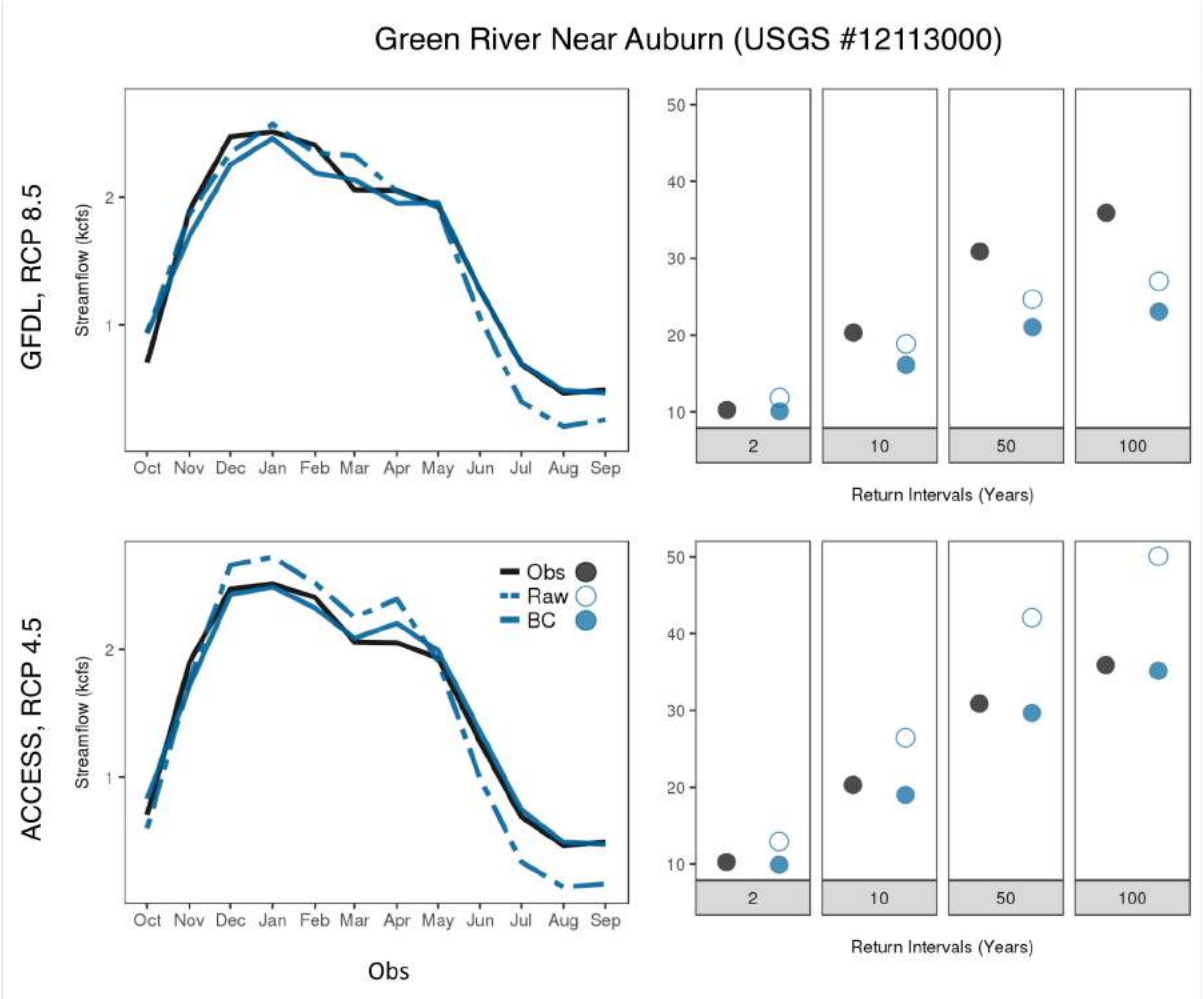

Figure 5.10 Comparing monthly average streamflows (left) and flood statistics for return intervals of 2-, 10-, 50- and 100-years (right) for naturalized flows on the Green River near Auburn. Plots show the observations (black) with raw (dashed lines, open circles) and bias-corrected (solid lines, solid circles) flows based on GFDL_RCP8.5 (top) and ACCESS_RCP4.5 (bottom).

(Figure 5.8). For the Snoqualmie River, the cumulative distribution function (CDF) of peak flows more closely matched the observations after the bias-correction, resulting in improved flood statistics for all return intervals. For the Green River, in contrast, the two missed peaks result in an underestimate of the high end of the CDF and resulting in underestimates of the magnitude of low frequency floods (50- and 100-year floods; Figure 5.8). Bias-correcting the streamflow also improved agreement for the GFDL- and ACCESS-based DHSVM simulations (Figures 5.10 and 5.11), with the one exception of the GFDL statistics for the Green River.

Finally, it is worth emphasizing that there is a trade-off between the quality of the bias correction and the resulting biases in the projected changes in streamflow after bias correction. The use of a constant scaling, as in our “Percentile-Delta” approach, means that all values within a certain quantile are subject to the same adjustment. Especially for the extreme statistics, this may not be appropriate, since the biases may be different for each. The result is that in a few cases the raw data agree better with the observations than the bias corrected flows. Although it is possible that the bias correction could be better tailored to extreme statistics, this is not feasible for the current project. As noted

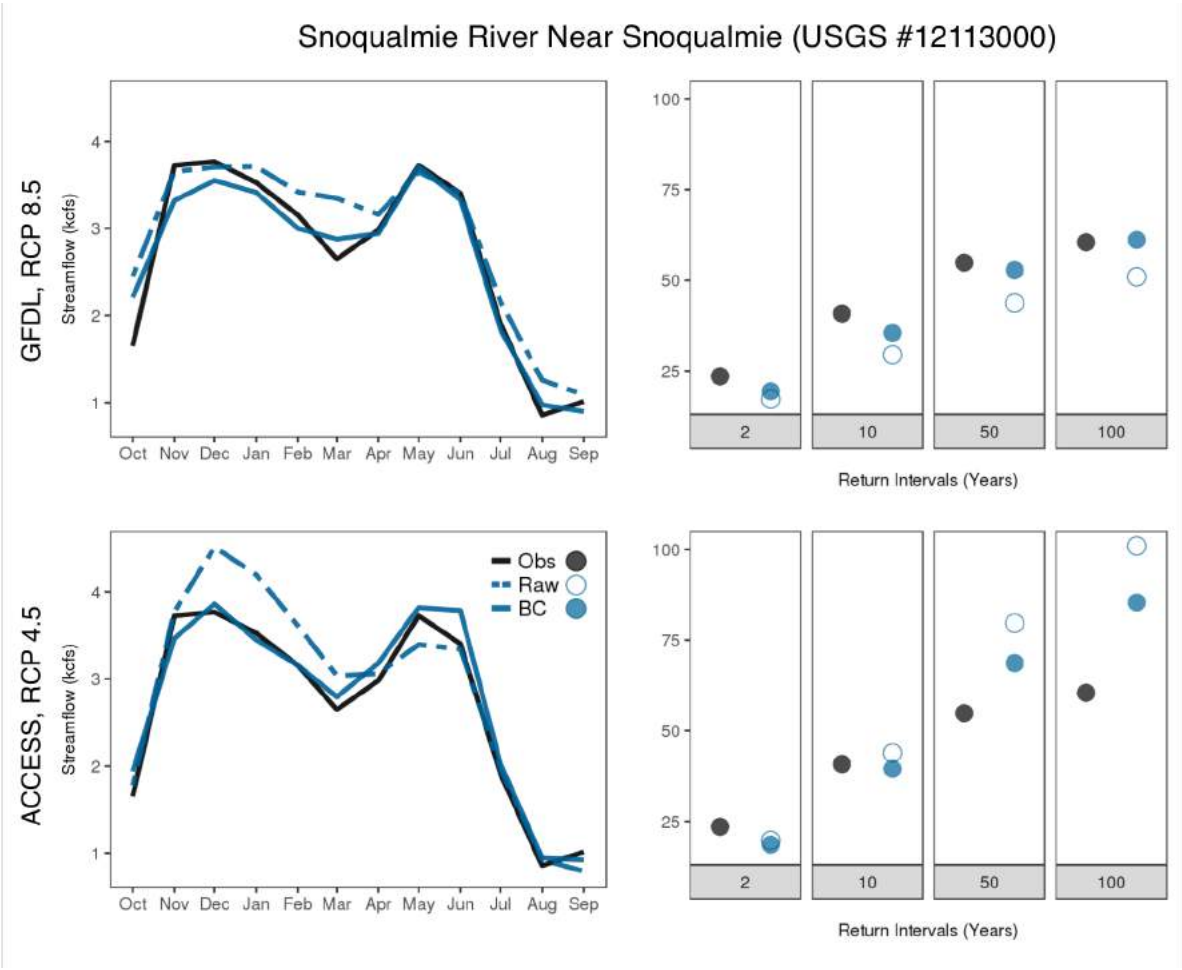

Figure 5.11 As in Figure 5.10 except that results are shown for the Snoqualmie River near Snoqualmie.

previously, we recommend using the percent changes in raw flows when absolute streamflow estimates are not needed.

6 Results

Projected Changes in Naturalized Streamflow

This section summarizes the changes in naturalized streamflow in the Green, Snoqualmie, and SF Skykomish river DHSVM simulations. As discussed in previous sections, all results are based on the bias-corrected MtClim-WRF forcings (meteorology), with humidity and radiation estimated using the empirically-based MtClim formulation. In addition to the bias correction applied to the forcings, we also developed a bias correction that we applied to daily streamflow as simulated by DHSVM. In this section, we present results based on bias-corrected streamflow when considering absolute flows, but use the raw streamflow results when considering the percent changes in flows. As discussed previously, using raw flows avoids potential artifacts associated with the streamflow bias correction.

Finally, in this section we also present the statistically-downscaled bcMACA projections alongside the results developed from the dynamically-downscaled WRF projections. As noted previously, the bcMACA projections are not able to produce reliable projections of changing precipitation extremes Nonetheless, these are included because they are constructed using a much larger ensemble of global model projections, and may provide some insight via comparison with the two WRF projections that are the primary focus of the current study.

Seasonal Cycle in Monthly Flows

Consistent with the observed and naturalized flows, historical simulations show that the Green, Snoqualmie, and SF Skykomish rivers all have dual peaks in winter and spring, a classic signature of snow-influenced watersheds in the Pacific Northwest (blue lines in Figures 6.1 and 6.2). Warming causes a greater proportion of precipitation to fall as rain, leading to increased winter flows, decreased snowpack, and decreased spring/summer flows. The result is a shift in the seasonal cycle of streamflow to a single winter peak occurring either in November, December or January for both rivers. All of the scenarios considered here exhibit this change by the 2080s, and many even by the 2050s. Although variability in seasonal and annual precipitation can cause some winters to have higher flows than others, all scenarios considered here project that the ratio of cool-season to annual flow volume is higher for the 2080s than for the 2050s. The GFDL-RCP8.5 and ACCESS-RCP4.5 projections show higher cool-season flow volumes for the 2050s than for the 2080s, but only because the two dynamically downscaled simulations also project higher annual flow volumes for the 2050s than for the 2080s. The ratio of cool-season flows to the total flows for the water year, in contrast, increases from the 2050s to the 2080s. These results are consistent with previous studies (e.g., Elsner et al. 2010, Hamlet et al. 2013), which show a clear temperature induced trend that is modulated by precipitation variability.

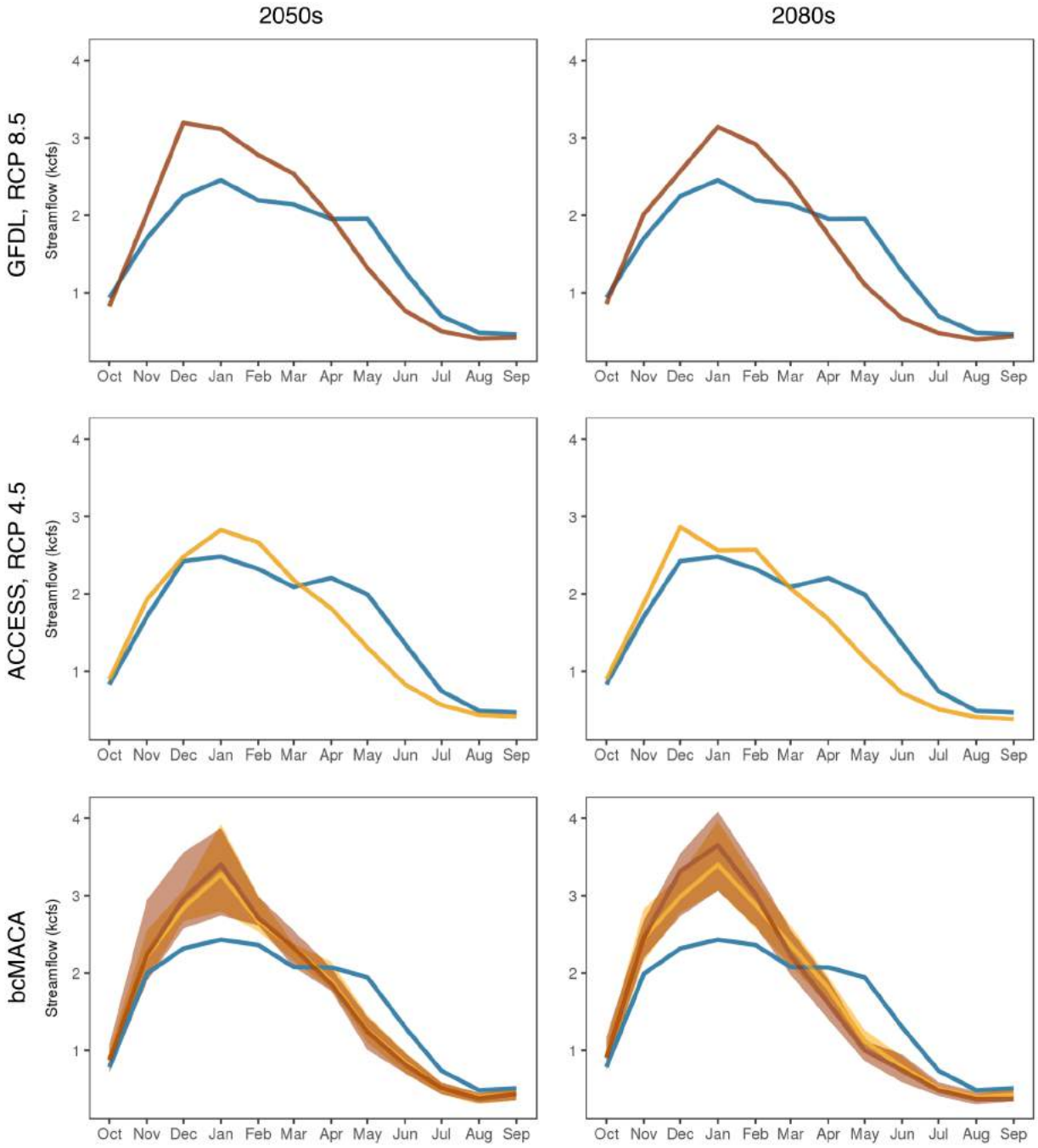

Figure 6.1 Seasonal cycle in monthly average naturalized streamflow for the Green River near Auburn, showing projections for GFDL-RCP8.5 (top), ACCESS-RCP4.5 (middle) and bcMACA (bottom) for the 2050s (left) and 2080s (right). The bcMACA results include projections for RCP 4.5 (yellow) and RCP 8.5 (brown). In all plots, the blue line shows the historical simulation for each set of projections (i.e.: average for the 1980s for WRF GFDL, WRF ACCESS, and bcLivneh, respectively). Since this figure concerns absolute flow estimates, bias-corrected streamflow data are shown.

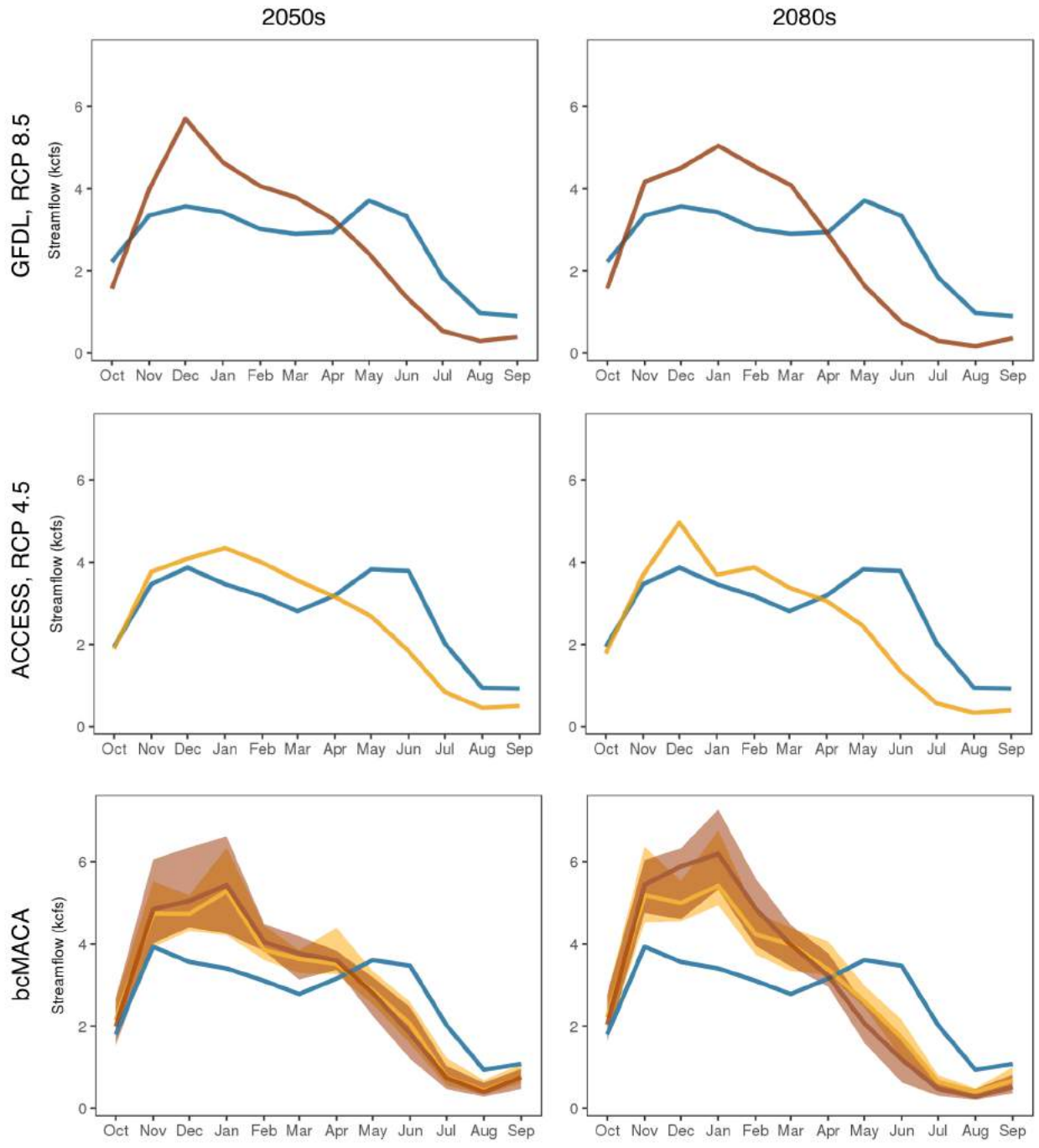

Figure 6.2 As in Figure 6.1 except showing results for the Snoqualmie River near Snoqualmie.

Other changes can also be observed in Figures 6.1 and 6.2. Specifically:

- The GFDL-RCP8.5 simulation projects a larger increase in winter flows than the ACCESS-RCP4.5 simulation, most likely because GFDL projects a slight increase in cool-season precipitation, while ACCESS projects a slight decrease (see Mauger et al. 2018);

- The GFDL-RCP8.5 simulation projects a smaller increase in winter flows than the median of the 10 bcMACA-RCP8.5 simulations, primarily because the GFDL-RCP8.5 simulation projects lower winter precipitation than the median of bcMACA;

- Similarly, the ACCESS-RCP4.5 simulation projects a smaller increase in winter flows than the median of the 10 bcMACA-RCP4.5 simulations. In contrast with GFDL-RCP8.5 and bcMACA, the ACCESS-RCP4.5 simulation projects a decrease in annual flow for both the 2050s and 2080s as compared to the 1980s, suggesting that these differences are driven by different precipitation projections. This means that the increase in winter streamflow for ACCESS-RCP4.5 is due to an increase in the proportion of precipitation that falls as rain, and that this increase more than compensates for the decrease in precipitation. In contrast, annual precipitation is projected to increase for the bcMACA-RCP4.5 simulations, compounding the increase due to the shift from snow to rain;

- The monthly peaks in streamflow for the 2080s are either similar to or greater than the peak monthly flows for the 2050s. The one exception is the GFDL-RCP8.5 projection for the Snoqualmie River, for which the December peak in the 2050s is higher than January peak in the 2080s. Since these are monthly averages, projected changes in flood statistics need not match the patterns outlined in this section (see following section on Streamflow Extremes and Figure 6.5).

Streamflow Extremes

Flood flows are projected to increase for all return periods and for all scenarios considered here except ACCESS-RCP4.5 (Figures 6.3-6.5, Tables 6.1-6.2). For the GFDL-RCP 8.5 simulation, both rivers show a large increase in peak flows from the historical simulation to the 2050s. For the Green River, the projected change for the 2080s is slightly larger for the 3-hour flood but significantly smaller for 3-day flood statistics relative to the projections for the 2050s. This suggests that GFDL-RCP 8.5 projects more 3-day consecutive precipitation for the 2050s than for the 2080s. Since there is no reason to expect precipitation extremes to first increase and then decrease with climate change, this is likely a reflection of natural variability. In contrast, changes in 3-hour flood for the 2080s are more pronounced for the Snoqualmie River – presumably because it is a cooler basin, meaning that declines in snowpack play a larger role in determining future peak flows. As a result, the large natural variability in precipitation extremes has a relatively smaller effect.

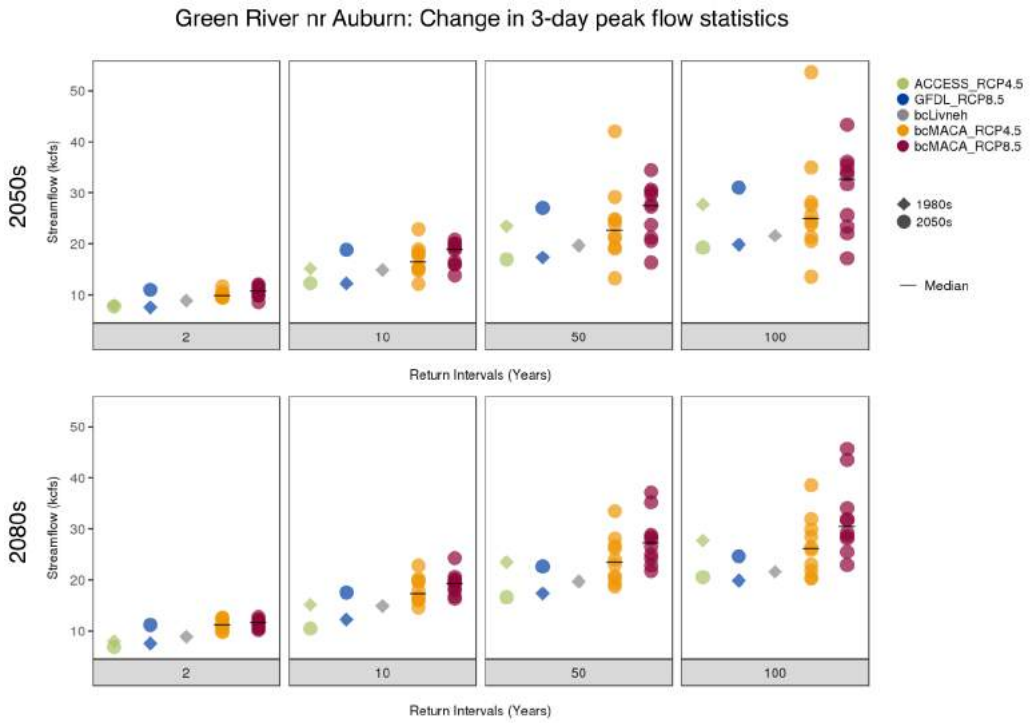

Figure 6.3 Future and historical flood statistics (2-, 10-, 50- and 100- year floods) using bias-corrected naturalized 3-day average flows for the Green River near Auburn. The plots include results for all DHSVM simulations for the 2050s (top) and 2080s (bottom). Historical flood statistics are based on water years 1971-2000.

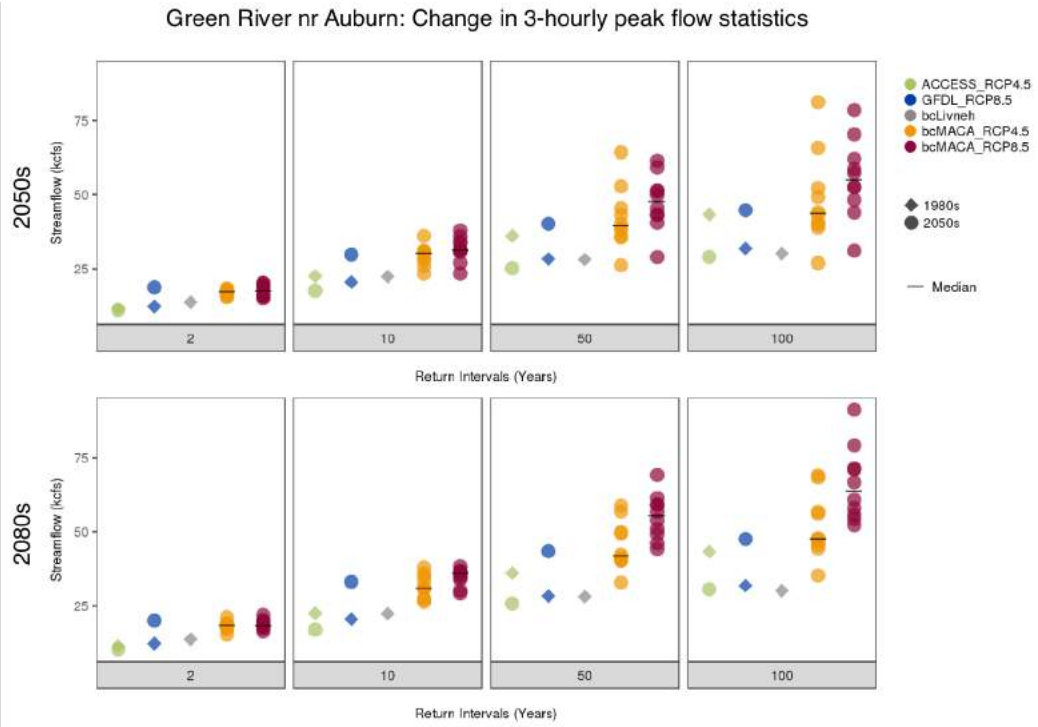

Figure 6.4 As in Figure 6.3 except for 3-hour peak flows for the Green River near Auburn.

		WRF		bcMACA	
site name	USGS ID	GFDL	ACSS	RCP 4.5	RCP 8.5
SF Skykomish R Nr Index	12133000	75%	-32%	30% (7%, 52%)	48% (8%, 64%)
Skykomish R Nr Gold Bar	12134500	71%	-31%	30% (7%, 49%)	47% (8%, 64%)
MF Snoqualmie R Nr Tanner	12141300	95%	-35%	30% (12%, 60%)	59% (17%, 72%)
Snoqualmie R Nr Snoqualmie Falls	12142000	74%	-36%	33% (20%, 60%)	56% (15%, 66%)
Snoqualmie R Abv Alice Cr	12143400	105%	-33%	40% (11%, 65%)	65% (28%, 86%)
Snoqualmie R Nr Snoqualmie	12144500	89%	-36%	27% (14%, 59%)	57% (14%, 64%)
Raging R Nr Fall City	12145500	36%	-19%	8% (-16%, 31%)	24% (-4%, 28%)
NF Tolt R Nr Carnation	12147500	48%	-33%	25% (13%, 53%)	48% (8%, 60%)
SF Tolt R Nr Carnation	12148000	56%	-36%	29% (16%, 57%)	53% (10%, 63%)
Tolt R Nr Carnation	12148500	48%	-32%	24% (14%, 55%)	47% (8%, 59%)
Snoqualmie R Nr Carnation	12149000	75%	-34%	23% (16%, 59%)	54% (12%, 59%)
Green R Nr Lester	12104500	77%	-29%	66% (35%, 104%)	85% (49%, 122%)
Green R Blw HHD	12105900	67%	-36%	44% (24%, 68%)	67% (36%, 86%)
Green R nr Palmer	12106700	66%	-36%	43% (24%, 67%)	66% (35%, 84%)
Newaukum Cr Nr Black Diamond	12108500	22%	-13%	10% (-5%, 33%)	25% (4%, 42%)
Big Soos Cr Abv Hatchery	12112600	11%	7%	8% (-3%, 39%)	23% (3%, 49%)
Green R Nr Auburn	12113000	56%	-33%	37% (20%, 64%)	61% (30%, 74%)

Table 6.1 Percent change in the 10-year extreme in 3-hour streamflow for the 2080s (2070-2099) relative to the 1980s (1970-1999). In the table header, “ACSS” refers to the ACCESS-RCP4.5 simulation. The bcMACA projections are included for comparison, showing the median for each scenario, plus the minimum and maximum among all 10 GCMs in parentheses.

		WRF		bcMACA	
site name	USGS ID	GFDL	ACSS	RCP 4.5	RCP 8.5
SF Skykomish R Nr Index	12133000	40%	-51%	26% (-10%, 104%)	41% (-10%, 87%)
Skykomish R Nr Gold Bar	12134500	41%	-52%	23% (-12%, 94%)	43% (-10%, 95%)
MF Snoqualmie R Nr Tanner	12141300	76%	-49%	14% (-7%, 67%)	47% (-8%, 114%)
Snoqualmie R Nr Snoqualmie Falls	12142000	49%	-54%	23% (-5%, 94%)	62% (-9%, 126%)
Snoqualmie R Abv Alice Cr	12143400	88%	-49%	38% (-9%, 90%)	73% (27%, 160%)
Snoqualmie R Nr Snoqualmie	12144500	85%	-51%	14% (-3%, 73%)	58% (-7%, 129%)
Raging R Nr Fall City	12145500	62%	-25%	25% (-27%, 77%)	61% (-9%, 132%)
NF Tolt R Nr Carnation	12147500	27%	-41%	19% (-2%, 125%)	73% (2%, 148%)
SF Tolt R Nr Carnation	12148000	31%	-48%	29% (-1%, 123%)	86% (5%, 159%)
Tolt R Nr Carnation	12148500	32%	-41%	18% (-3%, 122%)	71% (1%, 147%)
Snoqualmie R Nr Carnation	12149000	73%	-48%	17% (2%, 82%)	68% (-6%, 141%)
Green R Nr Lester	12104500	47%	-37%	137% (117%, 198%)	190% (112%, 288%)
Green R Blw HHD	12105900	50%	-41%	77% (39%, 159%)	133% (89%, 201%)
Green R nr Palmer	12106700	50%	-41%	75% (35%, 156%)	129% (85%, 200%)
Newaukum Cr Nr Black Diamond	12108500	42%	-0%	17% (-18%, 72%)	50% (18%, 129%)
Big Soos Cr Abv Hatchery	12112600	2%	60%	-8% (-32%, 59%)	11% (-15%, 128%)
Green R Nr Auburn	12113000	46%	-31%	65% (19%, 130%)	114% (73%, 200%)

Table 6.2 As in Table 6.1 except showing results for the 100-yr flood.

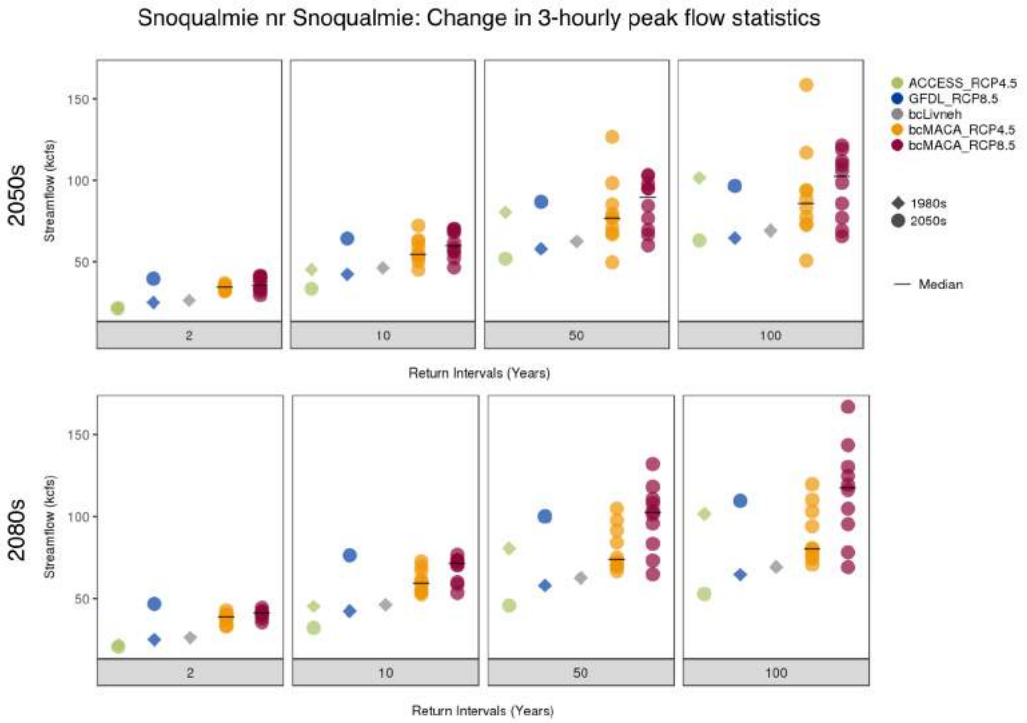

Figure 6.5 As in Figure 6.3 except showing results for 3-hour peak flows for the Snoqualmie River near Snoqualmie.

Projected changes for the GFDL-RCP8.5 are higher than the median of bcMACA for RCP 8.5 for the 2- and 10-year events and similar or lower than the median for the 50- and 100-year events (Figures 6.3-6.5). The GFDL-RCP8.5 simulation projects more than a 60% increase in the 10-year flood by the 2080s, relative to the 1980s, for all tributaries and the mainstem of the Green and Snoqualmie rivers, with the exception of the Raging and Tolt rivers and Newaukum Creek, for which the changes nonetheless exceed the median (or even maximum) of bcMACA for RCP 8.5 (Table 6.1). For the 100-year flood, the GFDL-RCP 8.5 simulation projects less than a 60% increase by the 2080s for all sites except Snoqualmie River above Alice Creek, which is generally lower than the median of bcMACA for RCP 8.5 (Table 6.2).

Figure 6.6 shows the time series in bias-corrected water year maximum 3-hour streamflow for the two WRF simulations for the Green and Snoqualmie Rivers. These results show a clear increasing trend in peak flows for the GFDL simulation, but no such change for the ACCESS simulation. Instead of showing a trend, the ACCESS simulation appears to be dominated by a few particularly large flood events that occur throughout the record. This suggests that the decreases in extreme statistics in the ACCESS projections are likely not associated with a long-term decline in peak flows, but instead a result of random variability in precipitation extremes. Figure 6.7 confirms this by showing the time series of annual maximum precipitation from the two WRF projections. For simplicity, results are shown for two points that are near the upper watershed for each basin: the NOAA rain gauge stations at Snoqualmie Falls (ID: 457773) and Mud Mountain

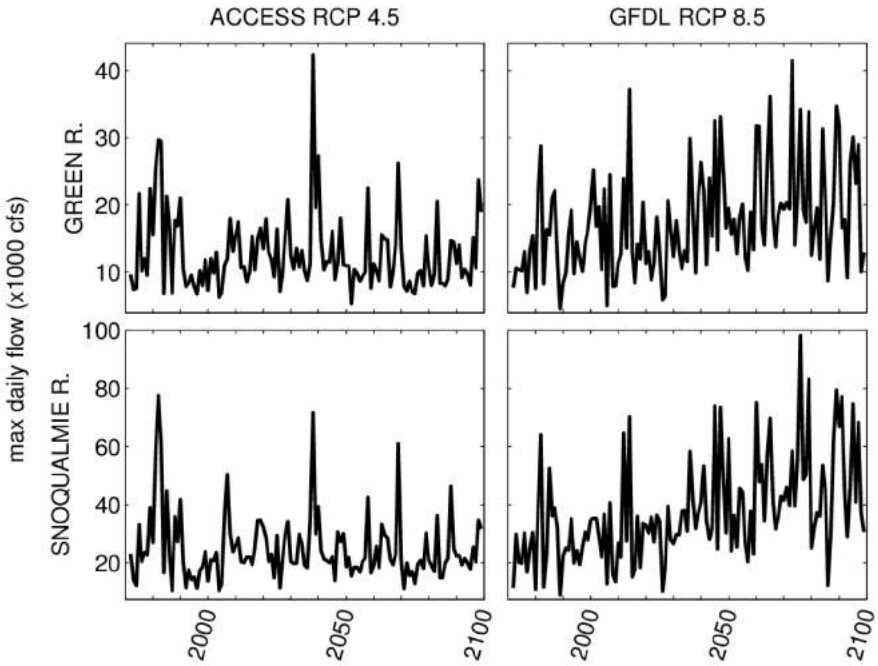

Figure 6.6 Time series of the water year maximum in 3-hour streamflow for the ACCESS (left) and GFDL (right) simulations. Results are shown for the Green River at Auburn (top) and the Snoqualmie River near Snoqualmie (bottom).

Dam (ID: 455704). Results are shown for the water year maxima in both 3-hour and 3-day precipitation. Although the patterns are somewhat different for each location, all show that a small number of events in the ACCESS simulation are much larger than the maxima in other water years, apart from which there is no apparent trend. In general, the ACCESS-RCP4.5 simulation shows much larger variability than the GFDL-RCP8.5 simulation. For the GFDL simulation, the long-term trend is much more pronounced for 3-hour than for 3-day precipitation, although both do show an increase over time.

In order to better control for the influence of peak flow events, we developed a time series for each extreme flow statistic (2-, 10-, 50-, and 100-year floods) using a moving 30-year window (Figures 6.8 and 6.9). In addition, we used a bootstrap approach in which we sub-sampled from each 30-year window in order to estimate the 95% confidence limits for the peak flow estimates. Specifically, we randomly selected a 20-year sub-sample and computed the extreme statistics for that sub-sample. This process was repeated 1,000 times, resulting in a probability distribution for each extreme statistic. From this we extracted the 95% confidence limits (2.5^{th} and 97.5^{th} percentiles) for each 30-year window. For the GFDL simulation, these results confirm the robust long-term increase in peak flows that are apparent in Figures 6.8 and 6.9. For the ACCESS simulation, the results suggest that natural variability dominates in all cases, with the two particularly large flood episodes (early 1980s, late 2030s) dominating the time series in most extreme statistics (recall that all CMIP5 simulations are “free-running”, meaning that each simulates a unique sequence of weather events that do not match the timing or sequence found in the observed record). That said, we cannot rule out a small negative trend, which

seems particularly plausible in the record for the 10-year flood. Additional ensemble members would be needed to determine if the apparent trend is real or simply a random consequence of the timing of one big flood event in the 1980s.

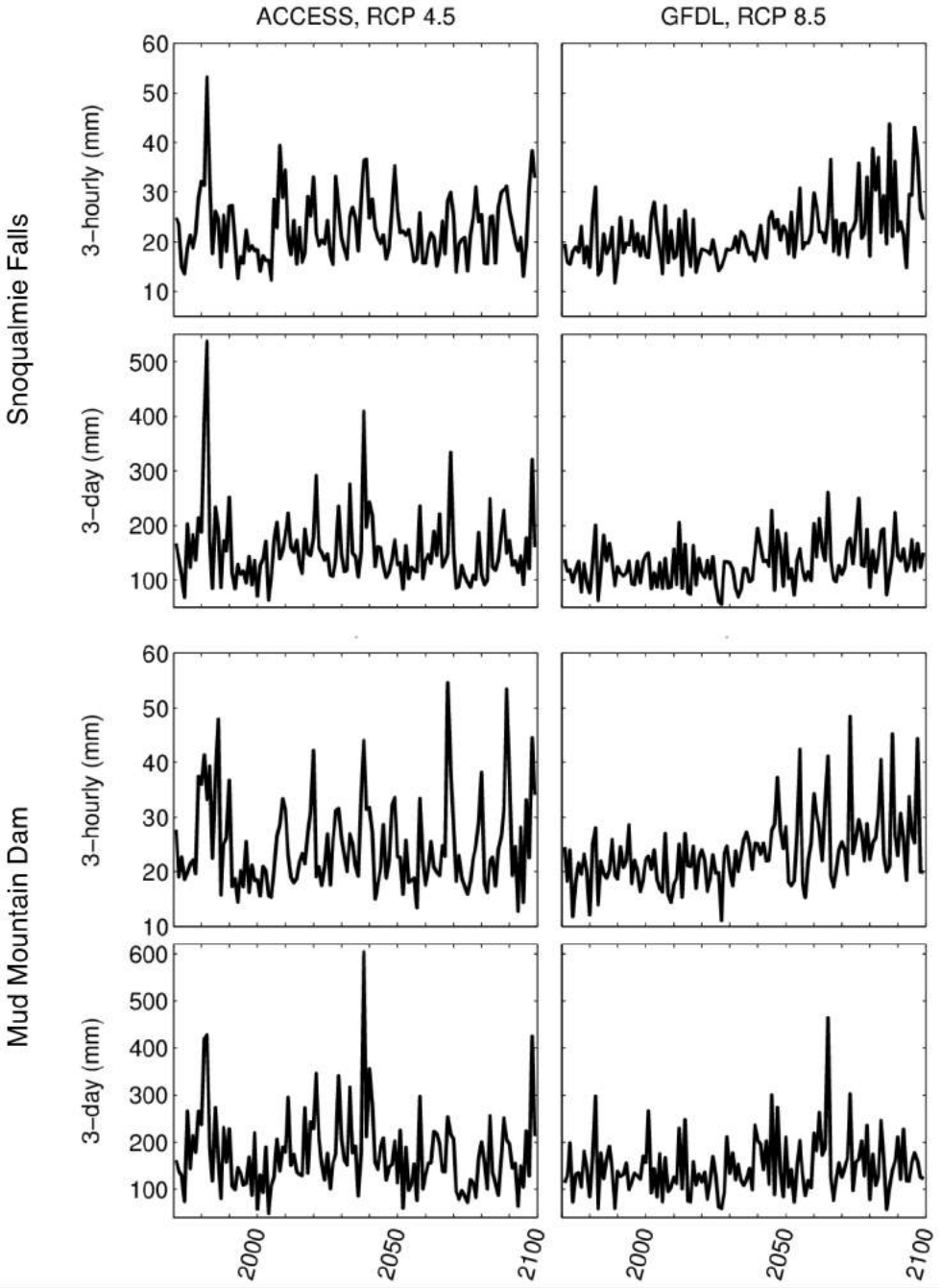

Figure 6.7 Time series of the water year maximum in 3-hour (1st and 3rd rows) and 3-day (2nd and 4th rows) ***precipitation*** for two NOAA weather station sites: Snoqualmie Falls (ID: 457773, top two rows) and Mud Mountain Dam (ID: 455704, bottom two rows). Results are shown for the ACCESS-RCP4.5 (left) and GFDL-RCP8.5 (right) simulations.

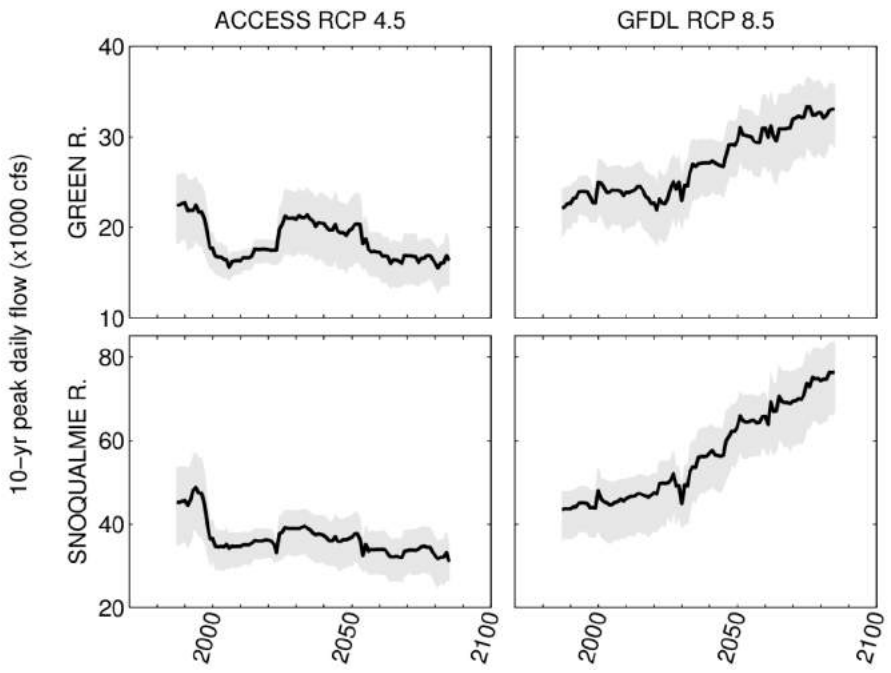

Figure 6.8 Time series of the 10-year peak in 3-hour flows for the ACCESS (left) and GFDL (right) simulations, based on a moving 30-year window. The shading denotes the 95% confidence limit, obtained by bootstrapping the extremes estimates for each 30-year sample. Results are shown for the Green River at Auburn (top) and the Snoqualmie River near Snoqualmie (bottom).

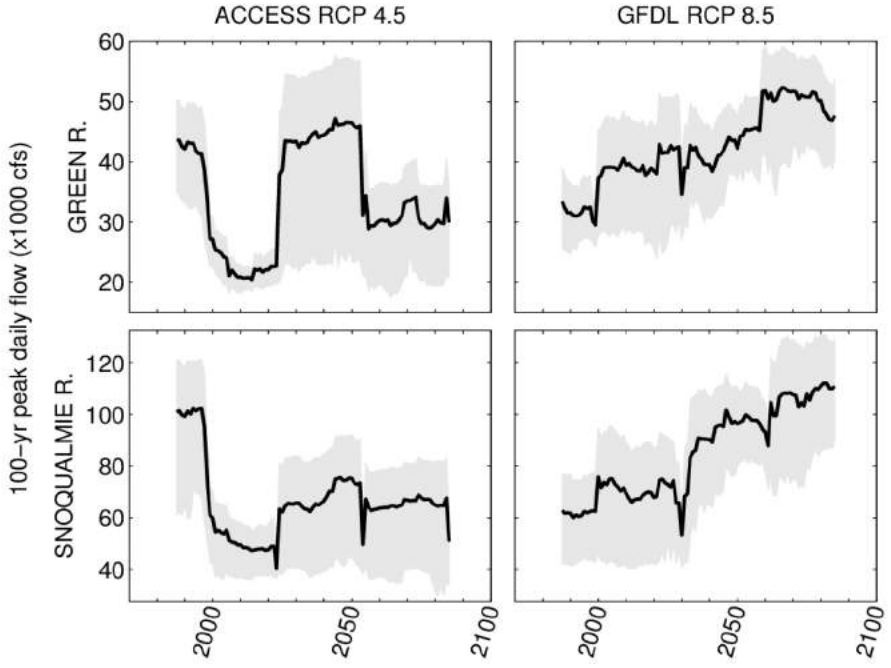

Figure 6.9 As in Figure 6.6 except showing results for the 100-year flood.

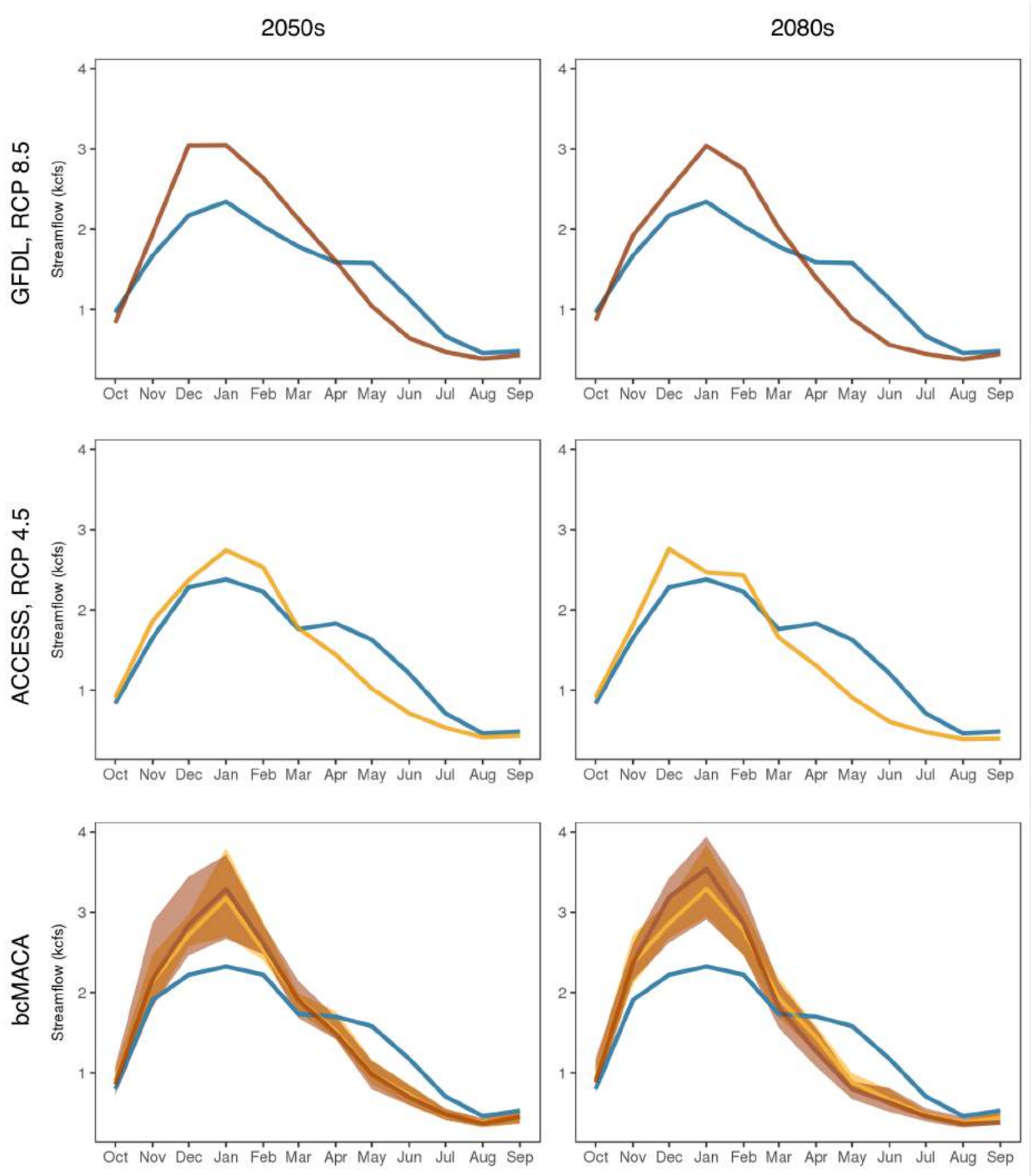

Figure 6.10 Seasonal cycle in monthly average regulated streamflow for the Green River near Auburn based on GFDL (top), ACCESS (middle) and bcMACA (bottom) for the 2050s (left) and 2080s (right). Since this figure concerns absolute flow estimates, bias-corrected streamflow data are shown.

Projected Changes in Regulated Streamflow

This section summarizes the changes in regulated streamflow in the Green River, based on the reservoir model simulations described previously. Howard Hanson Dam operations result in a very slight reshaping of monthly streamflow, due in part to the City of Tacoma diversion as well as providing flood control (compare Figures 6.1 and 6.10). In contrast, the effect on flood statistics is notable (Table 6.3; compare Figures 6.3 and 6.11). With the exception of a few bcMACA projections there is little to no change in regulated peak flows, especially for the largest floods (50- and 100-yr events).

For a few bcMACA scenarios whose 3-day average inflows exceed 35 kcfs, the dam does not have sufficient capacity to keep flows below the downstream target of 12 kcfs at Auburn. As in the above discussion regarding the episodic large events in ACCESS-RCP4.5 simulation, it is unclear if this result is due to random variability or a credible trend in the bcMACA projections – additional WRF projections would be needed to confirm these findings. Nonetheless, this result does highlight the potential for larger changes in peak flows, and is a reminder that the two WRF projections are unlikely to bracket the full range among projections in every situation.

Finally, it is worth noting that the current reservoir model only resolves daily average flows. Given the larger increases in short-duration peaks, it is possible that these

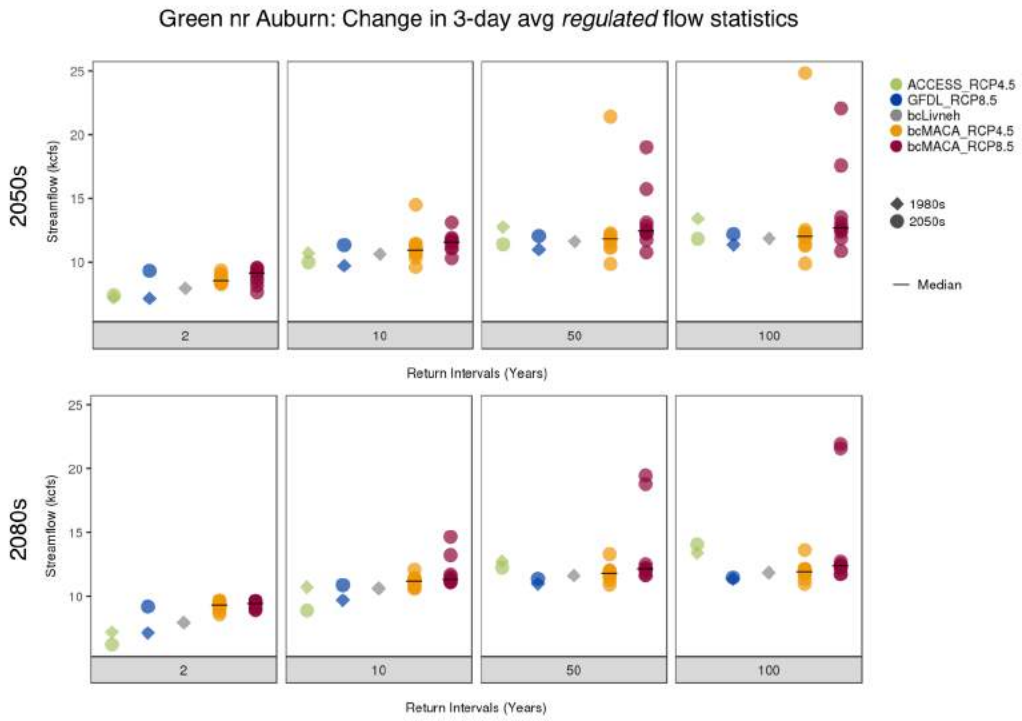

Figure 6.11 Future and historical flood statistics (2-, 10-, 50- and 100- year floods) using regulated flows for the Green River near Auburn. The plots include results for all DHSVM simulations for the 2050s (top) and 2080s (bottom). Historical flood statistics are based on water years 1971-1999

			WRF		bcMACA	
Agg.	**Freq.**	**Decade**	**GFDL**	**ACSS**	**RCP 4.5**	**RCP 8.5**
Daily	2-yr	2050s	22%	8%	+9% (+5%; +19%)	+12% (+1%; +18%)
		2080s	21%	-9%	+15% (+9%; +19%)	+15% (+11%; +18%)
	10-yr	2050s	14%	-2%	+1% (-9%; +46%)	+8% (-6%; +29%)
		2080s	10%	-14%	+2% (-1%; +17%)	+4% (+2%; +49%)
	50-yr	2050s	13%	-10%	-2% (-14%; +124%)	+8% (-11%; +87%)
		2080s	4%	-7%	-2% (-4%; +31%)	+4% (-3%; +132%)
	100-yr	2050s	14%	-12%	-2% (-15%; +173%)	+9% (-12%; +123%)
		2080s	3%	-2%	-3% (-5%; +38%)	+5% (-4%; +187%)
3-day	2-yr	2050s	32%	2%	+9% (+5%; +21%)	+16% (-1%; +21%)
		2080s	28%	-15%	+18% (+8%; +22%)	+19% (+11%; +23%)
	10-yr	2050s	19%	-5%	+3% (-10%; +43%)	+8% (-3%; +25%)
		2080s	13%	-18%	+5% (+0%; +13%)	+6% (+4%; +38%)
	50-yr	2050s	12%	-10%	+3% (-15%; +98%)	+7% (-8%; +62%)
		2080s	5%	-6%	+1% (-6%; +15%)	+5% (-1%; +70%)
	100-yr	2050s	10%	-11%	+2% (-17%; +129%)	+8% (-9%; +82%)
		2080s	3%	3%	+1% (-7%; +16%)	+5% (-2%; +91%)

Table 6.3 Percent change in regulated flows for the Green river near Auburn. Results are shown for the 2-, 10, 50-, and 100-year annual (water year) peak flow statistics for both 1-day and 3-day average flows. For bcMACA, the median is shown along with the minimum and maximum among all 10 models in parentheses. Results show a much larger increase for the 2-yr events than for the 100-yr events, suggesting that the reservoir is generally able to absorb increases in flow due to climate change.

increases could affect operations in the future. This risk could be assessed by working with the Army Corps to finalize their hourly flow reservoir model.

Projected Changes in Return Frequencies

As described in the Section 4, we also evaluated changes in the frequency of a number of key flow thresholds on the Snoqualmie and Green rivers (Table 4.1). Future return frequencies were estimated for all of the metrics described in Table 4.1 and are provided in the online material; here we provide a brief summary for a select subset of metrics (Tables 6.4 and 6.5).

The GFDL-RCP8.5 simulation projects that the historical 20- and 50-year flood (3-hour flows) for the Snoqualmie River near Snoqualmie will become 4- and 6-year flood events by the 2050s, respectively. The GFDL model projects the largest change among both the WRF and bcMACA simulations. The ACCESS-RCP4.5 simulation projects that these

events will occur less often, corresponding to 76- and 231-year flood events by the 2050s, respectively.

For naturalized flows at the Green River near Auburn, the 10,000 cfs threshold in 3-hour flows has historically corresponded to about a 1.4-year event. The projections indicate that these events will range from a 1.0- to a 1.6-year event by the 2050s.

A challenge in assessing changes in specific flow thresholds is that the modeled streamflow statistics do not perfectly align with the observations. To address this, we assessed changes in the 25,000 and 28,000 cfs thresholds with respect to the return frequencies that they approximate (100- and 200-yr events, respectively). Given the importance of absolute thresholds for operations at Howard Hanson Dam, this was only done for the 25,000 and 28,000 cfs thresholds. An important consideration for the other metrics is that the results are skewed by the fact that the GFDL-RCP8.5, ACCESS-RCP4.5, and bcLivneh simulations may all have different estimates of the historical return frequency for a particular threshold. For the 100-year threshold, simulations indicate that these will become 12- to >500-yr events by the 2050s, and 20- to 251-yr events by the 2080s. For the 200-year threshold, simulations indicate that these will become 21- to >500-yr events by the 2050s, and 49- to 402-yr events by the 2080s.

Regulated flows on the Green River are also projected to change. In the case of the 10,000 cfs threshold (in 3-day flows at Auburn), projections indicate this will be a 3- to 10-year event by the 2050s.

Overall, we find that this approach works well for evaluating changes in specific return intervals (e.g., 20-year event), but that additional refinement is needed to evaluate

	WRF		***bcMACA***	
metrics	***GFDL***	***ACSS***	***RCP 4.5***	***RCP 8.5***
Naturalized flows for the Snoqualmie Near Snoqualmie				
Historical 20-year extreme, 3-hour flow	4	76	9 (5 - >500)	6 (4 - 22)
Historical 50-year extreme, 3-hour flow	6	231	19 (7 - 33)	13 (6 - 67)
Naturalized flows (or unregulated flows) for the Green basin				
10 kcfs in 3-hour flow at Auburn (~1.4-yr)	1.0	1.6	1.1 (1.1 - 1.2)	1.1 (1.1 - 1.2)
100-yr for 3-day flow at Auburn (~25 kcfs)	12	>500	24 (9 - 165)	20 (11 - >500)
200-yr for 3-day flow at Auburn (~28 kcfs)	21	>500	43 (11 - 416)	27 (16 - >500)
Regulated flows for the Green basin				
10 kcfs in 3-day flows at Auburn	10	3	4 (3 - 6)	3 (2 - 6)
12 kcfs in 3-day flows at Auburn	43	139	46 (11 - >500)	22 (5 - 453)

Table 6.4. Future return intervals (in years) for a selection of flow thresholds listed in Table 4.1. Results are shown for the 2050s.

	WRF		*bcMACA*	
metrics	***GFDL***	***ACSS***	***RCP 4.5***	***RCP 8.5***
Naturalized flows (or unregulated flows) for the Snoqualmie basin				
Historical 20-year extreme, 3-hour flow	2	165	6 (4 - 11)	4 (3 - 10)
Historical 50-year extreme, 3-hour flow	3	>500	14 (6 - 27)	6 (5 - 353)
Naturalized flows (or unregulated flows) for the Green basin				
10 kcfs in 3-hour flow at Auburn (~1.4-yr)	1.1	1.9	1.1 (1.0 - 1.1)	1.1 (1.0 - 1.2)
100-yr for 3-day flow at Auburn (~25 kcfs)	20	251	31 (8 - 237)	15 (7 - 47)
200-yr for 3-day flow at Auburn (~28 kcfs)	49	402	49 (11 - >500)	22 (9 - 139)
Regulated flows for the Green basin				
10 kcfs in 3-day flows at Auburn	18	3	3 (2 - 5)	3 (2 - 4)
12 kcfs in 3-day flows at Auburn	>500	45	55 (9 - >500)	29 (4 - 50)

Table 6.5. As in Table 6.4 but for the 2080s.

changes for specific flow thresholds. In particular, the results are very sensitive to the accuracy of the model in representing the historical chance of exceedance for each threshold. Small differences in these estimates can significantly alter the resulting assessment of the future change in return frequencies. One way to address this issue is to re-calibrate the model for each extreme event of interest. Another potential workaround is to relate specific thresholds in the observations to a particular quantile in the observed extremes distribution (e.g., the 145-year flood, or 0.7% annual chance event), then evaluate model projections for that quantile as opposed to a specific flow threshold. This latter approach may not work on the Green, given that reservoir operations are tied to specific flow thresholds and the capacity of the reservoir.

7 Discussion

All of our simulations project an increase in winter flow volume due to an increase in the proportion of precipitation falling as rain over the course of the 21st century. Similarly, all scenarios also project that the Green and Snoqualmie rivers will become rain-dominant watersheds by the 2080s and in some instances even by the 2050s. As snowpack decreases, the proportion of winter precipitation falling as rain increases. Since winter precipitation is characterized by high variability and exhibits almost no long-term trend, the result is greater year-to-year variability in winter streamflow. For this reason, there are some instances in which winter streamflow is larger in the 2050s than in the 2080s. The influence of temperature is confirmed controlling for the variability in average annual streamflow, which is closely tied to precipitation: the ratio of winter to water year average streamflow increases from the 2050s to the 2080s in all simulations. This effect is greatest in the Green River basin, for which a smaller proportion of historical snowpack remains after the 2050s.

Changes in peak flows are driven by both increases in the proportion of winter precipitation falling as rain and increases in the intensity of heavy rain events. We selected the GFDL-RCP8.5 and ACCESS-RCP4.5 projections to bracket the range among projections. As a consequence, streamflow projections based on the GFDL-RCP 8.5 projection showed a systematic increase in peak flows, while projected changes for the ACCESS-RCP 4.5 simulation showed a decrease. Further inspection revealed that the decrease observed in the ACCESS-RCP4.5 projection is primarily a consequence of a few exceptionally large events in the 1980s and around mid-century. Based on the current results it is unclear if the decrease in the ACCESS-RCP4.5 projection is a real manifestation of declining peak flows or a random consequence of variability in extreme precipitation.

We present a separate analysis, showing that uncertainty in the estimates of extreme event statistics can be important. This is primarily a consequence of sample size, and is a challenge for both the observations and the model results. For example, our results suggest that for 60 years of observations (about the length of the Sea-Tac record), the uncertainty in the 100-year precipitation extreme is about ±10%. This means that changes in the 100-year storm that are smaller than 10% could potentially be masked by the noise in the observations. For the 30-year time periods used to evaluate projected changes, the uncertainties are greater. We present one approach, using a moving window, to begin account for this issue.

Reservoir simulations for Howard Hanson Dam, which the U.S. Army Corps of Engineers manages during flood season, indicate that future flooding is generally within the existing capacity of the reservoir. However, a few of the bcMACA projections did exceed the reservoir's capacity to mitigate peak flows downstream. As above, existing information is insufficient to determine if this is indicative of a real vulnerability or a result of model limitations, such as the use of statistically downscaled projections and a daily time step reservoir model.

Regardless of the interpretation, the balance of evidence suggests that peak flows will increase in the Green, Snoqualmie, and SF Skykomish river basins. However, there are two key questions that warrant further study:

1. With only two regional climate model simulations of the future, it is unclear if the projected changes are representative of what one would find from a larger set of regional climate model projections.
2. Other rivers in King County (e.g., Cedar, White) may respond differently to climate change. How they respond, and how each river exhibits different vulnerabilities, will be important for planning.

The first issue can be addressed by obtaining additional regional climate model projections and using these to drive new simulations of future streamflow change. These can be obtained via a collaboration with UW Professor Cliff Mass, who is currently producing several new regional model projections under a grant from the Amazon Catalyst program. These new projections would help elucidate our results in two ways: (a) by increasing the sample size, thereby improving the statistics; and (b) by evaluating results for new global models, each of which may respond differently to warming.

The second issue would be addressed by simply replicating our approach for additional rivers in King County. Since the approach has already been developed, this can be done much more quickly and with less effort than in the current study. New simulations for the Cedar River would make it possible to simulate the effects of regulation on both the Cedar and the South Fork Tolt. Flow regulation would also be simulated for Mud Mountain Dam on the White River.

In addition to the two issues outlined above, we believe there are a number of methodological choices that could be investigated further. These include the hydrologic model setup, the approach for generating meteorological inputs, the metrics used for optimizing the calibration, and the time step used for the reservoir modeling – all could be further investigated to more effectively capture the response of each basin to changing conditions.

Finally, the current study simply quantifies the amount of water during flood events, but does not specify which areas on the floodplain are affected, at what depth, and how often. Methods now exist to model the depth and extent of flooding over larger geographic areas. For example, a pilot study with the Snohomish Conservation District is currently producing future flood maps that cover all floodplains in the Snohomish and Stillaguamish river basins. In contrast with the very localized studies typically done for FEMA mapping, these allow for apples-to-apples comparisons of risk across an entire jurisdiction. This new flood mapping effort could be updated to include the new flood projections described in the current report, and expanded to cover all King County watersheds. These future flood maps could be used to inform floodplain management actions such as levee design

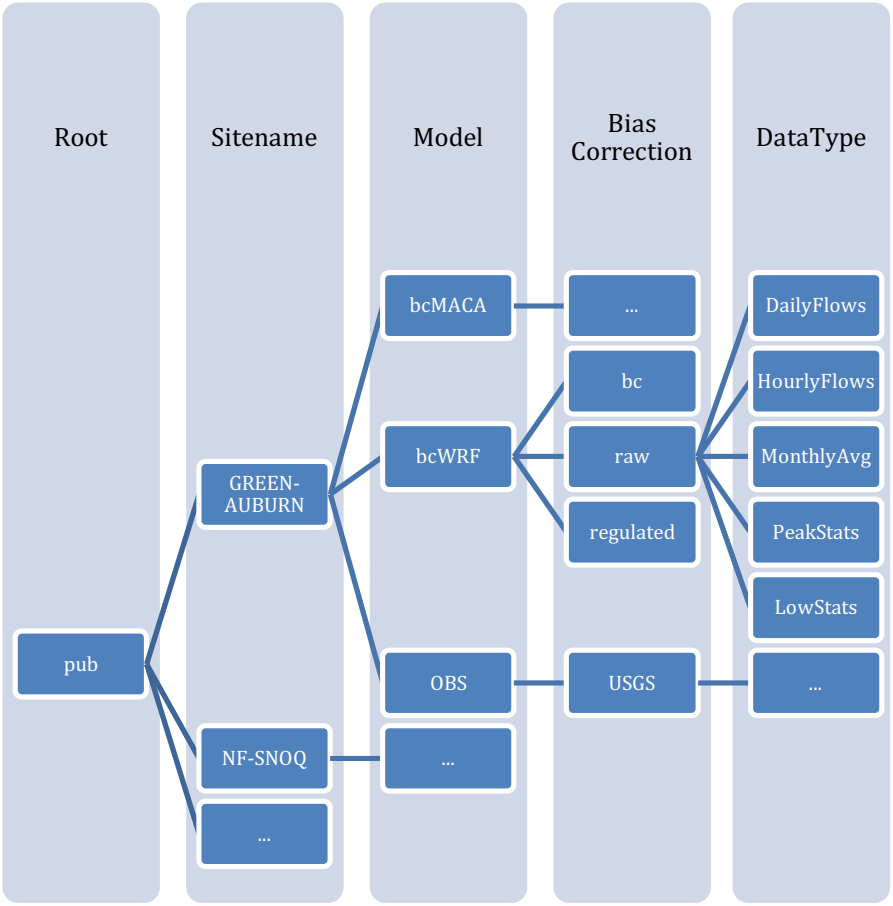

Figure 6.12. Data structure for study results.

for construction projects, flood preparedness, and potential priorities for acquisition or elevation of at-risk structures.

Accessing the Results

All of the results for this project can be accessed from the project website:

https://cig.uw.edu/our-work/applied-research/effect-of-climate-change-on-flooding-in-king-county-rivers/

Data are stored for each of the streamflow sites listed in Table 6.6, and are organized as shown in Figure 6.12. All files are comma- delimited (.csv), and all values are given in cubic feet per second (cfs). There are five types of output files, with the following naming conventions:

1. ***Time series files.*** Time series including the full record for the observations, raw simulated results or bias-corrected streamflow from the simulations. For the observations these are daily averages, whereas a 3-hourly time step is used for

the WRF and bcMACA results. In both cases, the file has four columns for year, month, day, and flow. Days are expressed as fractions for each 3-hourly time step (e.g., on day four of the month, the 3 AM results are expressed as 4.125).

File Naming:

Simulations:

```
<ShortName>_<Downscaling>_<GCM>_<RCP>_3hr_full_HourlyFlows.csv
<ShortName>_<Downscaling>_<GCM>_<RCP>_day_full_DailyFlows.csv
```

Observations:

```
<ShortName>_OBS_<TimeStep>_full_DailyFlows.csv
```

2. ***Statistics.*** Statistics are computed for each of the three time periods evaluated in the current study: 1980s (1970-1999), 2050s (2040-2069), and 2080s (2070-2099). Three different sets of statistics are included: (1) Peak flow statistics (2-, 10-, 50-, and 100-year for 3-hourly, daily, and 3-day average flows), (2) Low flow statistics (2- and 10-year for 7-day average flows), and (3) Monthly averages.

   File Naming:

Site Name	***Short Name***
Snohomish River basin	
SF Snoqualmie R. AB Alice Creek near Garcia	SF-SNOQ
MF Snoqualmie near Tanner	MF-SNOQ
NF Snoqualmie near Snoqualmie Falls	NF-SNOQ
Snoqualmie near Snoqualmie	SNOQ-NR-SNOQ
Raging R. near Fall City	RAGING-R
NF Tolt R. near Carnation	NF-TOLT
SF Tolt R. near Carnation	SF-TOLT
Tolt R. near Carnation	TOLT-CARNATN
Mainstem Snoqualmie near Carnation	SNOQ-CARNATN
SF Skykomish R. near Index	SF-SKY-INDX
Skykomish River near Gold Bar	SKY-GOLDBAR
Green River basin	
Green River near Lester	GREEN-LESTER
Green River at Howard A. Hanson Dam (HHD)	GREEN-HHD
Green R. at Purification Plant near Palmer	GREEN-PALMER
Newaukum Creek near Black Diamond	NEWAUKUM-CR
Big Soos Creek above Hatchery near Auburn	BIG-SOOS-CR
Green R. near Auburn	GREEN-AUBURN

Table 6.6. Short names used to label directories and data files for each streamflow site.

Simulations:

<ShortName>_<Downscaling>_<GCM>_<RCP>_<TimeStep>_<TimePeriod>_PeakStats.csv

<ShortName>_<Downscaling>_<GCM>_<RCP>_7dy_<TimePeriod>_LowStats.csv

<ShortName>_<Downscaling>_<GCM>_<RCP>_day_<TimePeriod>_MonthlyAvg.csv

Observations:

<ShortName>_OBS_<TimeStep>_1980s_PeakStats.csv

<ShortName>_OBS_7dy_1980s_LowStats.csv

<ShortName>_OBS_day_1980s_MonthlyAvg.csv

References

Abatzoglou, J. T., & Brown, T. J. (2012). A comparison of statistical downscaling methods suited for wildfire applications. *International Journal of Climatology*, 32(5), 772-780.

Andreadis, K. M., P. Storck, and D. P. Lettenmaier (2009), Modeling snow accumulation and ablation processes in forested environments, Water Resour. Res., 45, W05429, doi:10.1029/2008WR007042.

Bohn TJ, Livneh B, Oyler JW, Running SW, Nijssen B, Lettenmaier DP. 2013. Global evaluation of MTCLIM and related algorithms for forcing of ecological and hydrological models. Agricultural and Forest Meteorology, 176, 38-49.

Bowling, L.C. and D.P. Lettenmaier, 2001. The effects of forest roads and harvest on catchment hydrology in a mountainous maritime environment, in *Land Use and Watersheds: Human Influence on Hydrology and Geomorphology in Urban and Forest Areas*, M.S. Wigmosta and S.J. Burges, eds., AGU Water Science and Application Volume 2, p. 145-164.

U.S. Army Corps of Engieers (USACE). 2014. Climate change impacts and adaptation Study: Howard Hanson Dam, Green River Washington. Seattle District Army Corps of Engineers, April 2014.

Cristea N.C., Lundquist J.D., Loheide S.P., Lowry C.S., Moore C.E. 2014. Modelling how vegetation cover affects climate change impacts on streamflow timing and magnitude in the snowmelt-dominated upper Tuolumne Basin, Sierra Nevada. *Hydrological Processes* 28 : 3896-918.

Cuo L., Beyene T.K., Voisin N., Su F., Lettenmaier D.P., Alberti M., Richey J.E. 2011. Effects of mid-twenty-first century climate and land cover change on the hydrology of the Puget Sound basin, Washington. *Hydrological Processes* 25 : 1729-53.

Cuo, L., D.P. Lettenmaier D.P., M. Alberti, and J.E. Richey, 2009. Effects of a century of land cover and climate change on the hydrology of Puget Sound basin, *Hydrological Processes*, 23, 907-933.

Daly, C., W. P. Gibson, G.H. Taylor, G. L. Johnson, P. Pasteris. 2002. A knowledge-based approach to the statistical mapping of climate. Climate Research, 22: 99-113

Daly, C., Halbleib, M., Smith, J.I., Gibson, W.P., Doggett, M.K., Taylor, G.H., Curtis, J., and Pasteris, P.A. 2008. Physiographically-sensitive mapping of temperature and precipitation across the conterminous United States. International Journal of Climatology, 28: 2031-2064.

Elsner, M. M., Cuo, L., Voisin, N., Deems, J. S., Hamlet, A. F., Vano, J. A., ... & Lettenmaier, D. P. (2010). Implications of 21st century climate change for the hydrology of Washington State.*Climatic Change*, *102*(1-2), 225-260.

Hamlet, A.F., Elsner, M.M., Mauger, G., Lee, S.Y., and Tohver, I. (2013). "An Overview of the Columbia Basin Climate Change Scenarios Project: Approach, Methods, and Summary of Key Results." *Atmosphere-Ocean,* 1:4, 392-415, DOI:10.1080/07055900.2013.819555.

Homer, C.G., Dewitz, J.A., Yang, L., Jin, S., Danielson, P., Xian, G., Coulston, J., Herold, N.D., Wickham, J.D., and Megown, K., 2015, Completion of the 2011 National Land Cover Database for the conterminous United States-Representing a decade of land cover change information. *Photogrammetric Engineering and Remote Sensing*, v. 81, no. 5, p. 345-354

Hosking, J. R. M., & Wallis, J. R. (1993). Some statistics useful in regional frequency analysis. *Water Resources Research*, 29(2), 271-281.

Hosking, J.R.M., 1990. L-moments: analysis and estimation of distributions using linear combinations of order statistics. *Journal of the Royal Statistical Society*, Series B, 52,105-124.

King County. 2016. Flood Frequency Analysis of King County Rivers with an Emphasis on the January 2009 Floods. Prepared by Curtis DeGasperi, Water and Land Resources Division. Seattle, Washington.

Liang, X., Lettenmaier, D.P., Wood, E.F., and Burges, S.J. (1994). “A simple hydrologically based model of land surface water and energy fluxes for general circulation models.” *Journal of Geophysical Research*, 99(D7), 14415-14428.

Livneh B., T.J. Bohn, D.S. Pierce, F. Munoz-Ariola, B. Nijssen, R. Vose, D. Cayan, and L.D. Brekke, 2015: A spatially comprehensive, hydrometeorological data set for Mexico, the U.S., and southern Canada 1950-2013, *Nature Scientific Data*, 5:150042, doi:10.1038/sdata.2015.42.

Mass, C. et al., 2011. Extreme Precipitation over the West Coast of North America: Is There a Trend?. *Journal of Hydrometeorology,* 12(2), 310-318.

Mauger, G.S., J.S. Won, K. Hegewisch, C. Lynch, R. Lorente Plazas, E. P. Salathé Jr., 2018. New Projections of Changing Heavy Precipitation in King County. Report prepared for the King County Department of Natural Resources. Climate Impacts Group, University of Washington, Seattle.

Mauger, G.S., S.-Y. Lee, C. Bandaragoda, Y. Serra, J.S. Won, 2016. Refined Estimates of Climate Change Affected Hydrology in the Chehalis basin. Report prepared for

Anchor QEA, LLC. Climate Impacts Group, University of Washington, Seattle. doi:10.7915/CIG53F4MH

Naz, B.S., C.D. Frans, G.K. Clarke, P. Burns, and D.P. Lettenmaier, 2014. Modeling the effect of glacier recession on streamflow response using a coupled glacio-hydrological model, *Hydrol. Earth Syst. Sci.*, **18**, 787-802, doi:10.5194/hess-18-787-2014.

Nick, M., Das, S. and Simonovic, S.P. 2011. The Comparison of GEV, Log-Pearson Type 3 and Gumbel Distributions in the Upper Thames River Watershed under Global Climate Models, the University of Western Ontario Department of Civil and Environmental Engineering, Report No:077.

Rahman, A., Weinmann, P.E. and Mein, R.G. (1999). At-site flood frequency analysis: LP3-product moment, GEV-L moment and GEV-LH moment procedures compared. In: Proceeding Hydrology and Water Resource Symposium, Brisbane, 6–8 July, 2, 715–720.

Rahman, A., Karin, F, and Rahman, A. 2015. Sampling Variability in Flood Frequency Analysis: How Important is it? 21st International Congress on Modelling and Simulation, Gold Coast, Australia, Nov 29-Dec 4, 2015, 2200-2206.

Salathé Jr, E. P., Hamlet, A. F., Mass, C. F., Lee, S. Y., Stumbaugh, M., & Steed, R. (2014). Estimates of 21st century flood risk in the Pacific Northwest based on regional climate model simulations. *Journal of Hydrometeorology*, (2014).

Snover, A.K., Hamlet, A.F., Lettenmaier, D.P. 2003. Climate change scenarios for water planning studies: Pilot applications in the Pacific Northwest. Bulletin of the American Meteorological Society 84(11):1513-1518.

Storck, P., Bowling, L., Wetherbee, P., & Lettenmaier, D. (1998). Application of a GIS-based distributed hydrology model for prediction of forest harvest effects on peak stream flow in the Pacific Northwest. *Hydrological Processes*, *12*(6), 889-904.

Sun, N., J. Yearsley, N. Voisin, and D.P. Lettenmaier, 2013. A spatially distributed model for the assessment of land use impacts on stream temperature in small urban watersheds, *Hydrol. Process*. doi: 10.1002/hyp.10363.

Thornton, P.E., Running, S.W., 1999. An improved algorithm for estimating incident daily solar radiation from measurements of temperature, humidity, and precipitation. Agric. For. Meteorol. 93 (4), 211–228, http://dx.doi.org/10.1016/S0168-1923(98)00126-9.

Tohver, I. M., Hamlet, A. F., & Lee, S. Y. (2014). Impacts of 21st-Century Climate Change on Hydrologic Extremes in the Pacific Northwest Region of North America. *JAWRA Journal of the American Water Resources Association*, *50*(6), 1461-1476.

U.S. Army Corps of Engineers (USACE). (2014). Climate change impacts and adaptation study; Howard Hanson Dam, Green River, Washington. U.S. Army Corps of Engineers, Seattle District.

Vano J.A., Voisin N., Cuo L., Hamlet A.F., Elsner M.M., Palmer R.N., Polebitski A., Lettenmaier D.P. 2010. Climate change impacts on water management in the Puget Sound region, Washington State, USA. *Climatic Change* 102 : 261-86.

Vogel, R.M., McMahon, T.A. and Chiew, F.H.S. (1993). Flood flow frequency model selection in Australia, Journal Hydrology, 146, 421-449.

Wang, Q.J. 1997. LH moments for statistical analysis of extreme events. *Water Resour Res*, 33(12), 2841- 2848.

Whitaker, A., Alila, Y., Beckers, J., and Toews, D., 2003. Application of the Distributed Hydrology Soil Vegetation Model to Redfish Creek, British Columbia: Model evaluation using internal catchment data, *Hydrol. Process.* 17, 199-224.

Wigmosta, M. S., Vail, L. W., & Lettenmaier, D. P. (1994). A distributed hydrology-vegetation model for complex terrain. *Water resources research*,*30*(6), 1665-1679.

Wigmosta, M.S., and D.P. Lettenmaier, 1999. A Comparison of Simplified Methods for Routing Topographically-Driven Subsurface Flow, *Wat. Resour. Res.*, 35, 255-264.

Wigmosta, M.S., B. Nijssen, P. Storck, and D.P. Lettenmaier, 2002. The Distributed Hydrology Soil Vegetation Model, In *Mathematical Models of Small Watershed Hydrology and Applications*, V.P. Singh, D.K. Frevert, eds., Water Resource Publications, Littleton, CO., p. 7-42.

Yapo, P. O., H. V. Gupta, S. Sorooshian, Multi-objective global optimization for hydrologic models, J. Hydrol., 204, 83–97, 1998.